TIGHT JUNCTIONS AND ADHERENS JUNCTIONS: QUANTIFYING ADHESION AND ROLE IN MECHANOTRANSDUCTION IN EPITHELIAL CELLS

Dr. VEDULA SRI RAM KRISHNA
M.B.B.S, University of Pune
M.M.S.T, Indian Institute of Technology

A THESIS SUBMITTED

FOR THE DEGREE OF DOCTOR OF PHILOSOPHY

DIVISION OF BIOENGINEERING

NATIONAL UNIVERSITY OF SINGAPORE

2008

Acknowledgements

I would like to express my deepest gratitude to all those who have been instrumental in making this thesis possible. First and foremost, I would like to thank my supervisor Associate Professor Lim Chwee Teck for his able guidance, continuous support and sustained inspiration. If not for him, this thesis would not have been possible. I would also like to thank Associate Professor Walter Hunziker for his insightful suggestions, critical comments and for allowing the use of his lab facilities. I would like to thank my colleagues Mr. Lim Tongseng for helpful discussions and data analysis, Mr. Tan Swee Jin and Ms. Yan Lian for their help with designing and calibrating the cell stretcher and Dr. Jaya for help with the cell lines. I would also like to thank all my colleagues Ms. Tan Eunice, Mr. Hairul Nizam, Dr. Zhou Enhua, Mr. Li Ang, Ms. Shi Hui, Mr. Li Qingsen, Ms. Yow Sow Zeom, Ms. Sun Wei, Mr. Yuan Jian, Ms. Jiao Guyue, Dr. Earnest, Dr. Fu Hongxia, Dr. Yousheng and Dr. Yang Zhong at the Nano-biomechanics lab for providing a lively environment conducive for research. I am indebted to the Nano-bioengineering lab for allowing me to use their cell culture facilities.

I would also like to thank our collaborators Dr. Terence Dermody & Ms. Kristine Guglielmi from Vanderbilt Medical Centre, USA and Dr. Thilo Stehle & Ms. Eva Kirchner from University of Tubingen, Germany for providing protein samples for the experiments as well as for helpful discussions. I would also like to thank Dr. Yoshimi Takai from Osaka University for generously providing recombinant nectin-1 fusion protein. I would also like to thank Prof. Birgit Lane and Prof. Gunaretnam Rajagopal for their support.

I would like to thank National University of Singapore for providing me with a research scholarship as well as excellent research and recreational facilities. I would also like to acknowledge the Biomedical Research Council, Singapore for funding my research work.

I would also like to thank my friends Dr. Karthik, Dr. Dev Kumar, Dr. Sambit and Dr. Subha Narayan for making my stay in NUS delightful. Last but not the least I am grateful to my parents, brother and sister for their unconditional love and unwavering support throughout.

Table of Contents

Summary

Cell adhesion is one of the most important and basic biological phenomenon that is essential for cells to not only survive and proliferate but also to organize themselves into complex and better functional units. Cell adhesion allows adherent cell types like epithelial cells to form monolayers that not only act as barriers to invading pathogens but also regulate solute and solvent diffusion. The solute transport is not only regulated by the cells themselves but also by the intercellular adhesion proteins that hold these cells together. However, these intercellular adhesion proteins are not passive mechanical barriers to solutes but are highly dynamic, organized complexes that also regulate cellular processes such as proliferation, differentiation and migration. The expression, distribution and functions of these cell adhesion proteins are significantly affected by mechanical, chemical and biological stimuli coming from the surroundings. Apart from their normal physiological roles, several cell adhesion molecules also act as receptors for a variety of bacteria, viruses and several other pathogens. Furthermore, different cell adhesion molecules are bestowed with different structural, adhesive and kinetic properties so that they can serve different physiological functions. In this dissertation, the adhesion kinetics of specific intercellular adhesion proteins localizing at adherens junctions and tight junctions (nectin-1 and JAM-A) were elucidated using single molecule force spectroscopy. Also the effect of mechanical strain on the expression and localization of specific tight junction proteins was investigated. Results show that multiple binding configurations of homophilic nectin-1 interactions exist. Also, the relatively long bond half life of nectin-1 mediated interactions when compared to initial E-cadherin interactions provides a strong biophysical support for their role in initiating intercellular

adhesion. On the other hand, homophilic JAM-A interactions were found to be highly dynamic in nature. Such dynamic interactions provide a biophysical basis for the role of JAM-A in regulating paracellular diffusion of solutes as well as in trans endothelial migration of leukocytes. The interactions of the reovirus attachment protein sigma-1 with JAM-A (which acts as a cell receptor for sigma-1) were found to be kinetically more stable than homophilic JAM-A interactions and probably help the virus in attaching itself firmly to the cell. Finally, application of external mechanical strain was found to increase occludin expression and inhibit proliferation rate in MDCK cells. The increase was also associated with destabilization and re-localization of the tight junction adaptor protein ZO-2 from intercellular boundaries into the cytoplasm and nucleus. This strongly suggests that the tight junction complex plays an important role in regulating and modulating cellular response to external mechanical strain. The results provide an insight into the adhesive and mechanotransduction properties of specific intercellular adhesion molecules.

List of Tables

List of Figures

List of Symbols

k_B	Boltzmann constant
k_c	Spring constant of cantilever
k(f)	Dissociation rate under an acting force ‘f’
k_{off}	Unstressed dissociation rate
k_{eff}	Effective spring constant of the cantilever-molecular linker assembly
p(f)	Probability of the rupture of a bond under an acting force ‘f’
r_f	Loading rate
v	Retraction velocity of cantilever
x_β	Reactive compliance
$t_{1/2}$	Bond half life

Journal Publications & Book Chapters

Lim TS, **Vedula SRK**, Hunziker W, Lim CT, *"Kinetics of adhesion mediated by extracellular loops of Claudin-2 as revealed by single molecule force spectroscopy",* Journal of Molecular Biology, Vol. 381, Issue 3, pp. 681-691, 2008.

Lim TS, **Vedula SRK**, Shi H, Kausalya PJ, Hunziker W, Lim CT, "*Probing Effects of pH change on Dynamic Response of Claudin-2 Mediated Adhesion Using Single Molecule Force Spectroscopy*", Experimental Cell Research, 2008 Vol. 314, Issue 14, pp. 2643-51.

Vedula SRK, Lim TS, Hunziker W, Lim CT, "*Mechanistic insights into physiological functions of cell adhesion proteins using single molecule force spectroscopy*", Molecular & Cellular Biomechanics, 2008 Vol. 5, No. 3, pp.169-182.

Vedula SRK, Lim TS, Kirchner E, Guglielmi KM, Dermody TS, Stehle T, Hunziker W and Lim CT, *"A comparative molecular force spectroscopy study of homophilic JAM-A interactions and JAM-A interactions with Reovirus attachment protein sigma-1",* Journal of Molecular Recognition, Vol. 21, Issue 4, pp. 210-216, 2008.

Lim TS, **Vedula SRK**, Jaya Kausalya P, Hunziker W, Lim CT, *"Single Molecular Level study of Claudin-1 mediated adhesion"*, Langmuir (2008), Vol. 24, pp. 490-495.

Vedula SRK, Lim TS, Kausalya PJ, Lane B, Rajagopal G, Hunziker W, Lim CT, *"Quantifying forces mediated by integral tight junction proteins in cell-cell adhesion"*, Experimental Mechanics, 2008. (In press)

Vedula SRK, Lim TS, Hui S, Kausalya PJ, Lane EB, Rajagopal G, Hunziker W, Lim CT *"Molecular force spectroscopy of homophilic nectin-1 interactions"*, Biochemical and Biophysical Research Communications (2007), Vol. 362, Issue 4, pp. 886-892.

Vedula SRK, Lim TS, Rajagopal G, Hunziker W, Lane B, Sokabe M, Lim CT *"Role of External Mechanical Forces in Cell Signal Transduction"* , Biomechanics at micro- and nano-scale levels, World Scientific, Singapore, 2007.

Chong KF, Loh KP, **Vedula SRK**, Lim CT, Sternschulte H, Steinmuller D, Sheu FS, Zhong YL, *"Cell adhesion properties on photochemically functionalized diamond"*, Langmuir (2007), Vol. 23, pp. 5615-5621.

Lim CT, **Vedula SRK**, Lim TS, Kausalya PJ, Gunaretnam R, Hunziker W. *"Molecular interactions of tight junction proteins in cell-cell interaction"*, Journal of Biomechanics, 39, Supplement 1 (2006): S241

Lim CT, Zhou EH, Li A, **Vedula SRK,** Fu HX, "*Experimental techniques for single cell and single molecule biomechanics*", Materials Science and Engineering C: Biomimetic and Supramolecular Systems, Volume 26, Issue 8 , September 2006, Pages 1278-1288

Vedula SRK, Lim TS, Kausalya PJ, Hunziker W, Rajagopal G, Lim CT "*Biophysical approaches for studying the integrity and function of tight junctions*", Molecular & Cellular Biomechanics (2005), Vol. 2, No. 3, pp. 105-124

Conference Papers

Vedula SRK, Lim TS, Kausalya PJ, Hunziker W, Rajagopal G, Lim CT "*Quantifying inter cellular adhesion forces due to tight junction proteins*", Proceedings of the 12th International conference on Biomedical Engineering (ICBME), Singapore, 2005.

Lim C.T, **Vedula S.R.K.**, T.S. Lim., Kausalya P.J., Gunaretnam R., Hunziker W., *"Quantifying adhesion forces of tight junction proteins in cell-cell adhesion"*, Asia and Pacific workshop on Biological Physics, Singapore, 2006

Lim C.T, **Vedula S.R.K.**, T.S. Lim., Kausalya P.J., Gunaretnam R., Hunziker W., "*Molecular interactions of tight junction proteins in cell-cell adhesion",* 5th World Congress of Biomechanics, Munich, 2006

Lim TS, **Vedula SRK**, Kausalya PJ, Hunziker W, Rajagopal G, Lim CT, "*Quantifying adhesion forces of tight junction proteins*", poster presentation at the Summer Bioengineering Conference 2006, Florida.

Vedula SRK, Lim TS, Kausalya PJ, Hunziker W, Rajagopal G, Lim CT, "*Quantifying adhesion forces of tight junction proteins*", 2nd Tohoku-NUS Joint Symposium on the Future Nano-medicine and Bioengineering in the East-Asian Region, 2006, Singapore.

Vedula SRK, Lim TS, Kausalya PJ, Hunziker W, Rajagopal G, Lane EB, Lim CT, "*Molecular force spectroscopy of homophilic nectin-1 interactions*", OLS Official Opening & Conference, Singapore, Feb, 2007.

Vedula SRK, Lim TS, Kausalya PJ, Hunziker W, Rajagopal G, Lane EB, Lim CT, "*Molecular force spectroscopy of homophilic nectin-1 interactions in cell-cell adhesion*", 3rd Asian Pacific Conference on Biomechanics (AP Biomech), Tokyo, Nov, 2007.

T.S. Lim, **S.R.K. Vedula**, S. Hui, J.P. Kausalya, E.B. Lane, G. Rajagopal, W. Hunziker and C.T. Lim, "*Molecular force spectroscopy of homophilic nectin-1 interactions*",

Biochemical Society Annual Symposium - Structure and function in cell adhesion, Manchester, UK, Dec,2007.

Lim CT**, Vedula SRK**, Lim TS, Kausalya PJ, Hunziker W, Rajagopal G, Lane EB, "*Mechanical Insights into the Physiological Functions of Intercellular Adhesion Molecules*", 3rd Tohoku-NUS Joint Symposium on Nano-Biomedical Engineering in the East Asian-Pacific Rim Region, Singapore, Dec, 2007.

1 Introduction

1.1 Background

Cell adhesion is one of the most important and basic biological phenomenon that is essential for cells to not only survive and proliferate, but also to organize themselves into more complex and better functional units[1, 2]. Cell adhesion allows adherent cell types like epithelial cells to form monolayers that line several organ systems e.g. the respiratory tract, gastrointestinal tract, biliary tract and renal tract just to name a few. Apart from acting as barriers to invading pathogens, epithelial monolayers are also responsible for maintaining tissue homeostasis. They are responsible for critically regulating solute and solvent diffusion across the monolayers to maintain the internal milieu conducive for tissues to function normally. The solute transport is not only regulated by the cells themselves but also by the intercellular adhesion proteins that hold these cells together. However, these intercellular adhesion proteins are not passive mechanical barriers to solutes but are highly dynamic, organized complexes that also regulate cellular processes such as proliferation, differentiation and migration[3-5]. The expression, distribution and functions of these cell adhesion proteins are significantly affected by mechanical, chemical and biological stimuli coming from the surroundings. For suspended cell types e.g. leukocytes, adhesion is of primary importance in initiating and promoting the process of inflammation[6]. Apart from their normal physiological roles, several cell adhesion molecules also act as receptors for a variety of bacteria, viruses and several other pathogens[7-9]. Also, several diseases are associated with altered expression, distribution, structure and/or function of cell adhesion proteins either as a cause or effect[10]. Furthermore, different cell adhesion molecules are bestowed with different

structural, adhesive and kinetic properties so that they can serve different physiological functions[10]. Correlating the adhesion kinetics of specific intercellular adhesion proteins to their physiological functions and to study the effect of mechanical stimuli on cell adhesion proteins is the primary goal of this dissertation.

1.1.1 Intercellular adhesion complex in epithelial monolayers

The organization of a typical epithelial monolayer is shown in Fig. 1.1. There are two pathways for solutes to diffuse across epithelia. The *transcellular* pathway is actively regulated by the cells themselves while the *paracellular* pathway is guarded by the intercellular adhesion complex[4, 11]. The intercellular adhesion complex also stabilizes and maintains the overall architecture of the monolayer.

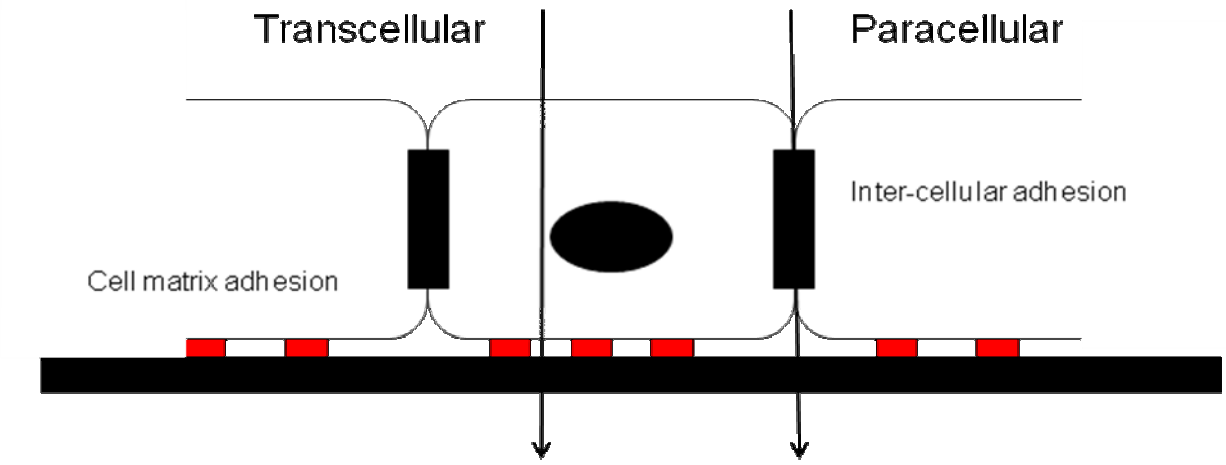

Figure 1.1 Schematic showing transcellular and paracellular pathways for solute diffusion across epithelial monolayers.

The intercellular adhesion complex can be classified broadly into four groups (Fig. 1.2)[4]:

(a) Tight junction complex: This is located at the top of the intercellular adhesion complex and forms a circumferential belt around the apical membrane of the cells. The complex itself is made up of several integral membrane proteins and their corresponding cytoplasmic adaptors. The tight junction (TJ) complex is considered the major regulator of the paracellular diffusion of solutes (gate function). The TJ complex also maintains a differential distribution of proteins (polarity) in the apical and basolateral membranes of epithelial cells by preventing diffusion of proteins. This function of TJ proteins is often referred to as the fence function. Apart from this, the cytoplasmic components of the TJ proteins are also involved in regulating the proliferation and differentiation of cells.

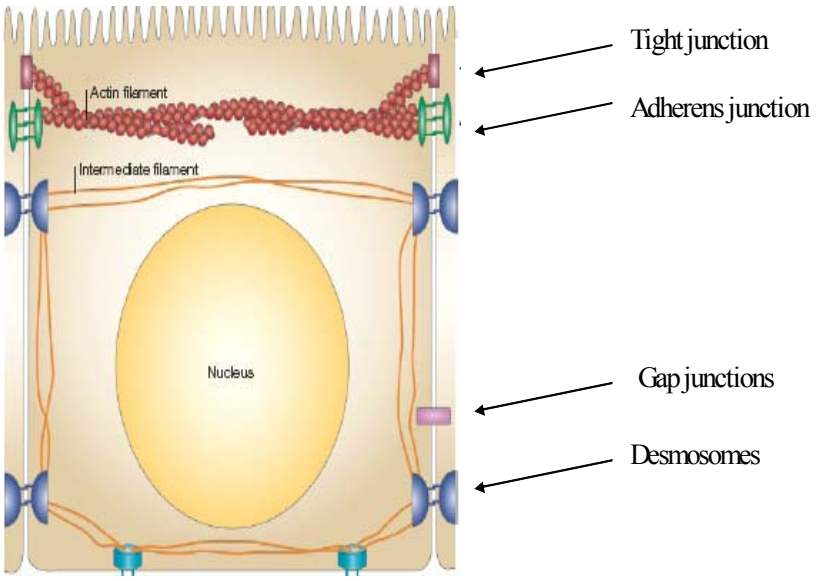

Figure 1.2 Schematic of the components constituting the intercellular adhesion complex in epithelial monolayers[4].

(b) Adherens junction complex: This complex is located just below the TJ complex. Similar to the TJ complex, adherens junction (AJ) complex is also constituted by different membrane proteins and their cytoplasmic adaptors. The primary function of AJ

complex unlike the TJ complex is to initiate, develop and maintain the adhesion between adjacent cells in the epithelial monolayer. The cytoplasmic components associated with the AJ proteins also play an important role in regulating cell proliferation.

(c) Desmosomes: Desmosomes are proteins that belong to the superfamily of cadherins and similar to E-cadherins, play an important role in providing mechanical stability to the intercellular junction. Their importance in maintaining the integrity of intercellular adhesion is evident in several diseases like pemphigus, where auto antibodies against the desmosomal protein e.g. desmogelin-1 make the epidermis very fragile leading to the formation blisters.

(d) Gap junctions: Gap junctions are proteins that provide conduits for neighboring cells to transmit signals and communicate with one another. Hemi channels of adjacent cells formed from hexamers of connexins come in contact with one another to form a complete channel that allows passage of ions and small chemical molecules.

1.1.2 Intercellular adhesion in suspended cells

The importance of intercellular adhesion in suspended cells is exemplified by leukocytes and monocytes during the process of inflammation. During inflammation, freely flowing leukocytes and monocytes in the blood are captured by the inflamed endothelial cells (Fig. 1.3)[6]. Activated endothelial cells express selectins (E-selectin and P-selectin) which can interact with their corresponding ligands present on the leukocytes (e.g. P-selectin glycoprotein ligand or PSGL). Furthermore, leukocytes also express molecules belonging to the integrin family (LFA-1 or leukocyte function associated antigen) which interact with intercellular adhesion molecule 1 (ICAM-1) thereby promoting adhesion.

While some of the adhesion molecules are involved in arresting leukocytes, others are involved in the crawling and transmigration of the leukocytes across the endothelial cell junctions (e.g. JAM-A).

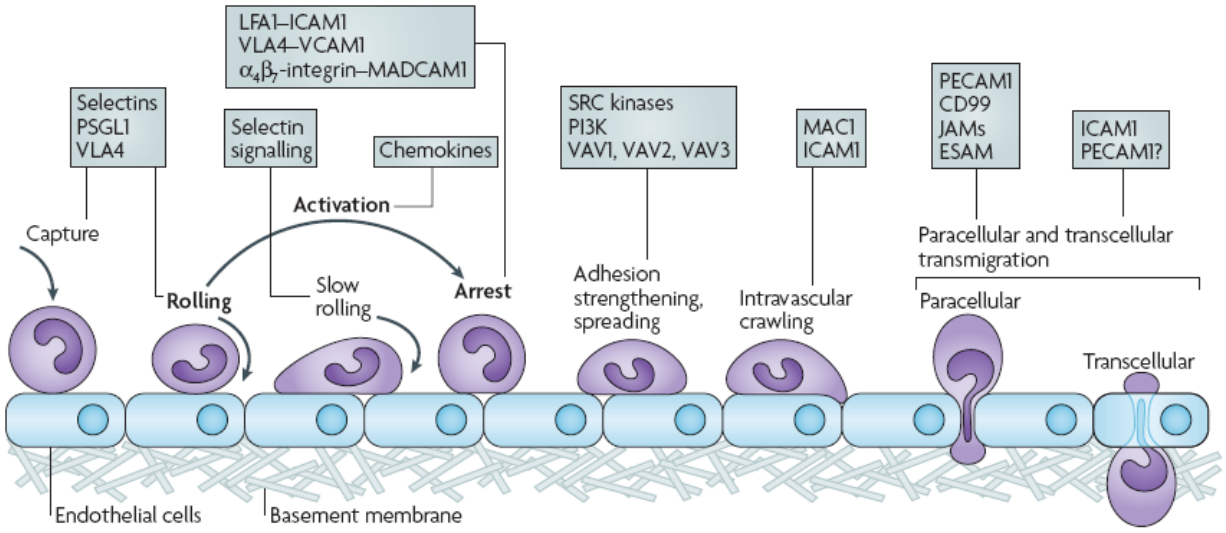

Figure 1.3 Schematic of adhesion process involving leukocytes during inflammation[6].

1.1.3 Cell-matrix adhesion

Cell matrix adhesion is mediated by a group of heterodimeric proteins called integrins. Integrins contain an α chain and a β chain (Fig. 1.4)[12]. They interact with RGD (Arginine, Glutamic acid and Aspartic acid) sequences present on ECM (extracellular matrix) proteins like collagen and fibronectin. The engagement of integrins with the ECM is the starting point for the formation of focal complexes and focal adhesion. The initial adhesion of integrins to the ECM proteins, called the focal complex, leads to their clustering and is later strengthened by recruitment of various kinases (e.g. focal adhesion kinase or FAK and Src), adaptor molecules and the cytoskeleton leading to the formation of the mature focal adhesion (FA). The FAK and Fyn/Shc pathways represent two main

signaling pathways activated by integrins. Apart from these main signaling pathways, integrins can also initiate several other signaling pathways leading to gene activation and expression[13-15]. Furthermore, externally applied mechanical forces play an important role in the maturation of the FA. This "force dependent stiffening" is a very important characteristic of integrin mediated cell substrate adhesion.

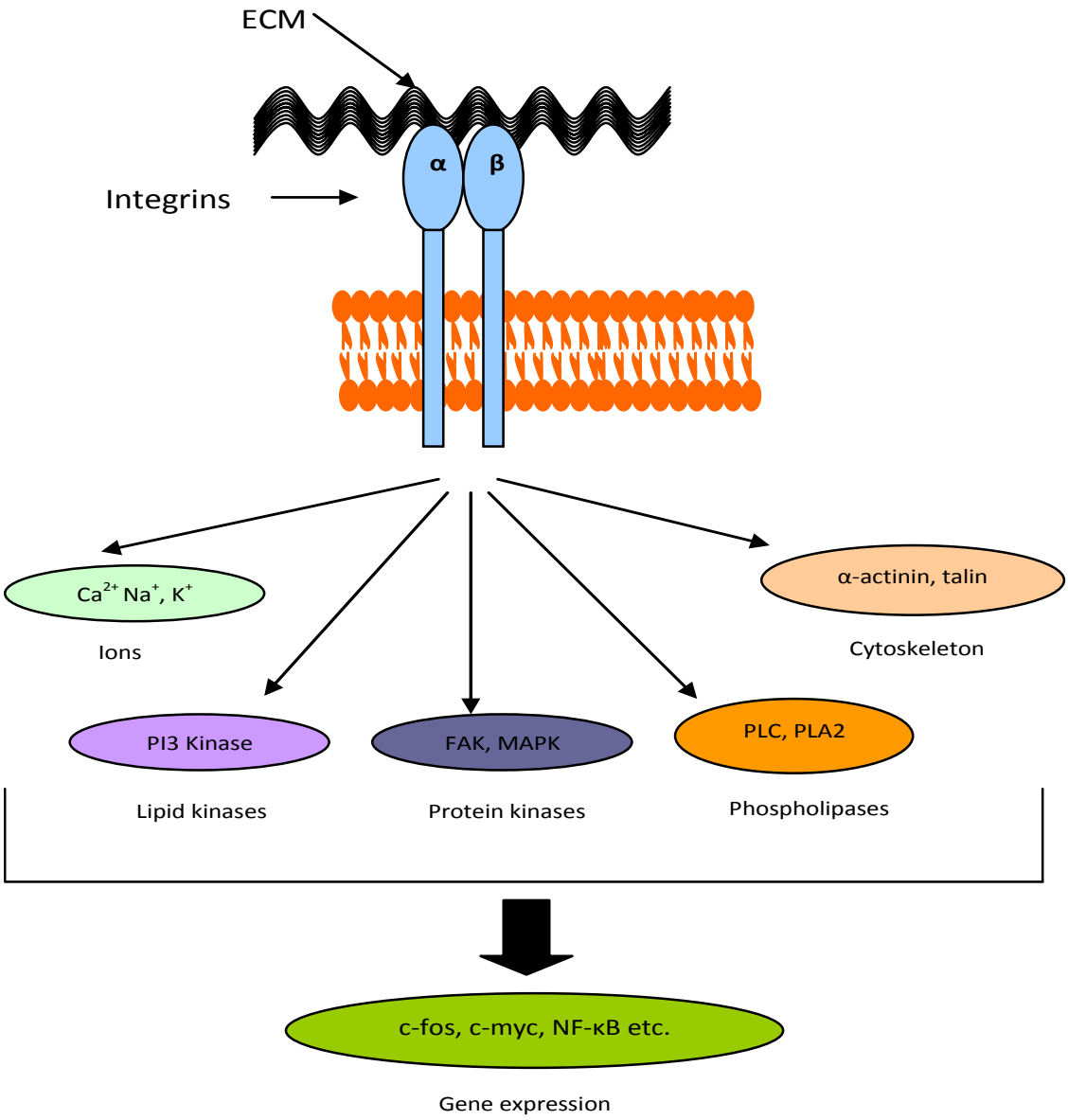

Figure 1.4 Heterodimeric integrins mediate cell-matrix adhesion. They are also important in initiating several cell signaling pathways[12].

1.1.4 Quantifying intercellular adhesion forces

Measuring the adhesion forces mediated by various cell adhesion molecules has been a topic of great interest for biologists as well as biophysicists. To this end, a number of experimental techniques have been devised for quantifying intercellular adhesion forces[16]. Initial studies could only be used for studying qualitative differences between different cell adhesion molecules. This was followed by semi-quantitative methods for estimating cell adhesion like flow chambers and centrifugation assays. Recent advances in nano-technological tools have significantly contributed to understanding and quantifying these adhesion forces in more detail. The advent of techniques based on micropipettes, optical traps and atomic force microscopy (AFM) has now enabled us to measure very weak forces, which was previously not possible. This section gives a brief overview of the different methods for estimating intercellular adhesion forces.

(a) Flow based methods: These methods are based on qualitative or semi quantitative estimation of the ability of cell adhesion to withstand shear forces. Simple washing[17, 18], shearing through fine bored needles[19], flow chambers and hydrodynamic focusing using flow cytometer[20] represent some examples of these methods. In the case of simple washing, one of the cell types labeled with a dye or radioactive substance, are incubated with a monolayer of the second type of cells. Following washing, the number of adherent cells is either counted or estimated colorimetrically. In the other methods, the cells types of interest are incubated for a specified period of time and then passed through a narrow gauge needle or a flow cytometer at different pressures. In both cases, the

number of conjugated cells (cells adherent to one another) in the effluent provides a rough estimate of the adhesion force between cells.

(b) Centrifugation methods: In these methods, the cell-cell adhesion complex is subjected to force due to centrifugation. McClay's method and Coulter counter are examples of methods that use this principle to estimate cell adhesion forces. McClay's method is similar to the washing method described above except that following incubation; the cells are centrifuged at different speeds. The centrifugal speed needed to separate 50% of adherent cells represents the index for estimating the intercellular adhesion force[21]. Alternatively, the Coulter counter is used to measure the number of single cells in suspension after a defined time period of rotation[22]. The decrease in the number of single cells in suspension with time is directly related to the strength of the cell adhesion forces. Coulter counter remains one of the most common methods currently used for qualitative estimation of intercellular adhesion.

(c) Micropipette assays: The dual micropipette assay and the biomembrane force probe utilize micropipettes for estimating adhesion forces. The step pressure technique introduced by Sung et al was the first micropipette based technique for studying cell-cell adhesion[23]. Here, one cell (right) is held tightly by a pipette by application of a large pressure. A second cell (left) is then manipulated close to this by a second pipette using a smaller suction pressure. After a specified period of contact, the left pipette is withdrawn away. If the adhesion force is stronger than the applied pressure, the cell slips away. The pressure in the left pipette is then increased step wise till it is sufficient enough to pull the left cell away from the right one[24].

(d) Optical trap method: The underlying principle of optical tweezers is the use of laser power to 'trap' cells or small beads attached to the cells. Prior calibration can give a correlation between laser power and the force that it produces. Using this knowledge, the adhesion forces needed to detach a cell from a substrate or another cell can then be computed[25].

(e) Magnetic bead method: In this method, cells are allowed to internalize small ferromagnetic beads. The internalized beads are subjected to a force using an externally applied magnetic field. The force on the beads is transmitted to the adherent cells and causes their separation.

(f) Atomic force microscopy: Dynamic force spectroscopy or single molecule force spectroscopy (SMFS) is a special application of the atomic force microscope. It has been used extensively to study protein unfolding, protein-protein[26], protein-cell[27] and cell-cell interactions[28]. There are two main advantages of SMFS over other currently available techniques. Firstly, the interactions can be studied under physiological conditions since the AFM allows the experiments to be performed on living cells. Secondly, the biophysical nature and adhesion kinetics of a given interaction can be probed at the level of single molecule.

Though several groups have explored the adhesion kinetics of a number of adhesion proteins like e-cadherins and selectins; details of interaction kinetics of a large number of intercellular adhesion molecules remain unknown. One of the main goals of this project is to elucidate and understand the interaction kinetics of some of the proteins localizing at the adherens junctions and tight junctions. This would not only help us in understanding

the physiological functions of these proteins in more detail but also hopefully guide us in developing and testing better methods for drug delivery across epithelial monolayers.

1.1.5 Cell adhesion proteins and mechanical stimuli

It has been observed that the expression and distribution of several cell adhesion molecules can be significantly influenced by stimuli coming from the surroundings. These stimuli include biological molecules, chemicals, toxins and mechanical forces[29-31]. Furthermore, different cell types respond in different ways to these stimuli. The influence of external stimuli, in particular mechanical stimuli, on endothelial cells lining blood vessels and epithelial cells lining the respiratory, gastrointestinal and urinary tract has been of intense research focus[30, 32-38]. This is due to its relevance to understanding normal physiological functions as well as the pathogenesis of several diseases. Endothelial cells are continuously subjected to mechanical strain with each heart beat, epithelial cells lining the alveoli in the lungs are stretched during inspiration, and epithelial cells lining the gastrointestinal tract and renal tract undergo mechanical strain during peristalsis. Cells have evolved over time to respond to these strains in a favorable manner. However, during the course of several diseases processes, the amount of mechanical strain on these cells can alter significantly leading to disruption of physiological functions. For example, alveolar epithelial cells can be subjected to excessive mechanical strains during artificial ventilation. Large pressures and strains can build up in the gastrointestinal and renal tracts when they get obstructed due to underlying pathology. It is only logical to assume that mechanical strains, both

physiological and pathological, would also significantly affect the intercellular adhesion complex and its functions.

Few experiments have been carried out previously to study the effect of mechanical strain on expression and localization of cell adhesion proteins as well as tight junction integrity in endothelial cells and respiratory epithelial cells[30, 39]. However, studies of a similar nature have never been done on renal epithelial cells. To study the effect of mechanical strain on the proliferation rate of renal epithelial cells, tight junction integrity and to correlate it with changes in the expression and localization of tight junction proteins is another important focus of this project.

1.2 Objectives and Scope of work

Considering that little work as been done to understand the adhesion kinetics of several intercellular adhesion proteins and elucidating their role in shaping the response of cells to mechanical stimuli, the main objectives of this study are to:

(a) Study the interaction kinetics of some of the proteins (nectin-1 and JAM-A in particular) localized at the adherens junction and tight junctions and correlate the kinetic parameters to their physiological functions.

(b) Study the effect of mechanical strain on cell proliferation rate and correlate it to the expression of tight junction proteins (occludin, JAM-A, ZO-1 and ZO-2) in renal epithelial cells.

It is expected that the results would provide us with a deeper understanding of the physiological functions of cell adhesion proteins and their role in regulating cellular

response to mechanical strain. To fulfill these objectives, the following experiments were carried out:

(a) Molecular force spectroscopy using AFM to study the interaction kinetics between two representative proteins at the adherens junctions (nectin-1) and tight junctions (JAM-A).

(b) Design and calibration of a cell stretching device that can apply uniform circumferential strain to epithelial monolayers.

(c) Immunofluorescence staining, western blotting and confocal microscopy to study the effect of mechanical strain on cell proliferation rate and expression levels of occludin, JAM-A, ZO-1 and ZO-2 in renal epithelial cells.

2 Literature Review

2.1 Structure, organization and functions of Adherens Junctions

Adherens junctions are probably the most important component for stabilizing the epithelial intercellular adhesion complex[40]. Proteins localizing at adherens junctions are not only important for initiating cell adhesion but also in stabilizing it. The two most important proteins localizing at adherens junctions are nectins and E-cadherins[41]. While nectins have been shown to be important for initiating cell adhesion, E-cadherins are important for cementing and stabilizing the adhesion[41]. The adherens junction proteins are associated with several transcription factors and are also linked to the cytoskeleton via adaptor molecules[42]. Previous work suggests that a strong functional and physical relation exists between the E-cadherin and nectin mediated adhesion systems[43]. Though the functional association between the two adhesion systems is well established, the physical association is not well understood till now.

2.1.1 E-cadherins

E-cadherins belong to the cadherin superfamily of proteins that contains >80 related proteins. They are amongst one of the oldest groups of cell adhesion molecules to have been discovered. The adhesion mediated by these proteins is characteristically dependent on the presence of Ca^{2+} ions[44].

Structurally, E-cadherin has been shown to have five extracellular domains, a short transmembrane region and a cytoplasmic tail (Fig. 2.1) [45]. The cytoplasmic tail interacts with β-catenin which interacts with α-catenin. α-catenin in turn links it to the

actin cytoskeleton[46]. There are pockets in between the extracellular domains for the binding of Ca^{2+} ions. The presence of Ca^{2+} is essential for the E-cadherin molecules to attain a conformation that is optimal for interacting with E-cadherin molecules from the neighboring cells[47].

The cell adhesion activity of E-cadherins is well established at the cellular level. L-cells transfected with E-cadherins have been shown to aggregate into clumps. It has also been shown that this adhesion is abolished by chelating Ca^{2+} from the medium[48]. Furthermore, micropipette based studies on E-cadherin transfected L-cells have also enabled us to quantify these adhesion forces[44].

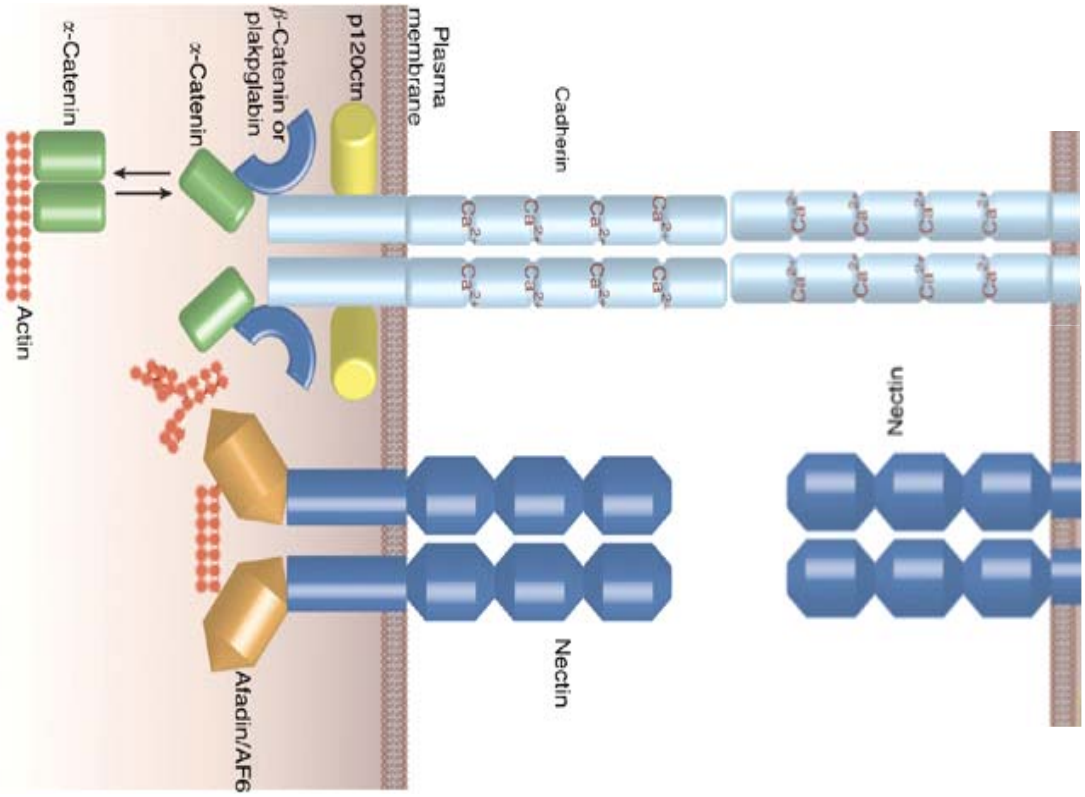

Figure 2.1 Schematic depiction of the adherens junctions. Extracellular domains of cadherins and nectins of adjacent cells interact with each other to form the junction. On the cytoplasmic end, they associate with adaptor molecules and actin filaments[49].

2.1.2 Nectins

Nectins belong to the immunoglobulin (Ig) superfamily of proteins and are characterized by their Ca^{2+} independent adhesion activity. They were first discovered as Polio virus Receptor Related (PRR) proteins[50-52]. However, later they were found to act as a receptor for infection by herpes group of viruses and not by polio virus[53]. Their role as an important and separate intercellular adhesion system from the E-cadherins has only recently been established[54].

Four different types of nectins have been discovered to date: Nectin-1, -2, -3, and -4. Nectins are highly conserved from humans to rodents[41]. Structurally, nectins contain three extracellular immunoglobulin-like loops, a short transmembrane region and a cytoplasmic tail (Fig. 2.1). The cytoplasmic tail contains a conserved Glu/Ala-X-Tyr-Val motif in most nectins. This motif binds the PDZ domain containing protein afadin. Afadin is the cytoplasmic adaptor molecule that links the cytoplasmic tail of nectins to the actin cytoskeleton. Nectins are ubiquitously expressed in several different cell types like fibroblasts, epithelial cells, B-cells, monocytes and neurons[41].

All nectins undergo homophilic *cis*-dimerization followed by homophilic *trans*-dimerization. Though heterophilic *trans*-dimerization has been observed for some nectin pairs e.g. nectin-1/nectin-3 and nectin-2/nectin-3, however, heterophilic *cis*-dimerization has not been observed. Studies using point and truncated mutants have shown that *cis*-dimerization is essential for *trans*-dimerization but not vice versa. It has also been shown that the first Ig loop is necessary for *trans*-dimerization while the second Ig loops is

essential for *cis*-dimerization. Furthermore, association of the cytoplasmic tail of nectin with afadin is not necessary for either *cis*- or *trans*- interactions between nectins.

Micropipette and centrifugation based assays have shown that transfection of nectins into L-fibroblasts causes an increase in adhesion force[55]. It has also been shown that the adhesion force imparted by nectins is much lower than that mediated by E-cadherins. Studies on L-cells stably transfected with E-cadherin and nectins show that nectin-1 or nectin-2 can recruit E-cadherin to the nectin based adhesion sites[56]. Also, over expression of nectins in L-cells has shown to increase the rate of formation of adherens junctions[57].

2.2 Structure, organization and functions of Tight Junctions

Tight junctions (TJs) are group of transmembrane proteins and their corresponding cytoplasmic adaptor molecules that form the most apical component of the intercellular adhesion complex[4]. The transmembrane proteins from adjacent cells come in contact with one another to form an apical belt that regulates not only paracellular diffusion of solutes but also maintains the polarity of epithelial cells by preventing some of the proteins in the apical membrane from diffusing into the basal membrane. These two functions of TJs are referred to as the ‘gate’ function and ‘fence’ function respectively[58].

2.2.1 Occludin and Claudins

Occludin and claudins are proteins that traverse the cell membrane four times forming two extra-cellular loops (Fig. 2.2)[59, 60]. The extracellular loops of these

transmembrane proteins on adjacent cells come into contact with each other forming the actual paracellular diffusion barrier.

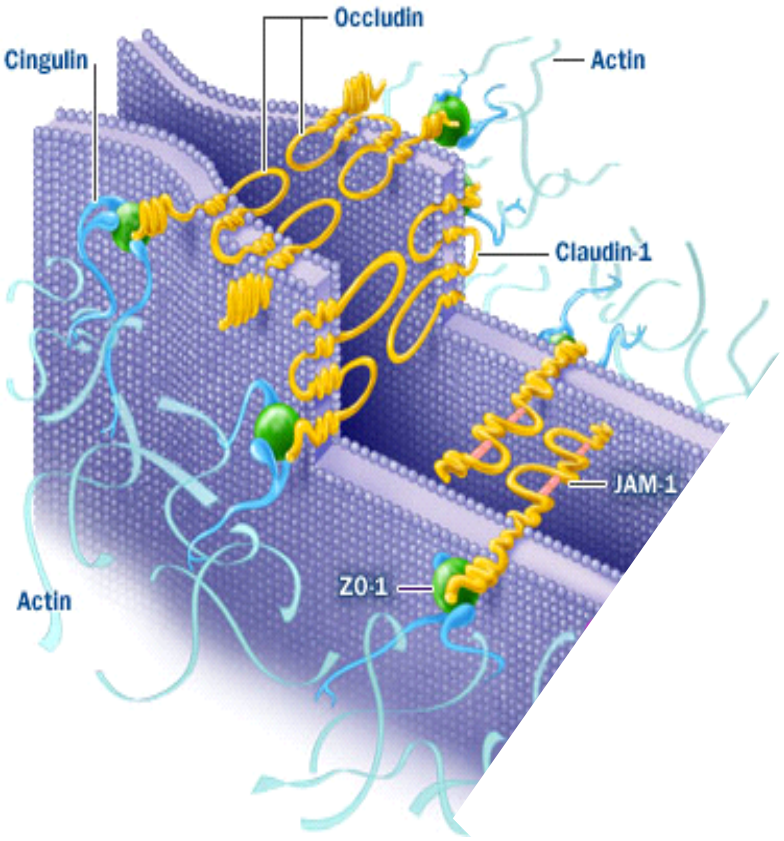

Figure 2.2 Schematic depiction of the tight junctions. Claudins and occludin possess two extracellular loops and four transmembrane segments. The extracellular loops from adjacent cells come together to form channels for solute diffusion. JAMs possess two extracellular immunoglobulin-like loops that undergo trans-interactions. (http://www.nastech.com).

On the other hand, the cytoplasmic tail interacts with adaptor, regulatory and transcription factors that link the transmembrane proteins to the actin cytoskeleton and are also important in the bidirectional signal transduction between the tight junctions and cell interior[61]. Occludin was the first discovered transmembrane TJ protein and was isolated from chick livers. As it could only be extracted using detergent, this suggested

that it was an integral membrane protein. Cloning and sequencing studies revealed that the protein was 504 amino acids long with molecular weight of 55.9kD[59]. The first and second extra-cellular loop and its C-terminal are considered to be extremely important for occludin mediated cell adhesion and localization, respectively[62, 63]. The C-terminal is linked to the actin cytoskeleton by ZO family of proteins. Occludin has quantitatively been well associated with barrier properties of tissues. Tissues that are less permeable have shown to have higher content of occludin as compared to more permeable tissues[64, 65]. In spite of this correlation, occludin expression is neither sufficient nor necessary for the formation of intact TJ strands or paracellular barrier function. Formation of TJ strands in occludin-deficient mice has led to the discovery of claudins[60, 66]. Also first discovered in chick livers, there are now about 24 types of claudins constituting the claudin gene family in mammals. In spite of having four transmembrane domains like occludin, they share no sequence similarity. These proteins have a molecular weight in the range of ~25kD. All claudins have been shown to have a C-terminal YV (except claudin-16, which has a type I TRV) PDZ-binding motif that is important for the interaction with the PDZ domain of the "cytoplasmic plaque" proteins like ZO group of proteins. Claudins associate laterally with each other to form the strands even in the absence of Ca^{2+}[48]. These associations can be homo- or heterogenic, but in the case of heterogenic interactions, only certain combinations are possible[67].

2.2.2 Junctional Adhesion Molecules (JAM)

JAM belongs to the immunoglobulin superfamily and in contrast to claudins and occludin, only spans the membrane once[68]. Apart from endothelial cells and epithelial

cells, JAM family members are expressed on leukocytes and platelets[69, 70]. JAMs belong to the immunoglobulin (Ig) superfamily and are implicated in tight junction formation[71], monocyte transmigration[68], platelet activation[70], angiogenesis[72, 73], and attachment of mammalian reovirus[8]. The JAM family includes JAM-A, JAM-B, JAM-C, JAM-4, and JAML proteins.

Structurally, all JAM proteins contain an N-terminal signal peptide, an extracellular region composed of two Ig-like domains (a membrane-distal, N-terminal D1 domain and a membrane-proximal, C-terminal D2 domain), a single membrane-spanning domain and a short cytoplasmic tail (Fig. 2.2)[74]. The cytoplasmic tail interacts with PDZ domain-containing scaffolding proteins including ZO-1, while the D1 domain interacts with the D1 domain of an opposing JAM-A molecule to form physiologically relevant homodimers[74, 75].

JAM-A was first discovered as an antigen on platelets for the F11 monoclonal antibody; engagement of platelets by F11 mediates granule release, fibrinogen binding, and aggregation[76]. JAM-A was subsequently found to localize at regions of intercellular contact in epithelial and endothelial cell tight junctions. While JAM-A is capable of undergoing only homophilic interactions within the JAM family, JAM-B and JAM-C are capable of both homophilic and heterophilic interactions with each other. Support for JAM-A-mediated homophilic adhesion comes from the observation that transfected CHO cells show localization of JAM-A to regions of cell-cell contact formed between transfected cells[77]. It has previously been shown that JAM-A plays an important role in regulating tight junction permeability in epithelial monolayers. Furthermore, a

monoclonal antibody J10.4 that binds to the dimer forming interface of JAM-A, has been shown to significantly delay the recovery of the tight junction barrier formation[71, 78]. On the other hand, inhibition of monocyte transmigration by monoclonal antibody BV11which binds JAM-A dimers, strongly suggested that JAM-A mediated interactions between monocytes and endothelial cells are important for transmigration[68]. However, recent experiments have demonstrated that only endothelial JAM-A is necessary for leukocyte transmigration[79]. Since, JAM-A can undergo heterophilic interaction with leukocyte function associated antigen-1 (LFA-1, $\alpha_L\beta_2$ integrin) expressed on neutrophils and T-lymphocytes, this means that a complex interaction of heterophilic and homophilic interactions mediated by JAM-A could be involved in leukocyte transmigration[80].

2.3 Single Molecule force spectroscopy using AFM

Atomic force microscope (AFM) belongs to a family of devices commonly referred to as Scanning Probe Microscopes (SPM). Scanning tunneling microscope (STM) was the first SPM to be invented and was able to image conducting as well as semi conductor surfaces with atomic resolution. The ability of AFM to operate in fluid environment has revolutionized high resolution imaging of biological samples like cells and tissues.

2.3.1 Working principle and applications of AFM

The first AFM built by Binnig et al consisted of a highly flexible cantilever with a sharp tip whose deflections during scanning of a substrate were monitored using an STM. The cantilever was made up of a thin foil of gold while the tip was made from diamond (Fig. 2.3)[81]. The newer AFMs, however, use the “optical lever” method instead of an STM to detect the deflections of the cantilever. The optical lever method consists of a laser

reflecting from the surface of the cantilever onto a split photodiode (Fig. 2.4). A piezoelectric scanner allows the relative distance between the tip and the surface to be controlled with nanometer resolution[82]. The deflections of the cantilever, as it scans the surface of interest, cause a change in the position of the reflected laser on the photodiode. A change in position of the laser spot causes a change in the relative current signal from the different segments of the photodiode.

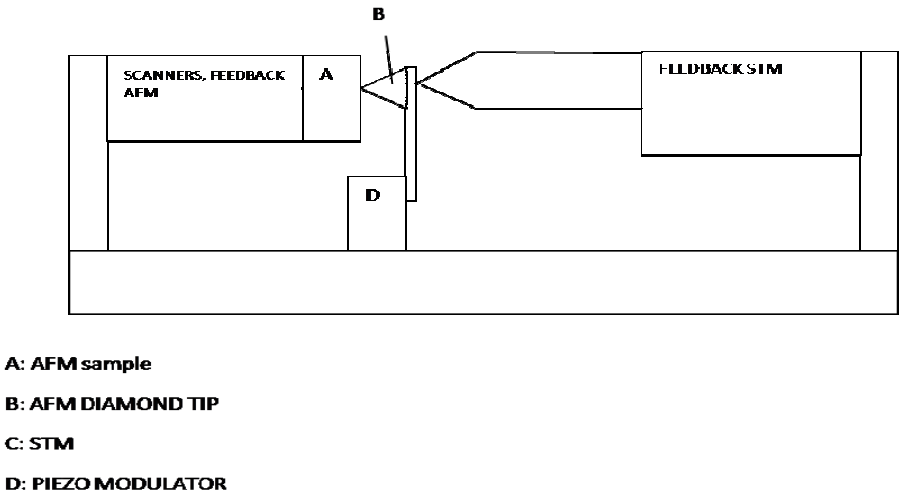

Figure 2.3 Schematic depiction of the first Atomic Force Microscope constructed based on the scanning tunneling microscope[81].

For example, for a photodiode containing two segments that give signals X and Y respectively, the net signal measured is given by (X-Y)/(X+Y)(Fig. 2.5)[45]. When the cantilever shows no deflection, the signal from both the segments is equal causing them to cancel out. When the cantilever shows no deflection, the signal from both the segments is equal causing them to cancel out. When the cantilever deflects, the signal from one of the segments is more than the other depending on which direction the cantilever deflects.

Since the photodiode essentially measures a change in the signal (voltage or current) due to the laser spot, it become necessary to calibrate the change in the signal for a given amount of deflection of the cantilever. This calibration is done by allowing the cantilever to press against a hard substrate mounted on a piezoelectric scanner and the constant is referred to as the deflection sensitivity of the cantilever (explained in detail in chapter 3).

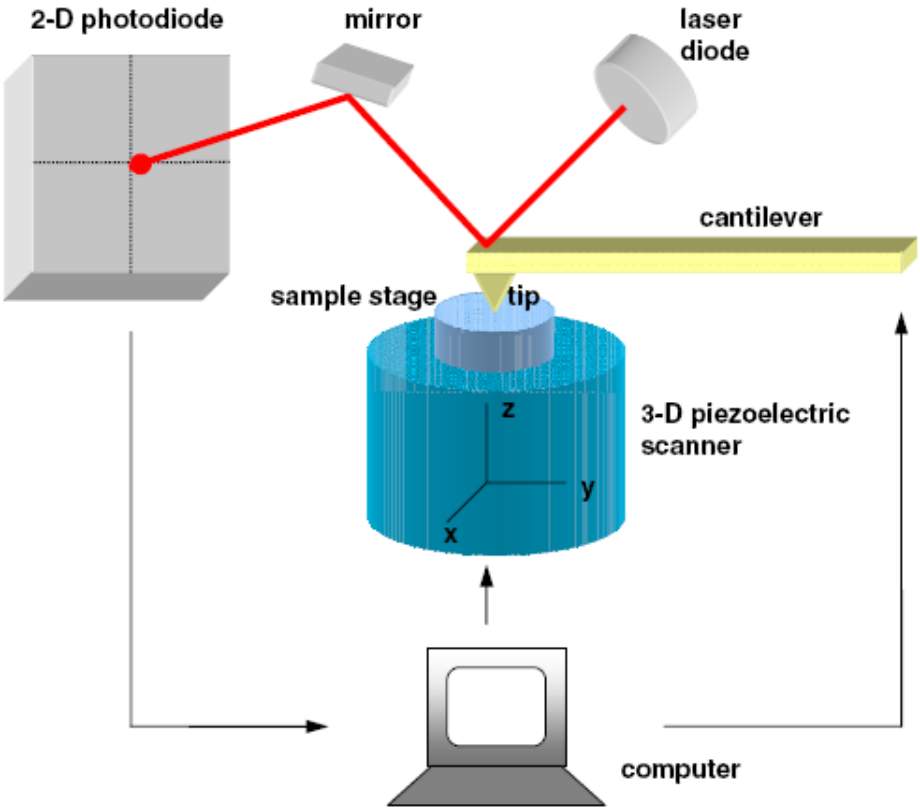

Figure 2.4 Schematic depiction of the components and working principle of modern AFM[24].

The deflection sensitivity of the cantilever is usually measured in mV/nm. Typically, soft cantilevers have high deflection sensitivity while stiff cantilevers show low deflection sensitivity. Data obtained from the movement of the piezoelectric scanner and the

cantilever deflection is used for reconstructing the topography of the scanned surface with high resolution.

The principle application of AFM in biology, for a long time, has been for imaging sample surfaces. High resolution imaging of biological surfaces using AFM, unlike scanning electron microscopy, has the distinct advantage that it can be carried out in fluid. Also sample preparation techniques are relatively simpler for imaging using AFM. Finally, AFM is capable of imaging live cells and allows us to monitor the dynamic changes occurring on cell membranes in response to various stimuli.

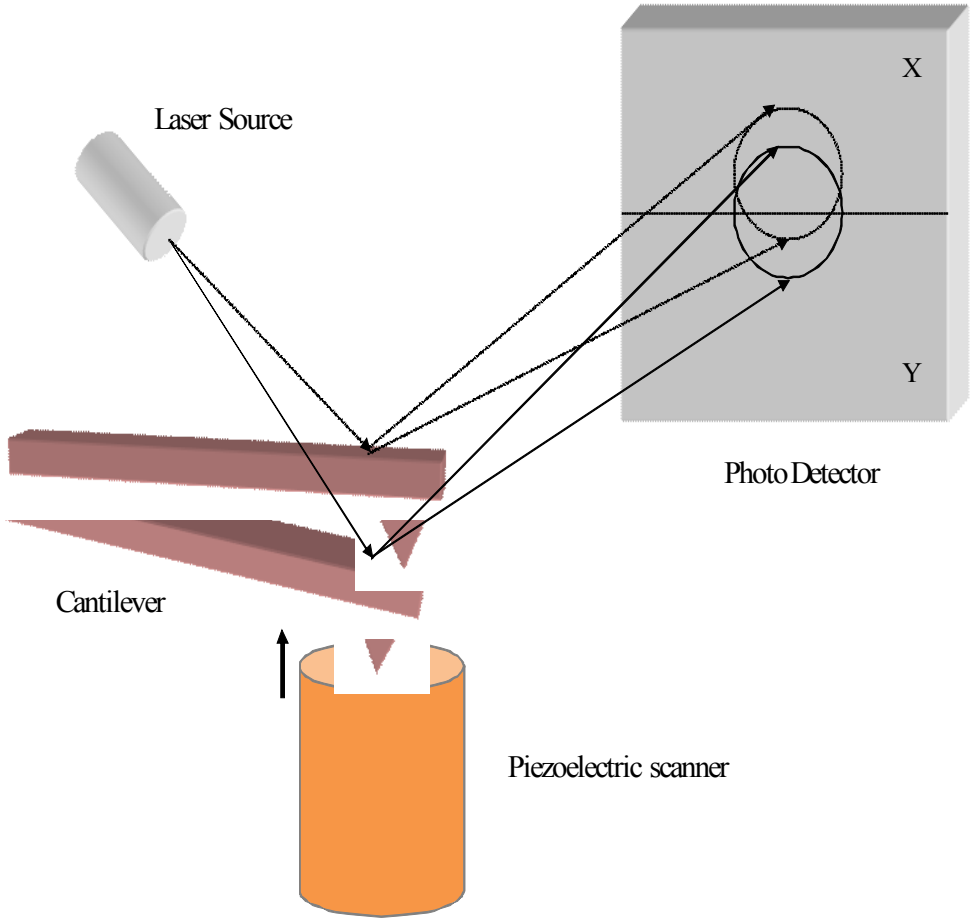

Figure 2.5 Schematic depiction of the principle of split photodiode and optical lever technique used in modern AFM.

Recently, AFM has emerged as a powerful tool for studying molecular interactions at the level of single molecule. In this mode of application of AFM, also called single molecular force spectroscopy or dynamic force spectroscopy, a protein or cell of interest is coupled to the cantilever tip using different strategies[83-85]. The cantilever is then made to approach a surface containing the other interacting protein or cell. After allowing contact for a defined time period at a defined contact force, the cantilever is made to retract at a predefined velocity. During the retraction process, bonds formed between the proteins or cells rupture. The changes in the characteristics of bond rupture events over a spectrum of applied loading rates are analyzed to extract the kinetic nature of the interaction under investigation[10].

2.3.2 Methods for functionalizing AFM tips

As mentioned in the previous section, single molecule force spectroscopy is a specialized application of the AFM in which the cantilevers are cross linked with proteins, molecules or even cells to study their interactions with ligands of interest. Such studies not only provide us with a wealth of information regarding the biophysical nature of different types of molecular interactions, but also give an insight into how these properties correlate to the physiological functions mediated by them.

One of the most important issues that needs to be addressed in SMFS experiments is the efficient and proper coupling (also called functionalization) of the molecule or cell of interest to the cantilever. A number of strategies have been developed for functionalizing cantilevers. However, there are several basic guidelines that have to be followed to assess the suitability of a given functionalization procedure[86]. First and foremost, the binding

strength of the molecule/protein to the cantilever should be much larger than that of the interactions being probed. Hence, it is preferable to covalently link the molecules to the cantilevers whenever possible. Other strong linkages like biotin/avidin and antigen/antibody interactions could also be used[83]. Secondly, the molecule or protein should have sufficient mobility following the linking procedure that will increase the probability of the interacting domains to come in contact with one another. For this purpose, several long flexible linkers or spacers are used. The linkers can be homobifunctional or heterobifunctional having reactive chemical groups on their ends for cross linking with proteins. One of the most commonly used spacer is PEG (polyethylene glycol) linker, the length of which can vary from 10nm to 30nm. Another common strategy employed to maintain proper orientation of proteins cross linked to cantilevers is to use fusion proteins. This would ensure that there is no interference for the functional domains to interact with one another. Proteins are expressed as fusion chimera with Fc fragment of human immunoglobulin[83], GST (glutathione-S-transferase)[87], histidine tag[88] or biotin. Thirdly, non-specific adsorption to the cantilevers should be minimized as much as possible. To prevent such non-specific protein adsorption, cantilevers are usually blocked in bovine serum albumin (BSA) prior to experiments. Finally, the concentration of the protein molecules on the cantilever and the substrate has to be optimal. This optimization is necessary because excessive protein can promote formation of multiple bonds (which can lead to incorrect characterization of the biophysical characteristics of a particular interaction) while a very low concentration can provide insufficient data. In view of the above requirements, surface modification of cantilevers using gold or silanizing agents have evolved as the major procedures for

functionalization. In the first method, advantage is taken of the strong chemisorption of thiols onto gold surfaces. In the second method, silanizing agents are used to introduce free amino groups onto the cantilever surface which can then be further cross linked using different strategies.

In the gold–thiol based functionalization method, the first step is to coat the cantilever with a thin layer (20-30 nm thick) of gold. This is usually achieved by thermal evaporation of an adhesive layer of chromium or titanium followed by deposition of gold. The gold surface can in turn bind to molecules containing thiol or sulfhydryl (-SH) groups with a strong affinity[89]. Thiol groups can be easily generated in protein molecules containing cysteine residues by cleaving them with suitable chemical reagents e.g. mercaptoethylamine hydrochloride (Fig. 2.6c). This method is highly suitable for coupling antibodies because of the presence of several disulfide linkages in antibodies[90]. Alternatively, N-Succinimidyl-S-acetylthiopropionate (SATP) can be used to generate protected thiol groups on proteins of interest. One end of SATP binds to free primary amines on the protein. The protected thiol groups on the other end can be made reactive by treatment with hydroxylamine[91]. The reactive thiol groups can crosslink with other thiol containing molecules (PEG linker or cleaved antibodies) to form a strong disulfide linkage. Furthermore, heterobifunctional flexible polymer linkers containing free thiol groups on one end and another functional group (carboxylic acid, amino or nickel-nitrilotriacetate) on the other can be used as spacers for attaching the molecule of interest. While carboxylic acid and amino terminating functional groups can be cross linked to free amino and carboxylic acid groups on the protein of interest using

EDC/NHS cross linker (Fig. 2.6b), nickel-nitrilotriacetate (Fig. 2.6a), can be used to bind to free histidine tags on proteins[88].

In the silanization based functionalization methods, free amino groups are first introduced on the silicone nitride cantilever surface directly by either vapor phase or liquid phase deposition of silanes. One of the most commonly used silanizing agent is APTES (3-aminopropyl triethoxysilane). For vapor phase deposition, cantilevers are kept in a dessicator along with triethanolamine for 2 hours[90]. For liquid phase deposition, cantilevers are immersed in a solution of APTES in acetone[84]. In either case, the free amino groups (-NH2) introduced on the cantilever surface can then be cross linked to the free carboxylic acid groups or amino groups(Fig. 2.7a&b) present on the protein or on PEG spacers using cross linkers like EDC/NHS or BS^3[92].

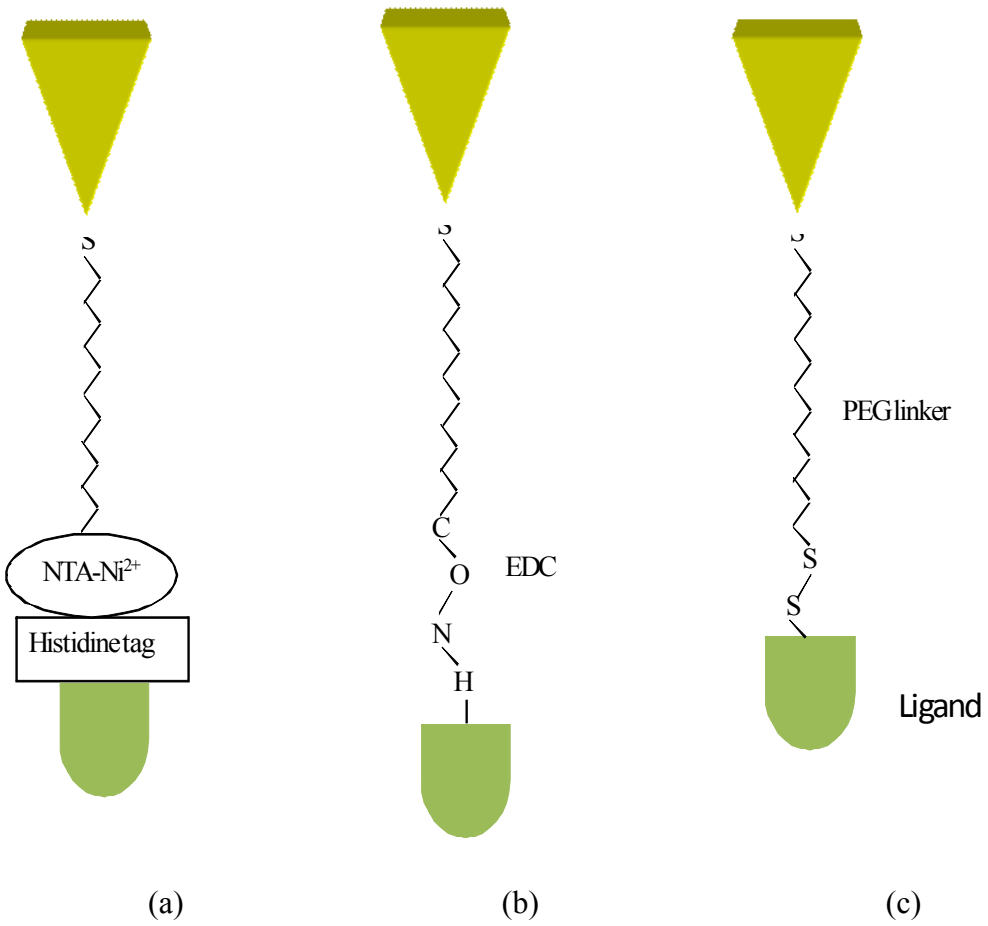

Figure 2.6 Schematic of AFM tip functionalizing using thiol based methods (a) proteins expressed with a histidine tag have a strong affinity to nickel nitrilotriacetate (b) amine groups in proteins can be cross linked to the free carboxylic acid group of the linker using EDC (c) thiol groups generated on the protein of interest can react with the thiol groups present on the spacer to form disulfide bonds.

Strategies for functionalizing cantilevers to attach live cells generally make use of the strong affinity of lectins to sugar residues on cell membranes. Since these sugar residues e.g. mannose are present on almost all cells, the functionalization method can be applied to attach practically any cell type. Two of the commonly used lectins are Concanavalin-A and wheat germ agglutinin[27, 93].

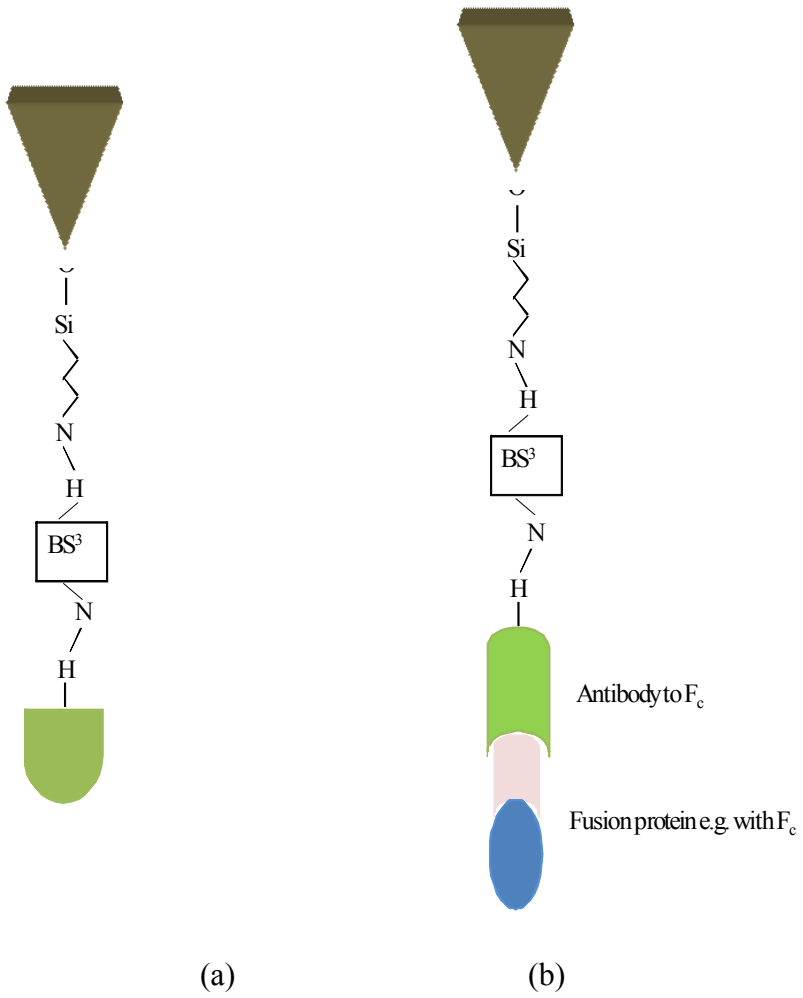

(a) (b)

Figure 2.7 Schematic of AFM tip functionalization using silanizing agents (a) free amine groups on the tips can be cross linked to free primary amine groups on the protein of interest by homobifunctional cross linker like BS^3 (b) free amine groups on the lysine residues present on the antibody to Fc fragment of human Ig can be cross linked to the free amine groups on the AFM tip using BS^3 following which a fusion chimera of the protein of interest with human F_c fragment can be linked.

2.3.3 Bell-Evans Model for extracting kinetic parameters in SMFS

Single molecular force spectroscopy attempts to study the behavior of a molecular interaction under an externally acting load. The observed characteristics of the bond over a spectrum of applied loading rates can be used to calculate the unstressed off rate as well

as to reconstruct the energy landscape of the dissociation[94]. Theoretical analysis of the effect of an externally acting force on a given molecular bond was first proposed by Bell in 1978[95]. According to the model proposed by Bell, the dissociation rate of a molecular bond increases as an exponential function of the applied external force. This can be written as:

$$k(f) = k_{off} \exp(\frac{Fx_\beta}{k_B T}) \tag{2.1}$$

Where k (f) is dissociation rate of the molecular interaction under an externally acting force F, k_{off} is unstressed off rate of the interaction, x_β is potential width of the energy barrier, k_B is Boltzmann constant and T is temperature.

Evans and Ritchie extended the model by using Kramer's theory for bond dissociation in liquids to show that the probability of a bond to rupture under an externally acting force is given by[94]:

$$p(F) = k_{off}^0 \exp(\frac{fx_\beta}{k_B T})\left(\frac{1}{\dot{F}}\right)\exp(-k_{off}^0 \int_0^F \exp(\frac{fx_\beta}{k_B T})(\frac{1}{\dot{f}})df) \tag{2.2}.$$

Where F* is the most probable rupture force and $\dot{F}$ is the loading rate. The maximum of this probability distribution (F*) can be obtained by differentiating the above equation i.e.

$$\frac{d}{dF}(p(f)) = 0 \tag{2.3}$$

If we assume that the applied loading rate is applied uniformly throughout the process of the bond stretch and rupture, it can be derived that:

$$F^*(\dot{F}) = \frac{k_B T}{x_\beta} \ln\left[\frac{\dot{F}}{k_{off}^0}\frac{x_\beta}{k_B T}\right] \tag{2.4}$$

Equation 2.4 is most commonly used to extract the kinetic parameters in single molecule force spectroscopy experiments and is called the Bell-Evans model. It predicts a linear correlation between the most probable rupture force and the logarithm of the corresponding loading rate. Hence, while the slope of the fitted line can be used to calculate x_β or the width of the energy barrier, the extrapolation of the fit to zero force can be used to extract the dissociation or unstressed off rate. Since both the loading rate and magnitude of rupture force can be obtained from the force-displacement curves, Bell-Evans model can be used to extract the unstressed off rate (k^o_{off}) and reactive compliance (x_β) for the interacting molecules.

2.3.4 Data acquisition in SMFS

Data acquisition in SMFS consists of monitoring repeated cycles of approach and retrace between a functionalized cantilever and substrate. The basic data unit in SMFS is called a force displacement curve or F-D curve[10, 16]. Each F-D curve represents a single cycle of approach and retraction. A single force displacement curve is obtained by tracking the deflections of the cantilever (force) and movement of the piezoelectric scanner (displacement) when they approach each other and then retract away.

An F-D curve consists of an approach curve and a retrace curve (red and blue colored respectively, Fig. 2.8). When the cantilever is approaching the substrate but is still far from it, there is no force induced or acting on the cantilever. In this case, the approach

curve is horizontal and represents the baseline for calculating forces acting on the cantilever ('approach' in Fig. 2.8). Fluctuations observed in the baseline represent the thermal vibrations of the cantilever. On coming in contact with the substrate, an upward force acts on the cantilever causing it to deflect. The deflection of the cantilever leads to a sharp rise in the approach curve. Once a specified contact force is reached, the cantilever stays in contact with the substrate for a predefined contact time and the cantilever then starts to retract away from the substrate. In the initial part of the retraction, the deflection of the cantilever starts to decrease till it becomes zero. If no bonds are formed between the cantilever and the substrate, the retract curve superimposes on the trace curve and the cycle is repeated. However, when a bond is formed between the cantilever and the substrate, the downward force acting on the cantilever due to the bond deflects the cantilever in the opposite direction. This is observed as a negative deflection (with respect to the baseline trace curve) in the retract curve. As the cantilever moves further away from the substrate, the bond initially is stretched and finally snaps restoring the cantilever to its normal undeflected state. The breaking of the bond is observed as a sharp jump in the retract curve. While the bond rupture events in the retract curve can be used to analyze the biophysical characteristics of the interactions between ligands receptor pairs on the cantilever and substrate, the trace curve can be used to extract the material properties of the substrate (e.g. stiffness). There are three important parameters that need to be controlled for obtaining proper F-D curves for analysis in SMFS. These are the contact force, contact duration and retraction velocity. The contact force and contact time critically determine the frequency of observed bond rupture events. A large contact force

and a long duration of contact can significantly increase the number of observed bond rupture events.

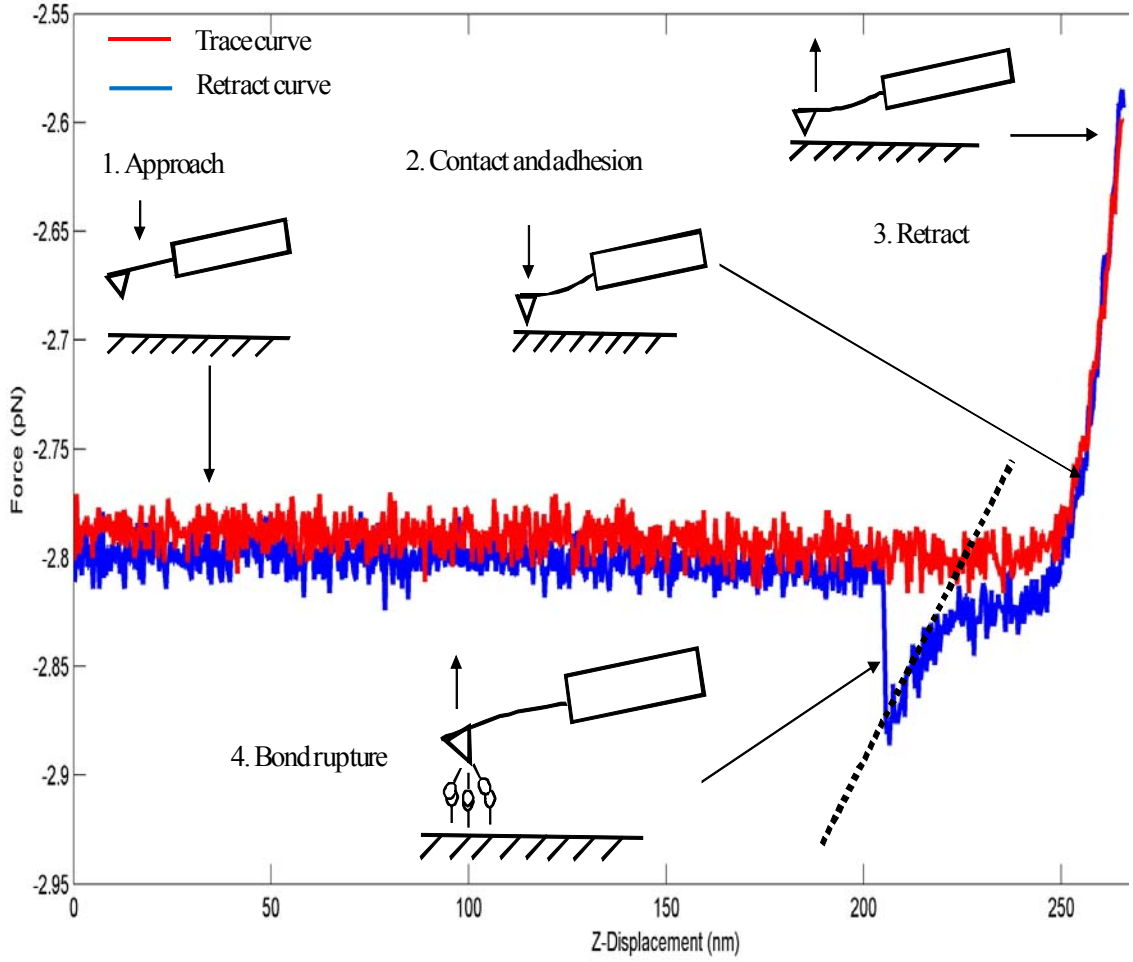

Figure 2.8 A typical force displacement curve showing a single bond rupture event[10].

However, a high frequency of bond rupture events is usually associated with multiple bond formation[96]. Low contact force and contact duration is hence necessary to increase the probability of forming single bonds[85]. The lowest force that can be applied is limited by the stiffness of the cantilever and the minimum distance that the scanner can move. Very low forces can lead to significant distortion of the F-D curves. Hence, the

contact force and contact time need to be optimized in such a way that the frequency of single bond formation is enhanced but the quality of the F-D curves is not compromised. The optimization of the contact force and contact time is a trial and error process. The two parameters are empirically changed till the observed bond rupture frequency is <30%. Based on Poisson's statistics, the probability of a bond rupture being due to a single bond is >85% when the observed bond rupture frequency is <30%[93].

The retraction velocity of the cantilever, unlike the contact force and contact duration, affects the loading rate on the bond. The loading rate on the bond is defined as the rate at which force is applied to the interacting molecules and is measured in pN/sec. The loading or pulling rate on a given molecular interaction is determined by the inherent 'stiffness' of the whole ligand-receptor-cantilever complex and the retraction velocity. As the stiffness of the cantilevers (~10 pN/nm) used is, in general, significantly higher than that of the interacting molecules (~0.3pN/nm) the effective stiffness of the whole ligand-receptor-cantilever complex is dominated by the inherent natural stiffness of the involved molecules. For a given pair of ligand and receptor, the stiffness of the molecules cannot be controlled; so the only way to apply different loading rates to the interaction complex is by varying the retraction velocity of the cantilever. Since the loading rate applied to a bond is directly proportional to the retraction velocity of the cantilever, the variation of bond rupture forces over a spectrum of applied loading rates is essentially obtained by analyzing F-D curves at different retraction velocities of the cantilever. This also means that the spectrum of loading rates that a bond can be subjected to is limited by the minimum and maximum velocities that the piezoelectric scanner can achieve. Furthermore, high retraction velocities of the cantilever can cause significant

hydrodynamic drag that can affect the measured parameters. Also, as the strength of a given molecular interaction under a given loading rate is a distribution, it is necessary to obtain a large number of F-D curves at each retraction velocity for analysis. Typically, over a few hundred curves are analyzed for each retraction velocity. The retraction velocity is varied at least over one order of magnitude to probe a sufficiently large spectrum of loading rates.

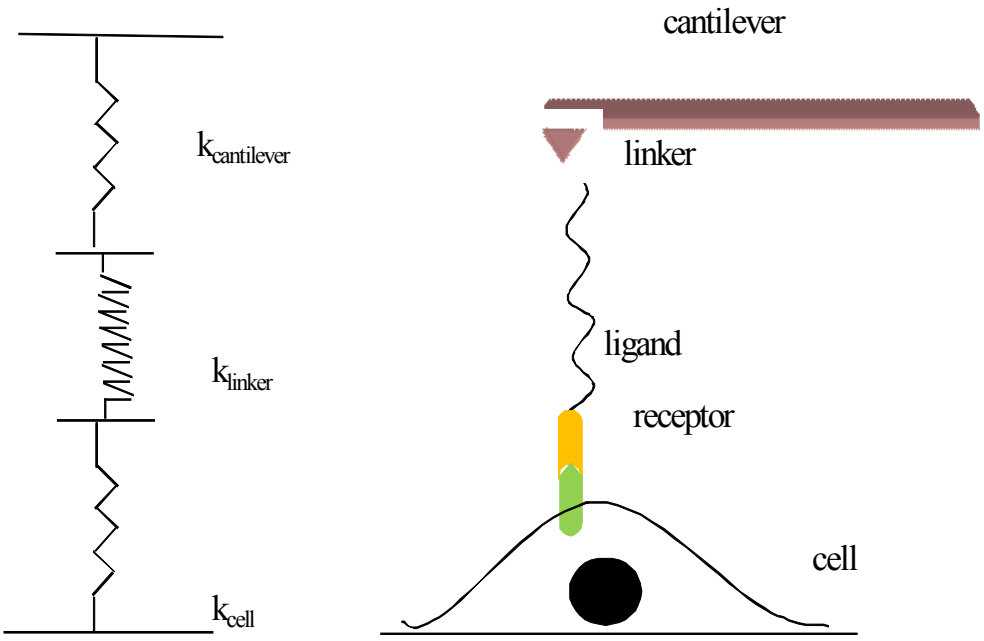

Figure 2.9 Schematic depiction of cantilever-linker-receptor-ligand-cell complex as springs arranged in series. The effective spring constant of the whole complex determines the loading rate acting on the interacting molecules. Here $k_{cantilever}$, k_{linker} and k_{cell} represent the stiffness of the cantilever, molecular linkers and the cell respectively.

2.3.5 Data analysis in SMFS

As mentioned in the previous section, to use the Bell-Evans model for extracting the kinetic parameters of two interacting molecules requires the magnitude of rupture force of the bond and the corresponding loading rate as input observations. Obtaining the

rupture force magnitude from an F-D curve is straight forward as it is the maximum deflection of the cantilever from the baseline prior to the rupture event. Previously, it was customary to multiply the velocity of the cantilever with the spring constant of the cantilever for computing the loading rate on the bond[26]. Loading rate computed in such a manner, also called the nominal loading rate, was extensively used in early SMFS experiments. In these experiments, it was assumed that for a given retraction velocity, the nominal loading rate remained constant. However, it soon became clear that the nominal loading rate did not reflect the actual loading rate on the bond. This was to be expected because the spring constant of the cantilever used in experiments is usually much larger than that of the spring constant of the interacting molecules. If we consider that the cantilever-linker-ligand-receptor-cell complex as a set of springs connected in series, the effective spring constant of the whole system is determined by the softest spring (Fig. 2.9). Since proteins and polymeric linkers are in general much less stiffer than the cantilever and the cell, the net stiffness of the whole system is closer to that of the linkers rather than that of the cantilever. Furthermore, the stiffness of the involved molecular linkers is unknown and also varies randomly from one F-D curve to another (even when obtained at similar pulling velocity). This variation in stiffness of the linkers and interacting molecules can arise from several factors such as [97]:

(a) fluctuations in the local environment surrounding the interacting molecules due to movement of ions and water molecules

(b) different orientations of the interacting molecules with respect to the direction of pull by the cantilever, and

(c) fluctuations within the molecule itself leading to subtle changes in the conformation of the molecules or the manner in which the molecules interact.

To overcome this difficulty, the concept of apparent loading rate was introduced. The apparent loading rate is derived separately for each F-D curve showing a rupture event and is calculated as the product of the slope of the linear portion of the retrace curve just before a rupture event and the retraction velocity of the cantilever[27]. This is because the initial non-linear extension observed before the rupture event reflects the unfolding of the linkers and interacting molecules. The linear extension just before the actual rupture event represents an elastic stretch of the interacting molecules and represents the effective spring constant ($k_{eff,}$ dashed line Fig. 2.8) of the system at that particular instant. Hence, the apparent loading rate is given by:

$$r_f = \frac{dF}{dt} = (\frac{dF}{dx})(\frac{dx}{dt}) = (k_{eff})(v) \tag{2.5}$$

Here, r_f is the apparent loading rate; k_{eff} is the effective spring constant of the cantilever-receptor-ligand complex and v is the retraction velocity of the cantilever.

F-D curves obtained at different retraction velocities are analyzed for rupture events in the retrace curve. For each F-D curve showing a single clear rupture event, the magnitude of rupture force (f) and the apparent loading rate (r_f) are extracted. After calculating the loading rate and the magnitude of rupture from the force curves, there are two methods by which they can be fit to the Bell-Evans model:

(a) In the velocity based method, the most probable loading rate and the most probable rupture force for all force-displacement curves obtained at a particular retraction velocity is computed. The most probable rupture force is then plotted against the logarithm of the corresponding most probable loading rate[98].

(b) In the binning based method, each force displacement curve yields a single value for rupture force and loading rate. The rupture force is plotted against the logarithm of the corresponding loading rate for all the force curves obtained at different velocities. The data points are then grouped into different loading rate bins and the average rupture force for each bin is calculated[84]. When the binning method is used, the average force rather than most probable rupture force is being computed. It can be shown from Eq. 2.2 that the average unbinding force <*f*> is given by:

$$< f >= \frac{k_B T}{x_\beta} \exp\left(\frac{k_{off}^0 k_B T}{x_\beta r_f}\right) E_i \left(\frac{k_{off}^0 k_B T}{x_\beta r_f}\right) \tag{2.6}$$

Here, $E_i(z) = \int_z^\infty t^{-1} \exp(-t)\, dt$ represents the exponential integral.

In either case, once the loading rate vs. rupture force data points are plotted, they can be fit using Eq. 2.4 or Eq. 2.6. While the slope of the curve fit can be used to calculate the reactive compliance (x_β), extrapolation of the fit to zero force can be used to obtain the unstressed off rate (k^o_{off}). The unstressed off rate, in turn, provides an insight into the kinetic stability of the bond. A low k^o_{off} is usually associated with protein interactions which are typically very stable (e.g. antigen–antibody interactions) while a large k^o_{off} is usually associated with protein interactions which are highly dynamic (e.g. claudins). In

some cases, protein interactions tend to show multiple values for k^{o}_{off} corresponding to different binding architecture or multiple energy barriers (e.g. E-cadherins, ICAM-1/LFA-1).

2.3.6 Determination of the cantilever spring constant

As the spring constant of the cantilever bears a direct correlation to the accuracy with which the bond rupture force is measured, it is very important to determine the spring constant of the cantilever as accurately as possible. Several methods have been devised to determine the spring constant of the cantilever[82].

(a) The spring constant can be derived directly from the geometrical features of the cantilever. For a triangular cantilever (whose length is *L*, width is *w*, opening angle is α and E is the elastic modulus) the spring constant k_c, is given by[99]:

$$k_c = \left(\frac{Ewt^3}{2L^3}\right)\cos\alpha\left[1+\frac{4w^3}{t^3}(3\cos\alpha-2)\right]^{-1} \qquad (2.7)$$

The main drawback of this method is that it is very difficult to precisely measure the geometrical features. Since the geometrical features of cantilevers are not perfectly homogenous, small errors in measurement can lead to a large difference in the spring constant.

(b) Cleveland et al proposed a method in which a known mass is suspended from the cantilever and the change in its resonance frequency is determined[100]. The spring constant is then given by:

$$k = \frac{4\pi^2 m}{\frac{1}{v_0'^2} - \frac{1}{v_0^2}} \tag{2.8}$$

Here, k is the spring constant, m is the mass added to the cantilever, v_0 is the resonant frequency before addition of the mass and v'_0 is the resonant frequency after addition of the mass.

(c) The thermal tune method proposed by Hutter et al is the most widely used method for determining the spring constant[101]. In this method, the thermal fluctuations of the cantilever are monitored. Considering the cantilever as a harmonic oscillator:

$$\frac{1}{2}k < \Delta Z^2 > = \frac{1}{2}k_B T^2 \tag{2.9}$$

Here, k is the spring constant of the cantilever, $<\Delta Z^2>$ is the mean square deflections of the cantilever and T is the temperature. Most commercial AFMs have an in built thermal tune module that implements this method for calculating the spring constant of the cantilever.

2.3.7 SMFS of cell adhesion molecules

Single molecule force spectroscopy has previously been applied to study the interaction kinetics of several cell adhesion molecules(Table 2.1)[10]. Some of the first studies were performed on the cell adhesion molecules expressed on leucocytes. P-selectin/PSGL-1, VCAM-1/$\alpha_4\beta_1$ and ICAM-1/$\alpha_L\beta_2$ are some of the important molecular pairs that mediate adhesion between leukocytes and endothelial cells. These cell adhesion molecules play an important role in the process of inflammation where leukocytes moving in the blood are

trapped by adhesion molecules expressed by the endothelial cells. Another cell adhesion molecule that has been extensively investigated using SMFS is E-cadherin that mediates intercellular adhesion in epithelial monolayers. The SMFS experiments on these cell adhesion molecules provide a deep insight into the physiological functions of these molecules. For example, it was observed that while P-selectin/PSGL-1 and VCAM-1/$\alpha_4\beta_1$ interactions show a large amplification in rupture force at high loading rates, ICAM-1/$\alpha_L\beta_2$ and E-cadherin/E-cadherin interactions show significant strength even at low loading rates.

Table 2.1 Overview of adhesion kinetics of different cell adhesion molecules probed using SMFS experiments.

Molecular pairs	**Substrate**	**Tip**	**k^o_{off} (s^{-1})**	**Physiological functions**	**Ref**
E-cadherin/ E-cadherin	E-cadherin	E-cadherin	~1.0* ~ 10^{-5}	Stabilizing intercellular junction	[102]
Desmoglein/ Desmoglein	Desmoglein/Fc	Desmoglein/Fc	5.88	Stabilizing intercellular adhesion	[103]
Integrin/ ligand	Type I collagen	$\alpha_2\beta_1$ integrin expressing CHO cell	1.3	Cell substrate adhesion	[98]
P selectin/ PSGL	PSGL expressing leukocytes	P-selectin/Fc	0.22	Leukocyte capture and rolling.	[83]
LFA1/ ICAM-1	ICAM-1	Leukocyte	4.0 and 57**§ 0.17 and 40**$^{\Psi}$	Leukocyte adhesion, crawling and transmigration	[27]

*Corresponds to different binding configurations
**Correspond to two different energy barriers
§Correspond to high affinity LFA and $^{\Psi}$low affinity LFA.

Considering that P-selectin/PSGL-1 and VCAM-1/ $\alpha_4\beta_1$ play an important role in trapping a fast moving leukocyte in the blood, it is necessary that they exhibit strong interaction strength when subjected to very high loading rates.

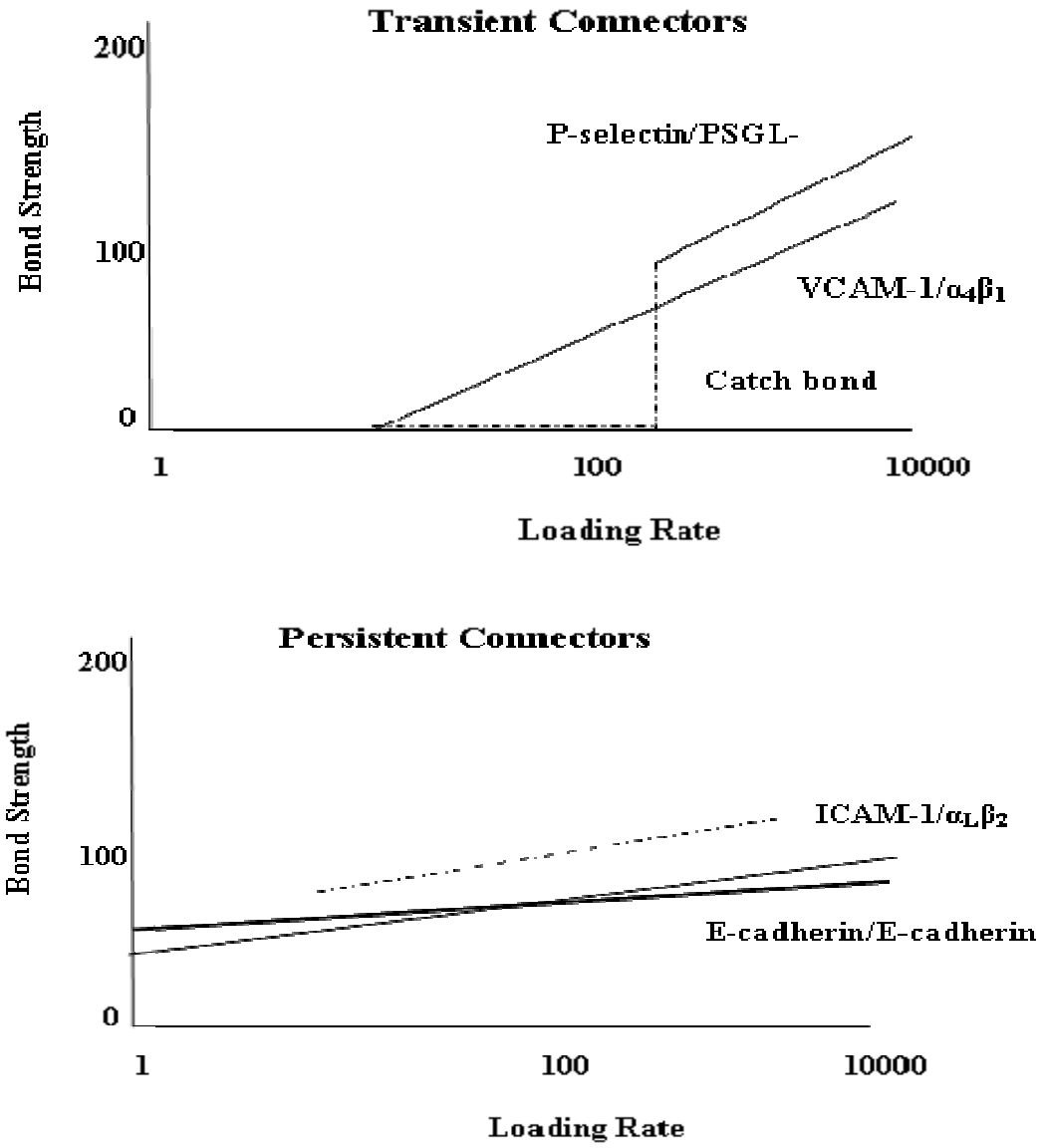

Figure 2.10 Relation between bond strength and loading rate on interactions mediated by (a) Transient connectors like P-selectin/PSGL-1 interactions and (b) Persistent connectors mediated by ICAM-1/ $\alpha_L\beta_2$ interactions[104].

On the other hand, once the leukocytes have been trapped, it is necessary that while they remain adherent to the endothelial cells, they should also have the flexibility to roll and crawl on the endothelium. This requires that the bonds formed are stable under low loading rates. ICAM-1/$\alpha_L\beta_2$ adhesion provides such a stable interaction for the leukocytes to adhere to the endothelial cells. These two types of interaction patterns have been broadly categorized as transient connectors and persistent connectors (Fig. 2.10).

Furthermore, P-selectin/PSGL-1 interaction shows a characteristic transition to a 'catch bond' behavior at higher loading rates. This means that the interaction shows almost no strength at very low loading rates but when it is loaded fast enough; the bond can resist a large magnitude of force acting on it. These experiments show how the adhesion kinetics of cell adhesion molecules probed using SMFS can provide a better insight into the physiological functions that they mediate. Despite extensive investigation of E-cadherin mediated interactions and interactions mediated by leukocyte adhesion molecules using SMFS, many important intercellular adhesion molecules are yet to be probed. As mentioned before, one of the main objectives of this dissertation is to understand the adhesion kinetics of some of the important intercellular adhesion molecules expressed by epithelial cells.

2.4 Diseases associated with changes in intercellular adhesion molecules

The primary reason for studying cell adhesion proteins and their interactions is not only due to their importance in physiological functions but also due to the role that these proteins play in several disease processes[10]. This section elaborates on the association of some of the cell adhesion molecules with different disease processes.

(a) Tight Junctions: Qualitative and quantitative changes in tight junction proteins are associated with diseases involving almost all organ systems of the body (Table 2.2)[16]. For example, mutations of claudins are associated with several diseases like familial hypomagnesaemia, hypercalciuria syndrome and hereditary deafness. While JAM-A has been found to act as a receptor for reoviruses, claudins have been recently found to act as co-receptors for HCV virus. Altered expression of tight junction proteins is also associated with several carcinomas making them potential candidates for new tumor markers.

(b) Adherens junction proteins: Altered expression and mutations of E-cadherin and nectin are also associated with several diseases (Table 2.3)[105]. While mutations in nectins have been shown to be associated with infertility, cleft lip and cleft palate; altered expression of E-cadherins has been shown to be associated with several carcinomas. Nectins have also been shown to act as a receptor for herpes group of viruses.

Table 2.2 List of diseases in various organ systems involving qualitative and/or quantitative changes in tight junction proteins[16].

Organ system	**Associated human diseases**
Central Nervous System	Multiple sclerosis, Alzheimer's disease, HIV encephalitis and dementia, auto immune encephalitis, astrocytomas and glioblastoma multiforme, hyperthermia , Duchene's muscular dystrophy, hypoxia.
Gastro-Intestinal System	Diarrhea induced by various bacterial toxins, inflammatory bowel diseases, colitis, Celiac disease, gastro-esophageal reflux disease (GERD), Menetrier's disease.
Hepato-biliary-pancreatic system	Cholestasis associated with common bile duct ligation, primary biliary cirrhosis and primary sclerosing cholangitis, cholelithiasis, acute pancreatitis

Respiratory system	Asthma, shock lungs, interstitial lung disease, ventilator induced lung injury.
Renal System	Familial hypomagnesaemia and hypercalciuria, pseudo-hypoaldosteronism.
Carcinomas	Hepatocellular carcinoma, endometrial carcinoma, GI tract carcinomas, pancreatic carcinoma, oral carcinomas, breast carcinoma
Other diseases	Autosomal recessive hearing loss, diabetic retinopathy, uveitis.

Table 2.3 List of diseases associated with altered expression and/or mutations in adherens junction proteins[105].

Protein type	**Associated human diseases**
Nectin-1	Receptor for herpes virus entry, mutation in Zlotogora-Ogur syndrome, microphthalmia in knockout mice.
Nectin-2	Receptor for herpes virus entry, male specific infertility in knockout mice.
Nectin-3	Receptor for herpes virus entry, male specific infertility and microphthalmia in knockout mice.
Nectin-4	Over expressed in breast carcinoma.
E-cadherin	Endometrial, gastric and breast carcinomas.

(c) Desmosomes: Mutations in desmosomes are typically associated with several diseases of the skin and in some cases heart, emphasizing their importance in maintaining the integrity of cell-cell adhesion in tissues subjected to extensive mechanical strain (Table 2.4)[106].

Table 2.4 List of diseases arising from altered/impaired function of desmosomal proteins[106].

Desmosome component	**Associated human diseases**
Desmogelin-1	Pemphigus foliaceus, pemphigus vulgaris, Staphylococcal scalding skin syndrome, bullous impetigo, striate palmoplantar keratoderma
Desmogelin-3	Pemphigus vulgaris
Desmogelin-4	Inherited hypotrichosis
Plakophilin-1	Autosomal recessive ectodermal dysplasia and skin fragility syndrome
Plakophilin-2	Arrhythmogenic right-ventricular cardiomyopathy (ARVC)
Plakoglobin	Autosomal recessive Naxos disease
Desmoplakin	Striate palmoplantar keratoderma, acantholytic epidermolysis bullosa, Carvajal syndrome

(d) Gap junctions: Mutations in connexins most often manifest as skin disorders and/or deafness. Peripheral neuropathy has also been observed in mutations involving connexin-32. Currently, over a hundred different types of mutations in connexin 32 have been identified and associated with the Charcot-Marie-Tooth syndrome (Table 2.5)[107].

Table 2.5 List of diseases associated with mutations in different connexins that form gap junctions[107].

Gap junction protein type	Associated human diseases
Connexin 26	Keratitis-ichthyosis-deafness and hystrix-like ichthyosis-deafness, Vohwinkel's syndrome, palmoplantar keratoderma
Connexin 30	Clouston's syndrome
Connexin 31	Erythrokeratodermia variabilis
Connexin 32	X-linked Charcot-Marie-Tooth syndrome
Connexin 43	Oculo-dento-digital dysplasia (ODDD)

2.5 Effect of mechanical strain on intercellular adhesion complex

The effect of mechanical strain on the expression of several genes and proteins has been studied in a variety of different cell types. For example it has been shown that mechanical strain can alter collagen and fibronectin production in fibroblasts (tendon, ligament, pulmonary and periodontal) and smooth muscle cells[108]. Also, mechanical strain has been shown to cause an increase in the expression of immediate early genes like *c-fos*, *c-jun* and *c-myc* in cardiomyocytes[109]. It has been shown that mechanical strain can activate both the classical MAPK pathway (ERK1/2) as well as the JNK and p38 MAPK pathway in endothelial cells[110]. Activation of ERK, JNK and p38 is followed by activation of downstream transcription factors, important among which are AP-1, Egr-1 and Elk-1. PKC, PI3K, tyrosine kinases, free radicals and tyrosine kinases have been shown to play an important role in the mechanical strain mediated activation of the

MAPK pathway in endothelial cells. Altered expression of a number of different genes has been associated with mechanical strain in endothelial cells. Important among them include ICAM-1, MCP-1, COX-1/2, eNOS and MMP[110]. Some of the important pathways involved in modulating the response of cells to external mechanical strain are shown in Fig. 2.11. Despite such a large number of studies conducted on the expression of various cellular proteins in endothelial cells in response to mechanical strain, few studies have focused on the effect of mechanical strain on the expression and localization of intercellular adhesion molecules. Some previous studies have been carried out on lung alveolar epithelial cells. It has been shown that mechanical strain can increase the proliferation rate of alveolar epithelial cells[111]. The increase in proliferation rate was shown to be mediated by phospholipase C-γ-protein kinase C pathway as well as ERK1/2 activation occurring through Src and focal adhesion kinase[112]. It was also demonstrated that mechanical strain can disrupt the intercellular tight junction barrier as well as decrease the expression of tight junction proteins e.g. occludin[30, 113]. Recent experiments conducted on endothelial cells show that mechanical strain can induce an increase in occludin and ZO-1 expression in endothelial cells subjected to mechanical strain[39].

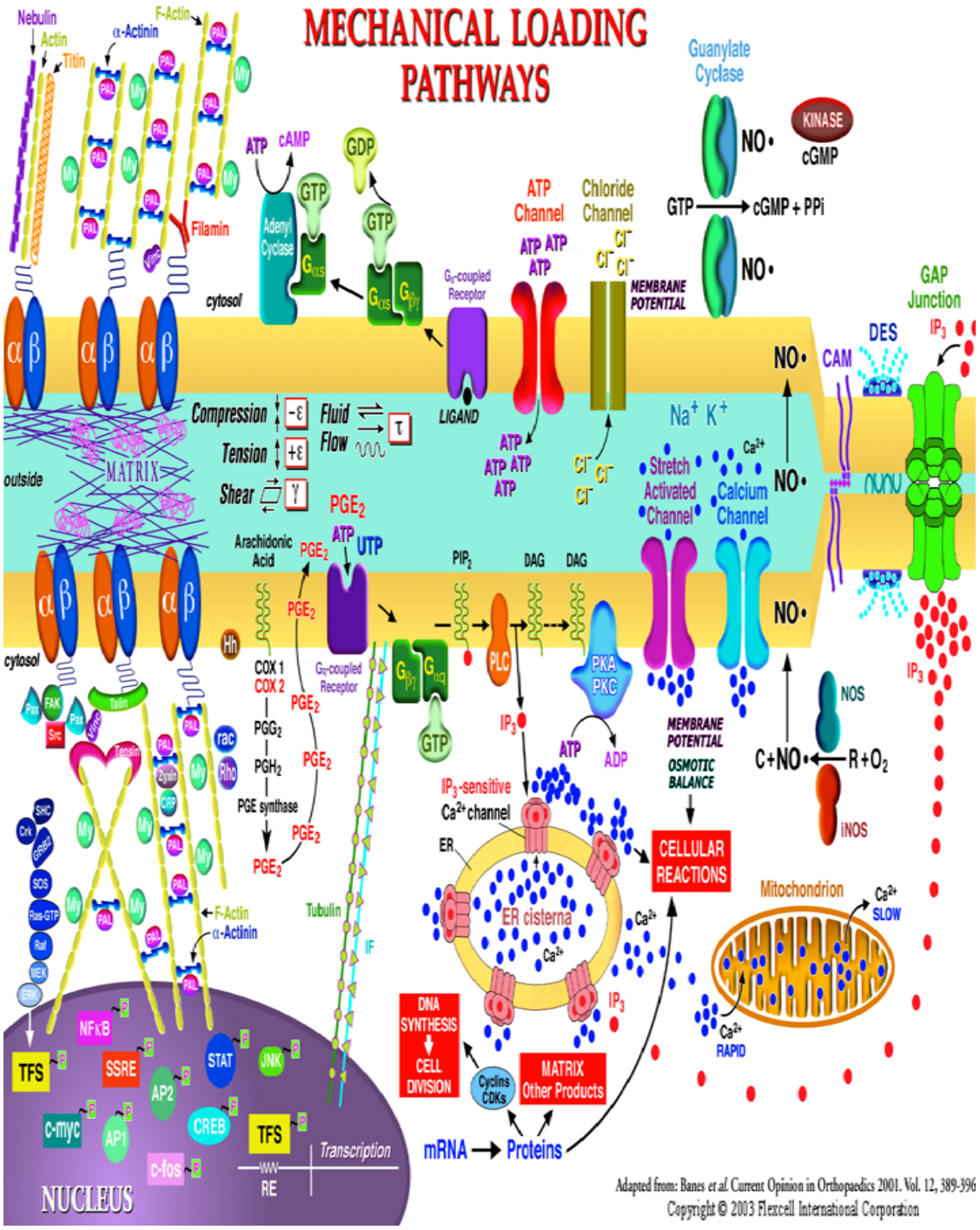

Figure 2.11 Schematic depiction of the various signaling pathways activated in response to mechanical strain in cells[114].

Such contradictory results show that the influence of mechanical strain on the expression and localization of intercellular adhesion proteins is highly dependent on the specific cell type under investigation. Furthermore, the experiments do not propose any possible mechanism or cause for the altered expression in occludin expression.

Considering that the renal tract epithelial cells are often subjected to large strains e.g. in case of obstruction arising from either stones or hypertrophic prostate (also called hydronephrosis) or cysts occurring due to genetic mutations (e.g. polycystic kidney); it is very likely that such strains induce significant alteration in the expression and distribution of intercellular adhesion proteins. Furthermore, since the renal tract is also responsible for strictly regulating the diffusion of solutes and ions, it is likely that any disturbance in the integrity of the tight junction proteins due to the mechanical strain would compromise the epithelial barrier. Though some studies have investigated the effect of mechanical strain on the proliferation rate of renal epithelial cells[115], the effect of mechanical strain on the expression and distribution of intercellular adhesion molecules in renal epithelial cells remains unknown. To probe the expression and distribution of some of the tight junction proteins in response to mechanical strain is another important objective of this dissertation.

3 Experimental setup, Methods and Materials

3.1 Cell culture, proteins and reagents

Mouse L-fibroblasts were cultured in Dulbecco's modified Eagles' medium (DMEM) supplemented with 10% fetal bovine serum and 1% penicillin. They were subculture every three days. For AFM experiments, cells were seeded on 13mm glass cover slips. The glass cover slips were used for SMFS experiments when the cells were about 50% confluent. Madin-Darby canine kidney (MDCK) cells were also cultured in the same medium. Nectin-1 fused to human Fc fragment was generated as described before and was a generous gift from Dr. Takai, Osaka University[55]. mJAM-A/Fc fusion protein was purchased from R&D systems (Minneapolis, USA). Purified head domain of reoviral attachment protein σ1 (residues 293-455) was provided by Dr. Dermody, Vanderbilt University, USA[116].

3.2 Single Molecule Force Spectroscopy Set Up

All single molecule force spectroscopy experiments were carried out on a MultiMode^{TM} Picoforce^{TM} AFM (Veeco, Santa Barbara, CA) with Nanoscope Controller IV coupled to an upright microscope. The microscope was connected to a monitor for visualizing cells. This helped in positioning the cantilever over the cell. Experiments were performed at room temperature using a fluid cell that allowed for injecting and changing culture medium during the course of the experiment (Fig. 3.1). This allowed the experiments to be performed on live cells.

3.3 Functionalization of AFM Tips

AFM cantilevers were functionalized with recombinant nectin-1/Fc or JAM-A/Fc fusion proteins using a previously described protocol[83, 84]. Silicon nitride tips (k=10pN/nm, Veeco, Santa Barbara, CA) were first cleaned in acetone and then UV irradiated for fifteen minutes. They were then incubated in a 30% solution of hydrogen peroxide in concentrated sulphuric acid for 30 minutes. Tips were then washed thoroughly with DI water and dried. Tips were discarded after one or two experiments because repeated treatment with acid caused damage to the reflecting surface of the cantilever leading to no detectable laser on the photodiode. They were silanized by incubating them in a 3% solution of 3-aminopropyltriethoxysilane (APTES, Sigma) in acetone for 3 minutes. Following this, they were rinsed in acetone three times and immersed in a solution of bis-sulfosuccinimidyl suberate (BS^3, 2mg/ml, Pierce, Rockford, IL) for 30 minutes. Tips were then washed in DI water and incubated in mouse anti-human Fc antibody (10μg/ml, Sigma, St. Louis, Missouri). Tips were washed to remove unbound antibody and the reaction was quenched by incubating tips in 0.1M glycine for 10 minutes. Finally, the tips were incubated in a 5μg/ml solution of nectin-1/Fc or JAM-A/Fc for two hours. They were then washed in PBS to remove unbound protein. Prior to experiments the tips were blocked in 1% BSA for 15 minutes. Glass cover slips were functionalized with nectin-1/Fc or JAM-A/Fc using the same method. For control experiments, all the steps were similar except that the tips were not incubated in nectin-1/Fc or JAM-A/Fc. For functionalizing tips with reoviral attachment protein σ1, a one step cross linking method using 1-ethyl-3-[3-dimethylaminopropyl] carbodiimide hydrochloride (1mg/ml, EDC, Pierce) was used[117]. Following silanization of the tips and treatment with BS^3as

described above, tips were incubated in a solution of homo-bifunctional mPEG-amine spacer (polyethylene glycol with free primary amine groups at both ends, 2 mg/ml, MW 2000, Nektar) for 2 hours. The tips were washed and quenched in 1M Tris buffer. The σ1 head domain (10μg/ml in PBS) and freshly prepared EDC (1 mg/ml in PBS) were mixed in equal amounts. Tips were rinsed in PBS and incubated in this mixture for 2 hours. Finally, they were rinsed in PBS and blocked in 1% BSA for 15 minutes.

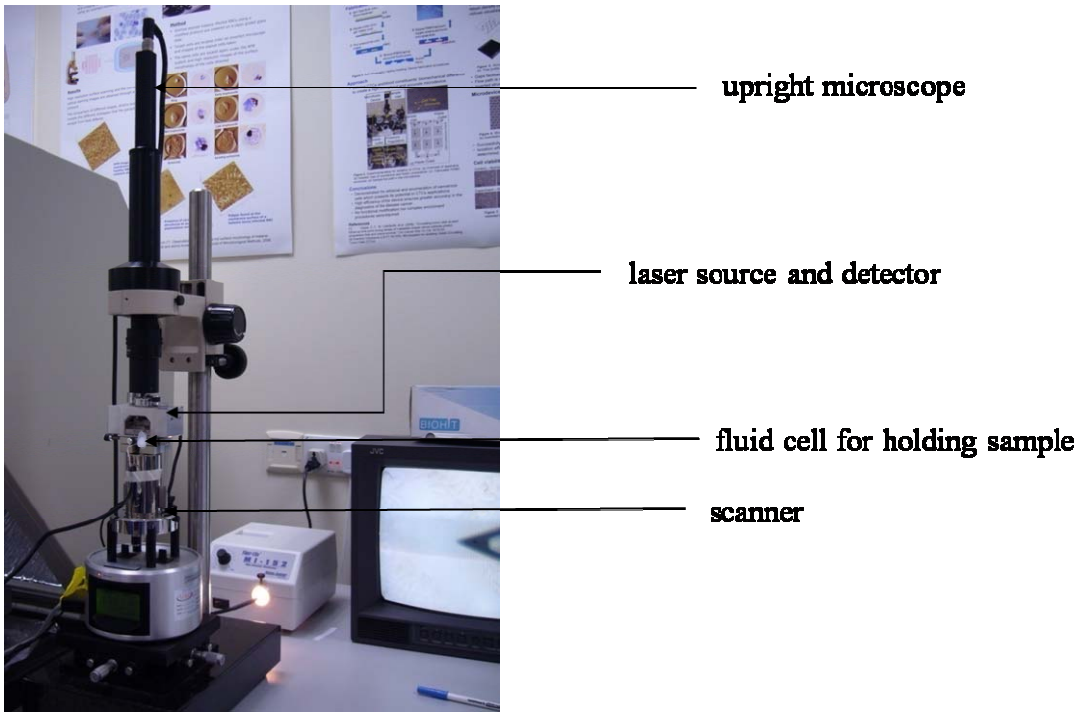

Figure 3.1 Experimental set up for SMFS experiments.

3.4 Single Molecule Force Spectroscopy Experiments on L-fibroblasts

Functionalized cantilevers were mounted on a fluid cell and the laser was aligned onto the largest cantilever (k=10pN/nm). Freshly cleaved mica was firmly glued to a metal disc and cover slips (on which L-fibroblasts were grown) were mounted on the mica

using a Scotch® double sided tape. The metal disc was then placed on the Picoforce™ scanner. A drop of culture medium was added over the cells and the fluid cell with the functionalized cantilever was placed on top of the cover slips. A small amount of culture medium was gently injected into the fluid cell to immerse the cantilever taking care to avoid formation of any air bubbles.

To obtain the deflection sensitivity of the cantilever, it was positioned over a region devoid of any cells. A force curve was obtained by allowing the cantilever to press hard against the glass cover slip (a contact force of ~2nN was applied). The deflection sensitivity was then calculated as the slope of the trace and retrace curve in the contact region (Fig. 3.2).

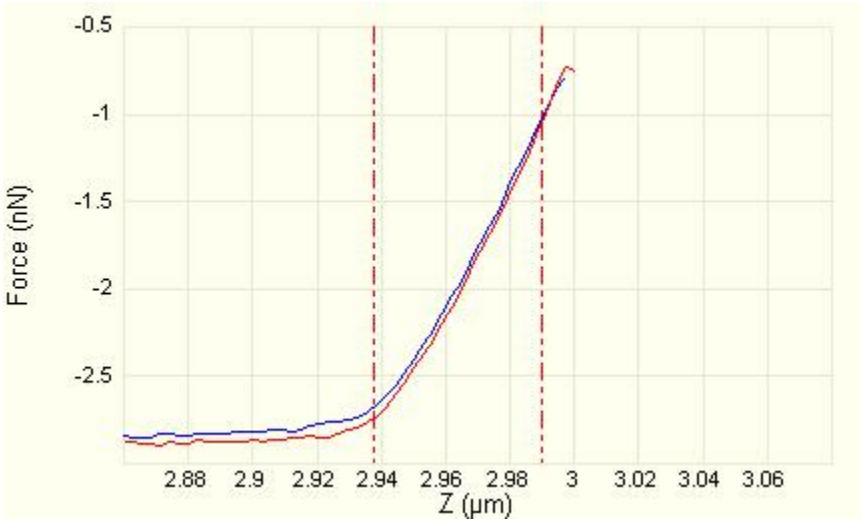

Figure 3.2 A typical force distance curve obtained on a hard substrate to calculate the deflection sensitivity of the cantilever. The slope of the trace and retrace curve between the two vertical dashed lines is used for calculating the deflection sensitivity.

The typical deflection sensitivity of the cantilevers used in SMFS experiments was ~90mV/nm. The deflection sensitivity of the cantilever so obtained is used by the in built

thermal tune module of the AFM to calculate the spring constant of the cantilever. The thermal tune module monitors the thermal fluctuations of the cantilever and derives the spring constant from the power spectrum. While monitoring the thermal fluctuations of the cantilever using the thermal tune module, the cantilever was moved far away from the substrate to prevent any interference from the substrate.

After calculating the spring constant, the cantilever was positioned over the centre of a well adherent and spread out L-fibroblast. Force curves were then obtained under conditions that minimized multiple bond formation. A contact force of 200pN and a contact time of 1ms were used in all experiments. Under these conditions, the frequency of bond formation was less than 30%. Poisson's statistics predicts a >85% probability of single bond formation for bond formation frequencies less then 30%. The retraction velocity of the cantilever was varied from $1\mu s^{-1}$ to $10\mu s^{-1}$. More than 500 force-distance (F-D) curves were obtained for each retraction velocity. These F-D curves were then analyzed to obtain the magnitude of rupture force and loading rate using a code written in MATLAB version 6.5 (The MathWorks, Natick, MA).

3.5 Detection of Rupture Events and Calculating Rupture Force & Loading Rate

Since a few thousand F-D curves need to be analyzed for statistically significant results, an automated data processing algorithm was implemented using MATLAB. A flow chart depicting the steps for detecting the rupture events in F-D curves is shown in Fig. 3.3. The data for the retract curve (scanner movement along X-axis and force along Y-axis) from all F-D curves was exported into ASCII format for further analysis using a custom written code in MATLAB for detecting the rupture events, calculating the magnitude of

rupture force and the loading rate. F-D curves were first smoothed using a sliding window of width *w* points (typically 5 by default) and the average force value of the data points was attributed to the window (Fig. 3.4). Smoothing was necessary to prevent the detection of small peaks and fluctuations arising from the inherent noise of the system.

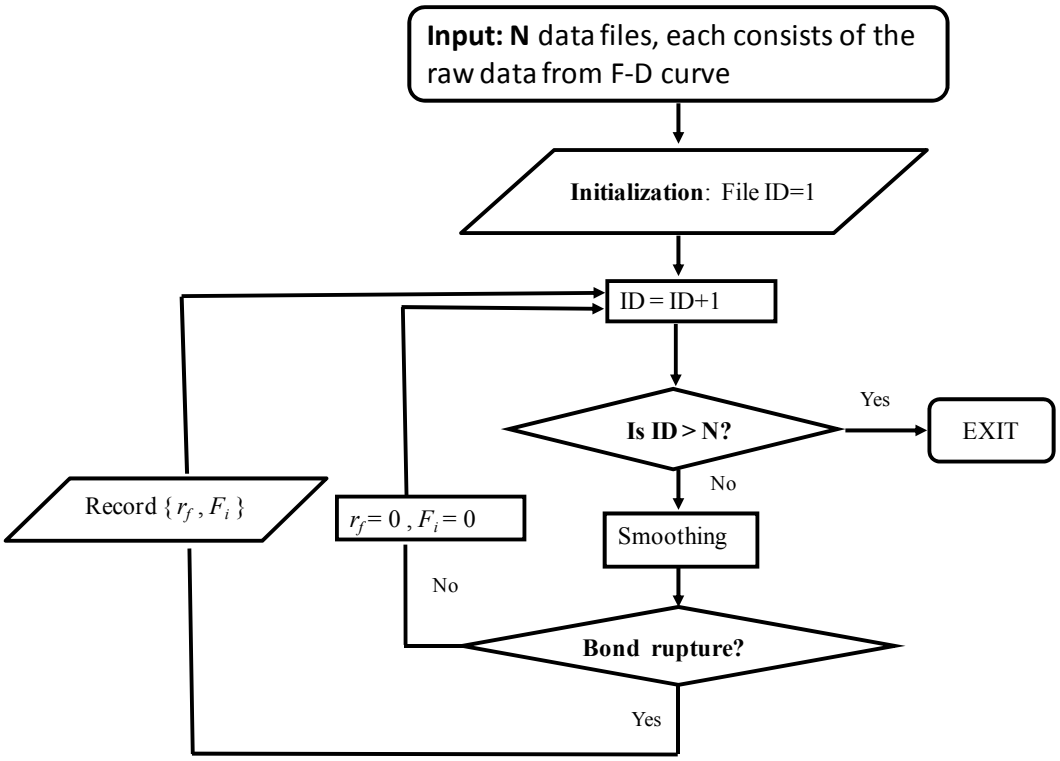

Figure 3.3 Flow chart depicting the sequence of steps in the analysis of F-D curves acquired in SMFS.

For detecting a rupture event in an F-D curve after smoothing, a profile of changes occurring in the force values was constructed within a sliding window of length L based on the difference between the first and last entries of the window (Fig. 3.5). Since unbinding events usually occur within very short pulling distances (~5 nm), the window length was calculated based on the ramp size (~2.5 to 5 μm) and the data points sampled

(typically either 1024 or 2048). Assuming that the force value corresponding to each data point is a result of a mutually independent force signal with a superimposed background noise, it can be shown that the profile of force changes follow a normal distribution. Thus, using Gaussian statistics it is possible to test if bond rupture event (i.e. a sharp transition) exists within the tested window. If the null hypothesis H_0 (there is no bond rupture (no sharp transition)) is true, the value of the back ground noise will be very close to zero since it is follows a Gaussian distribution with mean of zero.

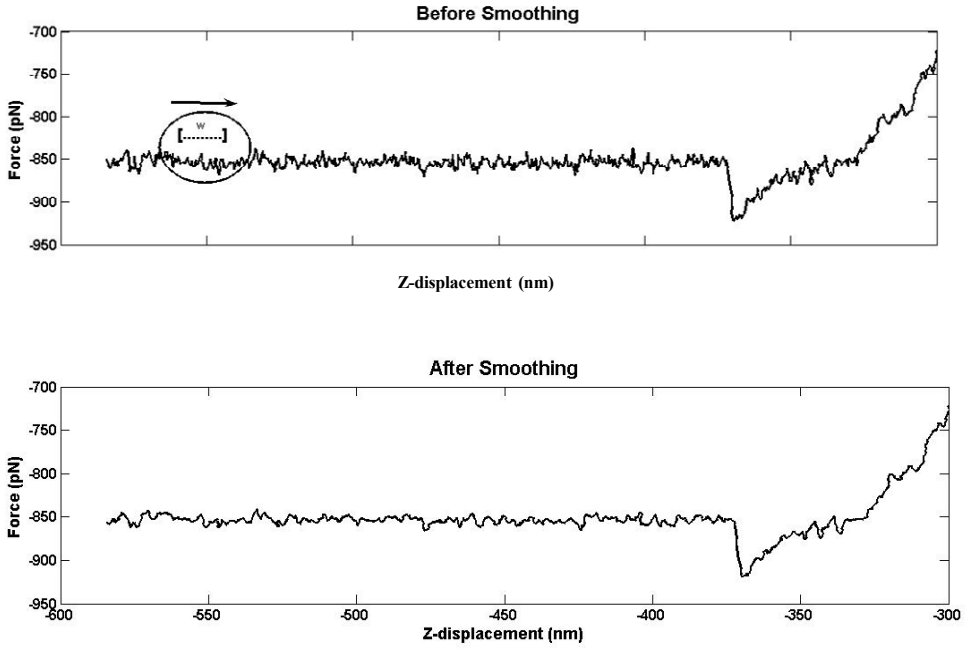

Figure 3.4 Smoothing of the F-D curve using a sliding window method.

In contrast, force values that deviate significantly from zero indicate that there is a sharp transition within the tested window suggesting the presence of a bond rupture event. To localize the position of the bond rupture event, a threshold (T, dotted red line, Fig. 3.5) is set based on the mean and standard deviation of the observed changes in the force profile.

Only F-D curves containing a rupture event show a change in the force profile greater than the threshold. After localizing the peak position, original experimental values (non-smoothed) are used to evaluate the amplitude of the force and the z-displacement position of each rupture event. Only those curves that display a single rupture event are included in the analysis. Each rupture event is mapped as a single scatter point $\{r_{fi}, F_i\}$ where F_i is the rupture force and rate r_f is the corresponding loading rate.

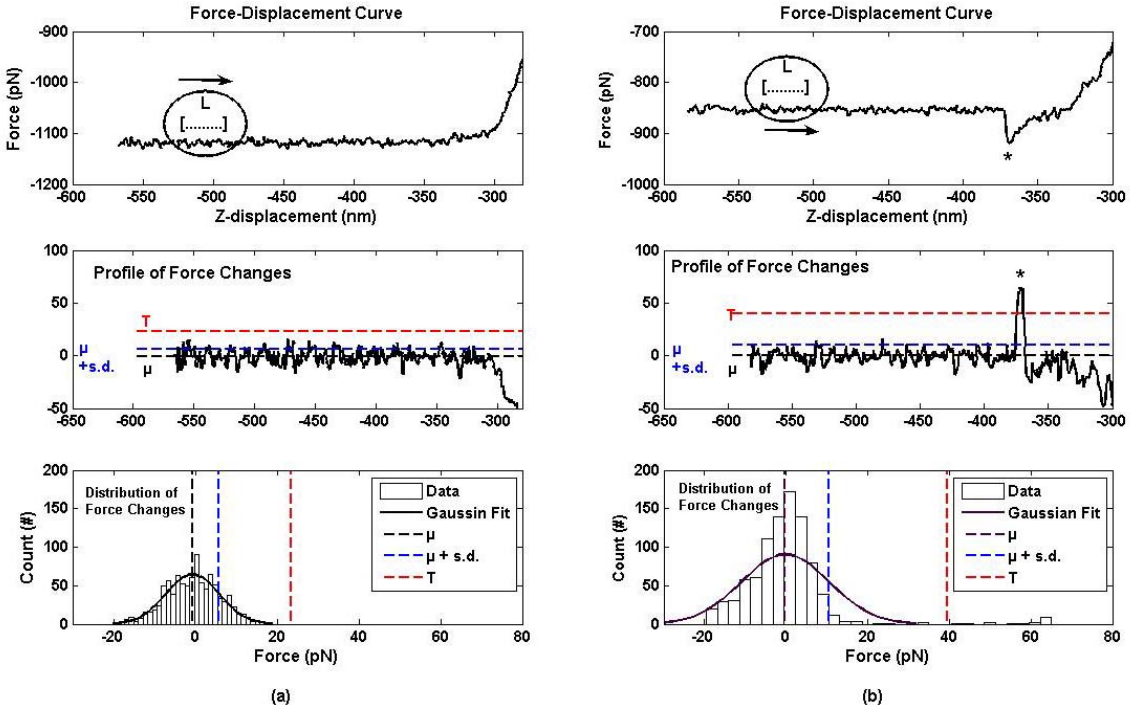

Figure 3.5 Two typical retract curves containing (a) no bond rupture and (b) a single bond rupture are shown in the first row. Sliding window of width L (~5 nm) is used to calculate the profile of changes in the force for all data points along the Z-displacement (arrow indicates the direction of sliding). Profiles of force changes are fitted using Gaussian distribution (third row) with mean (μ) and standard deviation (s.d.). Value of μ (black dashed line), μ + s.d. (blue dash line) and 99.99% threshold T (red dash line) of Gaussian test (p=0.0001) used for detecting the bond rupture (*) are superimposed on the observed changes in the force values for the data points (second row). Only F-D curves with bond rupture (*) will have force values greater than the threshold set (i.e. values fall outside the red line).

The loading rate is derived by multiplying the reproach speed (v) and the effective spring constant k_{eff} (obtained from the slope of the reproach curve prior to the rupture of the

bond, Eq. 2.5). The rupture force measurements are partitioned by using binning windows of 50 pN/s for loading rates between 100 and 1000 pN/s and by binning windows of 500 pN/s for loading rates between 1000 and 10,000 pN/s[83, 85]. Each bin yields a mean force or peak force by Gaussian fitting. By plotting the force in each bin as a function of loading rate, the unstressed dissociation rate and reactive compliance for the molecular interactions can be extracted. These parameters characterize the binding interactions at the single molecule level.

3.6 Design, Fabrication and Calibration of Cell Stretcher

A microscope mountable cell stretching device was designed based on a previously described set up[118]. The fabrication was done by AEC engineering, Singapore. The device basically consists of three parts: base, clamp and a press (Fig. 3.6a). The base contains a groove and sits on the microscope stage. The clamp holds a flexible silicone membrane and is placed on the base. When the press pushes the membrane into the groove in the base, the membrane is subjected to a uniform and circumferential mechanical strain (Fig. 3.6b). The depth to which the press indents the membrane determines the magnitude of mechanical strain applied. A motor controls the depth, duration and frequency of indentation by the press. The motor in turn is controlled by a computer through a LABVIEW^{TM} based user interface programme. The whole cell stretching system with the microscope is enclosed in an incubation chamber that allows for maintaining the temperature at 37^0 C. Furthermore, a mixture of 95% air and 5% CO_2 is introduced into the "press" through a small valve located at the rear. Regulating the temperature and CO_2 makes it possible to apply mechanical strain to cell monolayers for

long durations. The cell stretcher is mounted on a Nikon microscope equipped with a laser confocal scanning head and a perfect focus system (Fig. 3.7). The confocal microscope allows for obtaining optical sections while the perfect system prevents drifting of the objective focus during observations involving long periods.

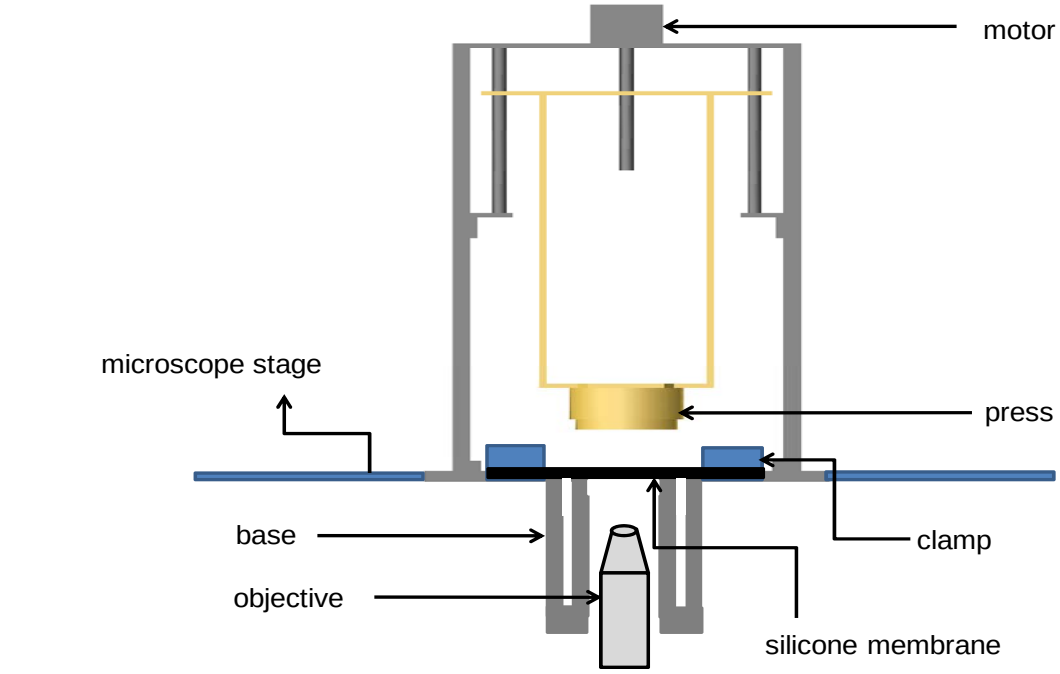

(a)

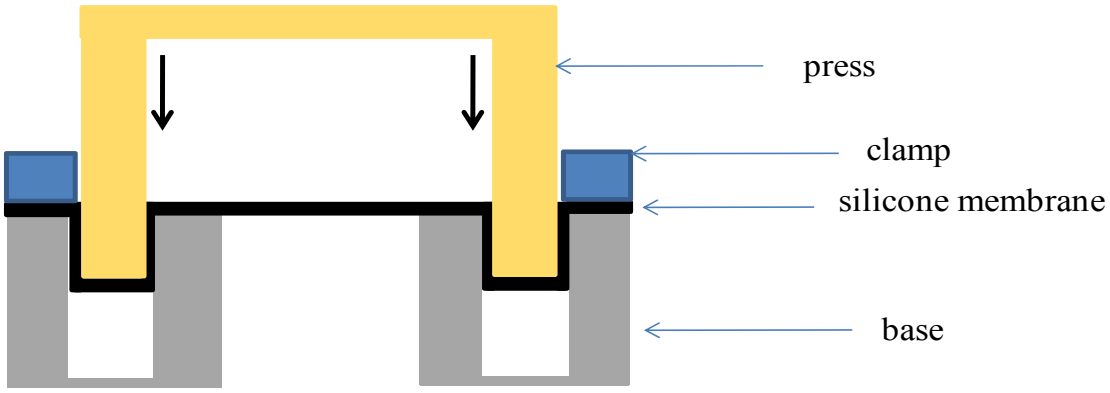

(b)

Figure 3.6 (a) Schematic of the microscope mountable circumferential cell stretcher and (b) close up view of the press, base and clamp of the cell stretcher.

Silicon membranes (250µm thick) were purchased from Specialty Manufacturing (Saginaw, MI). The membranes were cut to the appropriate size and placed inside the clamp to be firmly held by screws. The clamp with the membrane was then mounted on the base for stretching. For calibrating the cell stretcher, a previously described method was used[118]. Roughly equidistant markings were made on the membrane starting from the centre and radiating out using a marker. Images of the membrane with the markings were captured for different magnitudes of indentation by the 'press'.

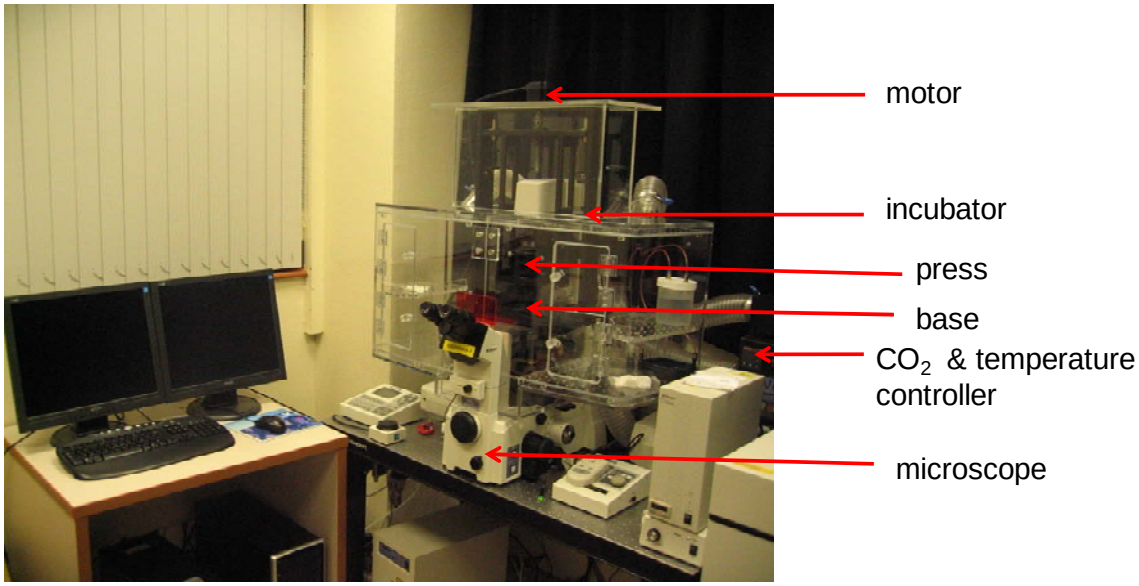

Figure 3.7 Cell stretching device mounted on a laser confocal microscope enclosed in an incubation system.

Using ImageJ software, the distance between the markings was calculated in pixels. The strain was then calculated as the ratio of the change in distance between two markings after stretch to that of the distance between the markings before stretch. For assessing the uniformity of the stretch in all directions (radial strain), strain was calculated along different directions (0^o, 90^o, 180^o and 270^o). For assessing the uniformity of stretch at the

centre and the periphery (circumferential strain), strain was calculated for one pair of points at the centre (blue arrows, Fig. 3.8) and another pair of points at the periphery (red arrows, Fig. 3.8). Results show that the strain in different directions and at the centre of the membrane as well as at the periphery for different magnitudes of indentation by the press is relatively uniform (Fig. 3.9). The maximum strain that could be achieved was ~60%. Also, the magnitude of strain showed a linear correlation with the indentation of the press for strain magnitudes between 5% and 60% (dashed lines, Fig. 3.9). However, at very low strain magnitudes (<5%), the correlation was not linear. Since 20% strain was applied in all our experiments, we were well within the linear range.

Before seeding cells on the silicone membranes, the membranes were plasma cleaned for 30 minutes and left exposed to UV in a laminar hood overnight. The membranes were then incubated with bovine collagen (0.3mg/ml in PBS, Nutragen) overnight in an incubator. The excess collagen was washed off using PBS. MDCK cells were seeded at a density of 40,000 cells/cm^2. They were allowed to grow to ~100% confluence to form a uniform monolayer of cells (~2-3 days).

At confluence, one membrane was transferred to the cell stretcher while the other was left as a control in the incubator. Cells were subjected to a mechanical strain of 20% at a frequency of 0.25Hz (2 seconds of stretch and 2 seconds of relaxation) for a duration of 24 hours. At the end of 24 hours, the cells were either fixed and stained for TJ proteins or lysed and subjected to protein gel electrophoresis. For cell proliferation assays using BrdU method, BrdU (1:500 diluted in culture medium) was added to the cells one hour before the end of stretching.

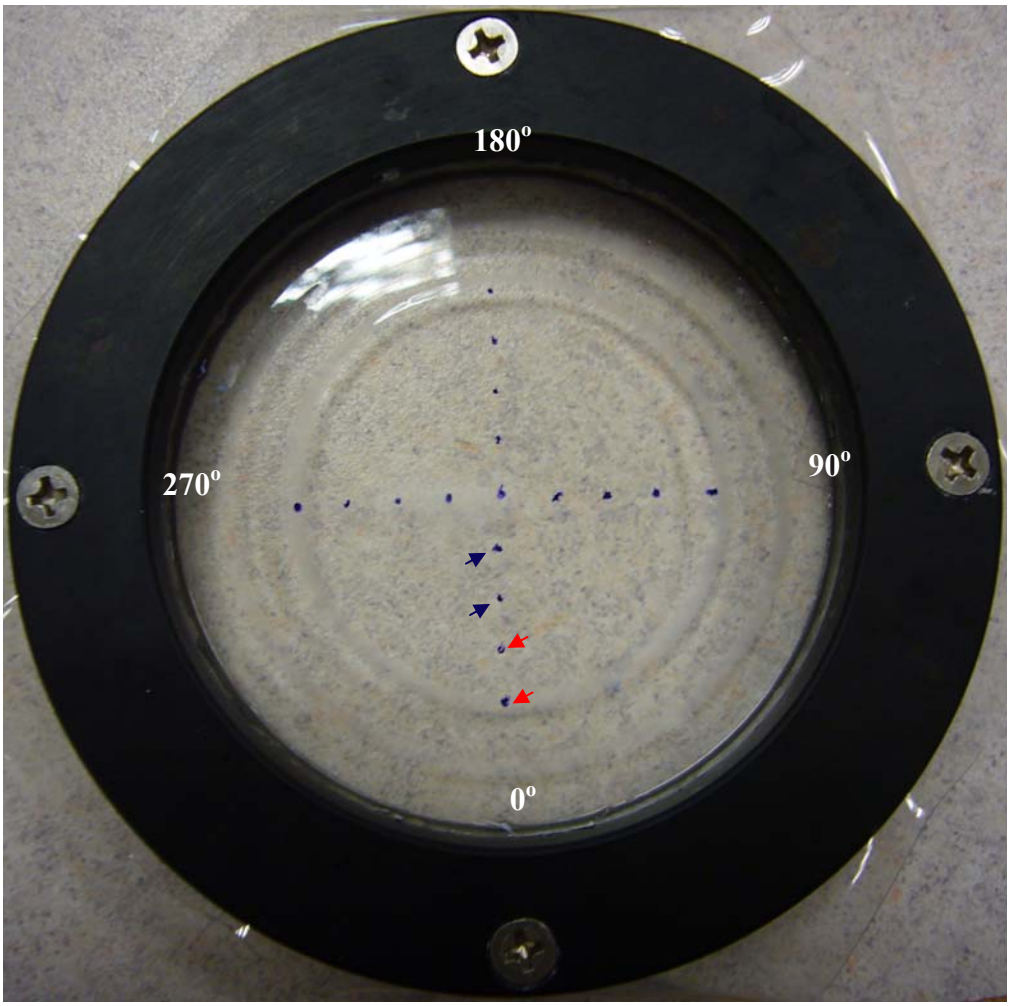

Figure 3.8 Clamp with a silicone membrane showing markings used for calibration. Strain was obtained in four perpendicular directions (0^0, 90^0, 180^0 and 270^0) and for points at the centre (blue arrows) and at the periphery (red arrows) of the membrane.

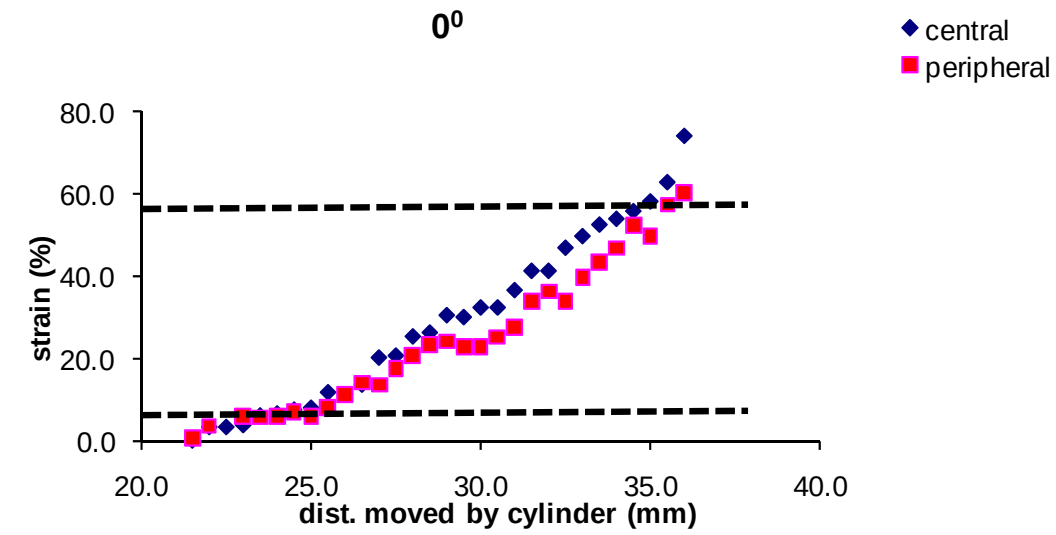
0^0
central
peripheral
80.0
60.0
40.0
20.0
0.0
strain (%)
20.0
25.0
30.0
35.0
40.0
dist. moved by cylinder (mm)

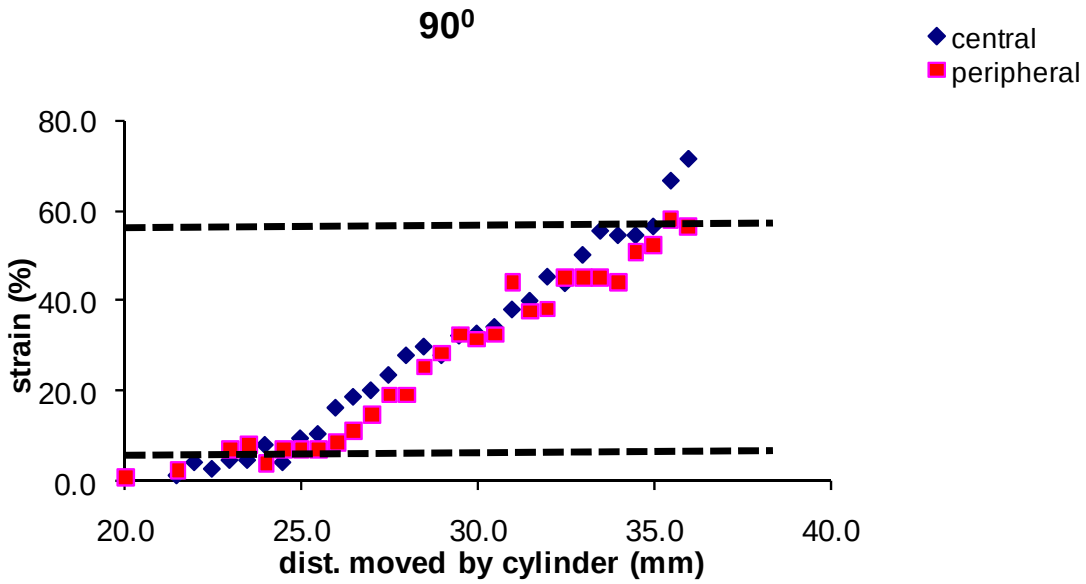
90^0
central
peripheral
80.0
60.0
40.0
20.0
0.0
strain (%)
20.0
25.0
30.0
35.0
40.0
dist. moved by cylinder (mm)

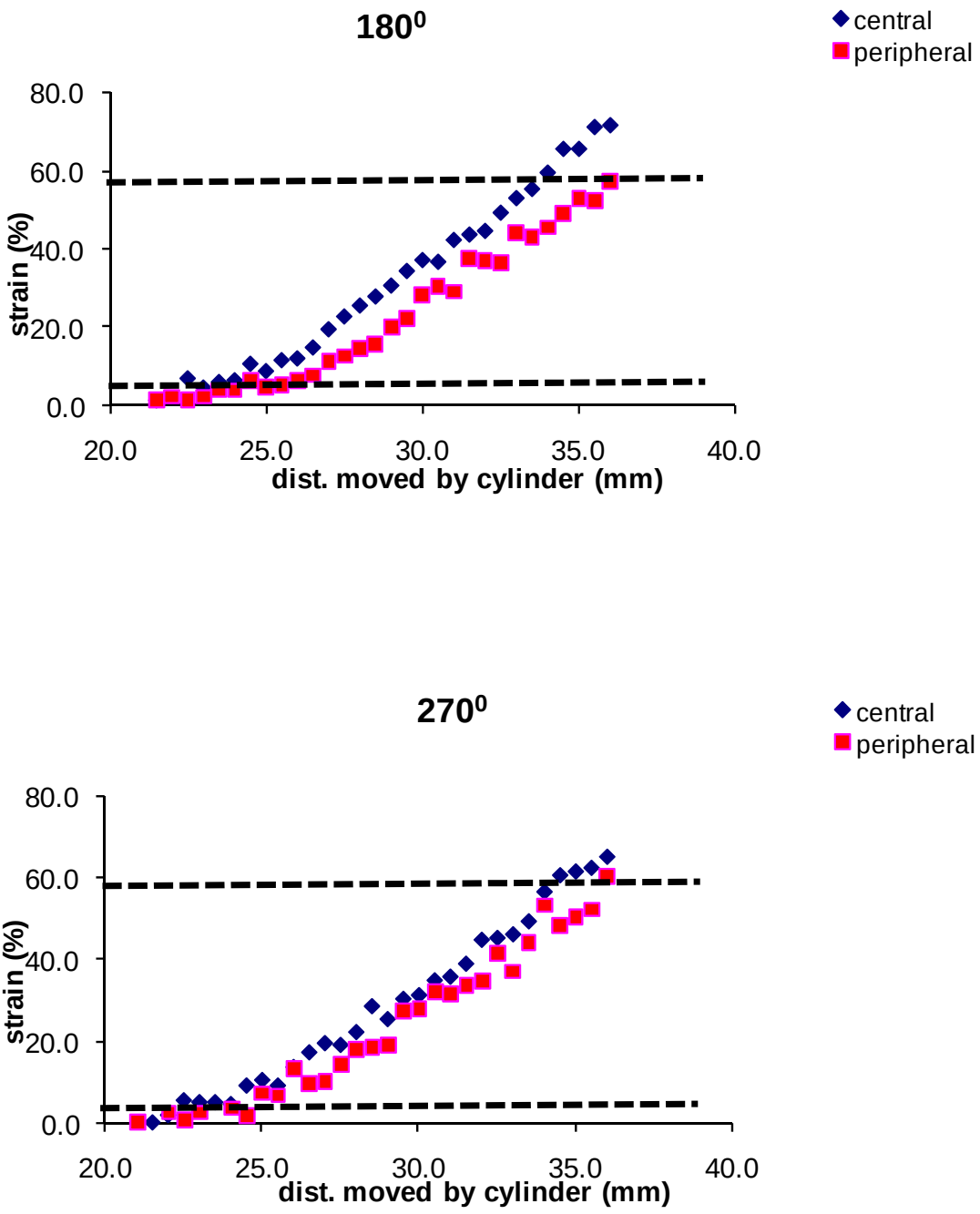

Figure 3.9 Plot of strain in different directions and for points at the centre and periphery of the membrane for different magnitudes of indentation by the press. Dashed lines represent the region within which the magnitude of strain increases linearly with the indentation distance of the press.

3.7 Immunofluorescence Staining, Protein Gel Electrophoresis and BrdU Staining

(a) Immunofluorescence Staining

Cells grown on membrane were washed in PBS and fixed using 4% paraformaldehyde (PFA) in PBS for 15 minutes. For staining occludin, cells were subjected to a gentle pre-extraction step using a pre-extraction buffer (0.2% Triton X-100 in 100mM KCL, 3mM MgCl2, 1mM CaCl2, 200mM sucrose, and 10mM Hepes (pH 7.1) for 2 min on ice) prior to fixation. After fixation, cells were permeabilized with 0.1% Triton X-100 for 10 minutes followed by blocking with 10% normal goat serum in 0.1% triton X-100 for half an hour. They were then incubated for one hour with primary antibodies (Zymed) diluted 1:20 to 1:50 times in the blocking solution. Cells were washed thrice in PBS and then incubated in fluorescent labeled secondary antibodies (Zymed). The membranes were then mounted on cover slips using Fluorsave (Calbiochem). Images were captured using a Nikon confocal laser scanning microscope. Images of each set of control and stretched samples were acquired using the same acquisition parameters (laser intensity, pixel dwell time, pinhole size and gain).

(b) Protein Gel Electrophoresis

Cells were lysed using RIPA buffer containing 1:1000 protease inhibitors CLAP (chymostatin, leupeptin, antipain, pepstatin, Sigma,). After vortexing for 15 minutes, the lysate was homogenized by passing through a fine gauge needle. Protein content in the lysate was estimated using Bradford assay. The lysate was boiled in sample buffer for 4 minutes and 50ug of protein sample was loaded into each well of a 10% polyacrylamide gel. The proteins were then transferred to a PVDF membrane. Membranes were blocked

in 5% non-fat milk in 0.1% TWEEN 20 in PBS for one hour. The membranes were then incubated with primary antibodies (1:1000) followed by HRP tagged secondary antibodies (1:4000). Detection of the protein bands was done using Super Signal West Pico Chemiluminescent Substrate (Pierce). The membranes were exposed to autoradiography films (GE healthcare) for five minutes and then developed in a developer (KODAK).

(c) BrdU Staining

For studying cell proliferation rate, BrdU labeling and detection kit was used (Roche, USA). After 23 hours of stretch, stretching was stopped and medium was replaced with BrdU containing culture medium (1:500 dilution of stock). Stretching was resumed again for one hour. At the end of 24 hours of stretching, cells were washed and fixed in a mixture of 70% ethanol and 30% 50mM glycine (pH 2.0). Following this, they were incubated in a solution of primary antibody against BrdU mixed with nucleases. Nucleases are necessary to enhance the accessibility of incorporated BrdU to the antibodies. Following this, cells were incubated in fluorscein labeled secondary antibody. The cell nuclei were counterstained with DAPI (1μg/ml). Images were acquired on an inverted fluorescence microscope (Leica, Germany) using a 20X objective. For every region, an image of BrdU positive nuclei was first collected (by exciting with blue light) followed by the total nuclei in the region (by excitation with UV light). Six different regions were captured for analysis in each experiment and three independent experiments were carried out. Nuclei were counted manually and the proliferation rate was defined as the ratio of BrdU positive nuclei to that of the total nuclei in a given region.

4 Single molecule force spectroscopy study of homophilic nectin-1 interactions

4.1 Introduction

Nectins are cell adhesion molecules (CAMs) that localize at adherens junctions along with E-cadherins. They belong to the immunoglobulin (Ig-) superfamily of proteins. There are four types of nectins- nectin-1, -2, -3 and -4. Nectins were first discovered during the search for the physiological functions of the polio virus receptor (PVR). Southern blot hybridization analysis revealed that the murine genome contained a homologous receptor identical to polio virus receptor[50]. The discovery of the murine PVR homologue (MPH) was followed by the discovery of two proteins in human placenta that closely resembled PVR. These were named Polio virus receptor related proteins (PRR1 and PRR2)[52]. It was also shown that PRR2 was the true homologue of MPH.

Despite a significant sequence and structural similarity, both MPH and PRR proteins did not bind to any of the three serotypes of polio virus. It was, however, found that replacing the first domain of the murine homologue with that of the PVR conferred the homologue with ability to bind to polio virus. Further experiments showed that both PRR1 and PRR2 are glycoproteins that are expressed ubiquitously in several tissues including hemopoietic cell lines. Cells transfected to express PRR2 showed marked aggregation which was inhibited by the addition of a PRR2/Fc fusion chimera[51, 54]. This strongly suggested that PRR2 mediated aggregation was mediated by a homophilic mechanism. This

adhesion was shown to be independent of the presence of divalent cations. Furthermore, immunostaining showed that PRR2 localized to intercellular junctions and was absent from free cell edges. It was also found that l-afadin (a novel actin filament binding protein localizing at AJs) and PRR co-localized at cadherin-based cell-cell AJs in various tissues and cell lines[42, 119]. The PRR proteins were renamed nectins (taken from the Latin word "necto" meaning "to connect"). Using L-cells transfected with nectin-1 (PRR1) and nectin-2 (PRR2), it was shown that adhesion mediated by nectins, similar to that mediated by several other Ig- superfamily CAMs, can occur even in the absence of Ca^{2+} ions. The Ca^{2+} independent adhesion activity of nectins distinguishes them from adhesion mediated by E-cadherins. This established the nectin/afadin complex as an independent intercellular adhesion system at AJs. The nectin/afadin intercellular adhesion system has now been shown to be widely distributed in different tissues and cells. Apart from epithelial cell junctions, some of the locations in which it has been shown to play an important role are endothelial cell junctions, neuronal synapses, germ cell/Sertoli cell and Sertoli cell/Sertoli cell junctions (Fig. 4.1).

4.1.1 Structure and Organization of Nectins

Structurally, all nectins have an extra cellular region, a single transmembrane region and a cytoplasmic region (Fig. 4.2a)[41]. The extracellular domains consist of three Ig-like loops (two membrane proximal C domains and one membrane distal V domain). Most members of the nectin group of proteins contain a conserved four residue motif (Glu/Ala-X-Tyr-Val) in the cytoplasmic region that interacts with the PDZ domain of the adaptor molecule afadin.

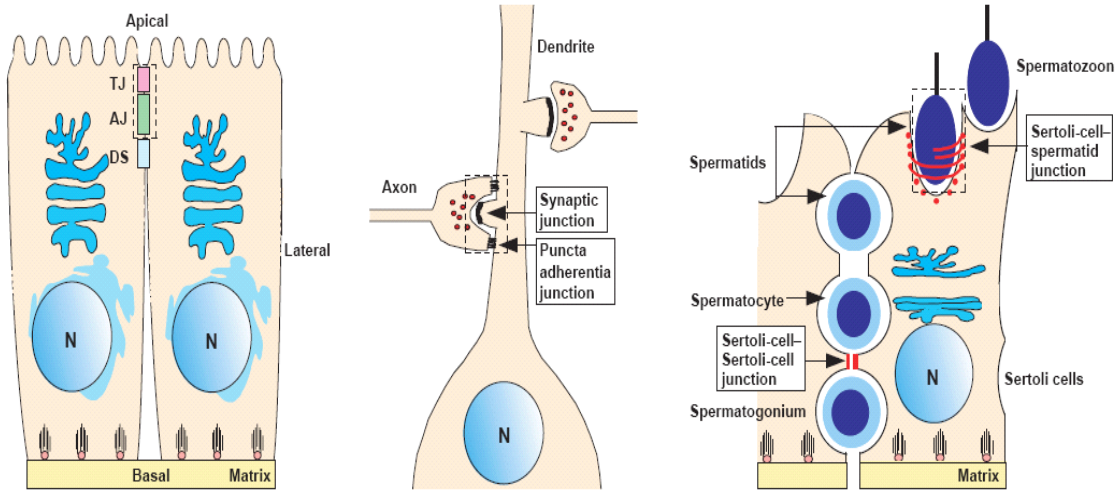

Figure 4.1 Distribution of nectins in different intercellular junctions (a) Epithelial cells (b) neuronal synapses and (c) Sertoli cell-spermatid junction[41].

Afadin is a large adaptor molecule (MW ~205kD) that contains a PDZ domain, three proline rich regions and an F-actin binding domain (Fig. 4.2b)[42]. While the PDZ domain interacts with the cytoplasmic tail of nectins, the F-actin binding region connects it to the actin cytoskeleton. In this manner, afadin acts as an adaptor molecule that connects nectins to the actin network of the cell. Nectins are conserved from humans to rodents. When nectin-2 transfected cells were trypsinized into single cell suspensions, treated with a cell membrane impermeable cross linking agent (e.g. BS^3), lysed and probed with anti-nectin antibody; it was found that in addition to the ~70kD band (that represents monomeric nectin), there was another band of approximately 140kD. This strongly suggested that nectins undergo cis-dimerization on the cell membrane [54, 120]. Mutational studies showed that the second extracellular loop is essential for cis-

dimerization of nectins. Mutant nectins, where the second extracellular loop was deleted (nectin-ΔIg2), did not show the characteristic higher molecular weight dimeric band following cross linking with BS^3.

As mentioned before, L-cells stably transfected with full length nectins showed increased aggregation. Several lines of evidence point towards the role of the membrane distal first extracellular loop in mediating the trans-interactions that cause increased aggregation in these cells[121]. Point mutations in the first extracellular loop abrogate the trans-dimer formation but not cis-dimerization. Herpes glycoprotein D, which binds to the first extracellular loop of nectin, prevents trans-dimer formation but not cis-dimerization. An antibody against the first extracellular loop also prevents trans-dimer formation. Finally, fragments of the first extracellular loop have been shown to form trans-dimers. Thus, the first extracellular loop of nectin is essential for the formation of trans-dimers. Also, L-cells stably transfected with nectin-ΔIg2 (nectin with its second extracellular loop deleted) did not show cell aggregation behavior seen in cells transfected with full length nectin. This suggested that the second extracellular loop was essential for both cis and trans-dimerization. Taken together these facts show that (a) nectin cis-interactions are mediated by the second extracellular loop (b) nectin trans-interactions are mediated by the first extracellular loop and (c) cis-interactions are a pre-requisite for trans-interactions to take place. It was also seen that a nectin mutant that lacked the C- terminal four amino acids (essential for binding to afadin) showed similar cell adhesion activity when transfected into L-cells. This showed that the trans-interactions between nectins can occur independent of their association with afadin i.e.,

nectin trans-interactions do not require their anchoring to the actin cytoskeleton. The function of the third Ig-like loop currently remains unknown.

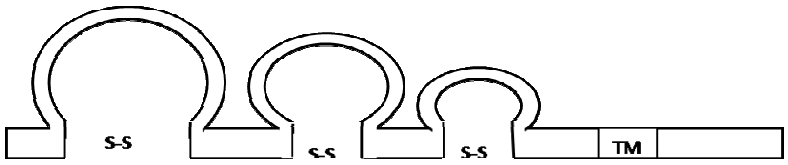

(a)

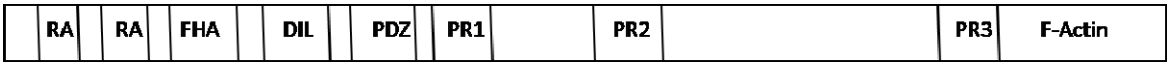

l-afadin

(b)

Figure 4.2 Schematic of (a) nectin showing the three extracellular Ig-like loops, a short transmembrane region, a cytoplasmic tail and (b) afadin showing the PDZ domain that binds nectin and the F-actin binding region that links it to the actin cytoskeleton[41]**.**

4.1.2 Role of Nectins in Cell Adhesion

As mentioned in the previous section, the primary function of nectins is intercellular adhesion. For a long time E-cadherins were considered the primary anchors of intercellular adhesion complex. This was strongly supported by the fact that transfection of E-cadherin into non-adherent cell types (e.g. L-fibroblasts) conferred strong aggregation properties to the cells[44, 122]. Furthermore, Ca^{2+} chelating agents like EDTA strongly inhibited intercellular adhesion in a variety of cell types. Since E-cadherin adhesion is strongly dependent on the presence of extracellular Ca^{2+} ions, it provided additional support that E-cadherins mediated adhesion formed the basis for

intercellular adhesion. Based on the crystal structure of E-cadherin, it was proposed that dimers of E-cadherins undergo *trans*- interaction with corresponding dimers on adjacent cell to form the intercellular adhesion (Fig. 4.3)[45]. However, the discovery of nectins has brought about a totally new perspective on how intercellular adhesion is initiated and maintained. It is becoming increasingly clear that nectins and E-cadherins function in a well coordinated manner to establish a mature intercellular adhesion complex.

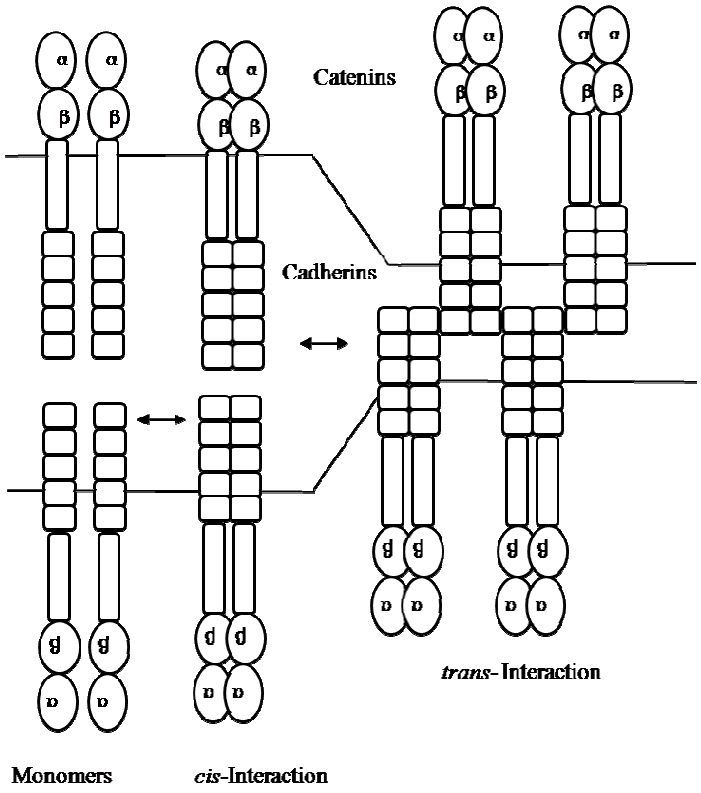

Figure 4.3 Schematic depiction of adhesion mediated by E-cadherins. Initial cis-dimerization is followed by trans- interactions with dimers from adjacent cells to form adherens junction[41].

Over expression of nectin-1 in cells was shown to increase the velocity of formation of E-cadherin based junctions while addition of nectin-1 inhibitors decreased the velocity[55, 57]. This demonstrated for the first time that the assembly of E-cadherins was modulated

by nectin-1 mediated interactions. Further investigations showed that *trans*-interactions mediated by nectin-1 recruit E-cadherins in an afadin dependent manner[56]. The recruited E-cadherins, in turn, bound $p120^{ctn}$, β- catenin, and α-catenin. However, the adhesion strength of interactions mediated by the initially recruited E-cadherins was found to be very low. Activation of small G proteins e.g. Rap1 caused by the *trans*-interactions between nectin-1, was found to significantly enhance the interaction strength of the recruited E-cadherins. Together, these facts suggest that while *trans*-interactions occurring between nectin-1 are responsible for recruiting E-cadherins to the adherens junctions, Rap1 activation via nectins plays an important role in strengthening E-cadherin mediated adhesion[56].

4.1.3 Single Molecule Force Spectroscopy Study of Homophilic Nectin-1 Interactions

The emergence of nectins as a relatively new intercellular adhesion system has made them a focus of extensive research. In spite of the significant biochemical and molecular biology work carried out to elucidate their structural and functional properties, little work has been done to characterize their adhesion properties particularly at the level of single molecule. Most of the previous studies focusing on the intercellular adhesion forces mediated by nectins have been predominantly qualitative. The initial experiments that discovered the adhesion properties of nectins were based on centrifugation assays performed on transfected L-cells[55]. These experiments merely showed that transfection of nectins lead to an enhanced cell aggregation. Later, experiments performed on transfected L-cells using dual micropipette assays gave some quantitative information

regarding the adhesion forces mediated by nectins[44]. It was observed that nectin mediated cell adhesion was weak when compared to that mediated by E-cadherins. Furthermore, while adhesion mediated by E-cadherins was abolished in the presence of a calcium chelator like EDTA, nectin mediated adhesion was unaffected. However, no experiments were performed to analyze the kinetics or magnitude of nectin mediated interactions at the level of single molecule.

As described in previous chapters, single molecule force spectroscopy using AFM has emerged as a powerful tool to understand the interaction forces and dynamics of molecular interactions. Moreover, SMFS using AFM also allows us to probe the interactions under more physiological conditions. This chapter describes how the elucidation of adhesion kinetics of homophilic nectin-1 interactions using SMFS experiments provides additional support for the role of nectins as initiators of cell adhesion.

4.2 Materials and Methods

The atomic force microscopy setup for SMFS experiments, cantilever functionalization with nectin-1/Fc fusion protein (Nef-1), data acquisition and analysis are described in detail in Chapter 3.

4.3 Results

4.3.1 Force Spectroscopy of L-cell/Nef-1 Interactions

AFM cantilevers functionalized with Nef-1 were used to probe L-fibroblasts (Fig. 4.4). These cells were chosen because they express low levels of endogenous nectin-1[120].

Furthermore, since they do not express nectin-3 (with which nectin-1 can interact in a heterophilic manner), all observed interactions can be attributed to homophilic nectin-1 interactions. Also, fusion of the F_c fragment to the C-terminal of nectin-1 provides optimal access of the N-terminal extracellular loops which mediate *trans*- interactions.

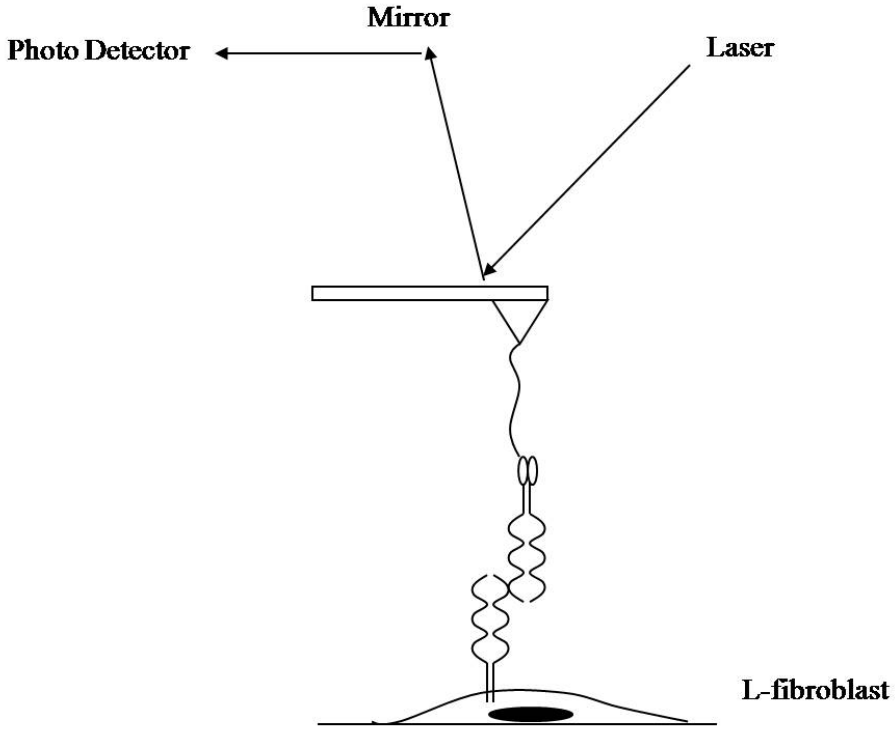

Figure 4.4 Schematic of SMFS set up for probing nectin-1 mediated interactions.

Force-distance curves were obtained by lowering the functionalized cantilever on to a well adherent L-fibroblast (Fig. 4.5). A contact force of 200pN was applied for a duration of 1ms. The retraction velocity of the cantilever was varied from 1 to 10μm/s. More than 500 F-D curves were obtained for each velocity at a binding frequency of <30%. The curves were analyzed for the loading rate and rupture force magnitude as described under methods.

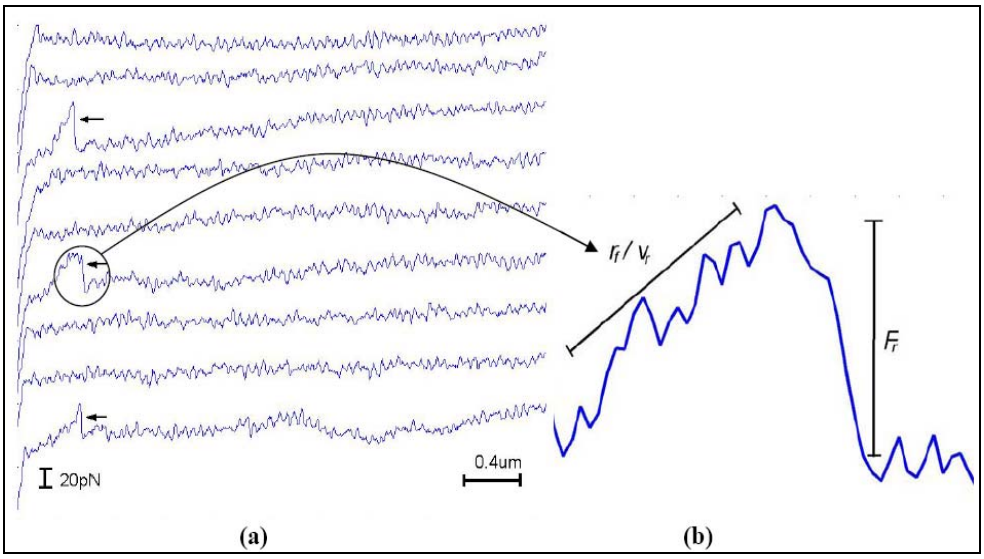

Figure 4.5 Typical force-distance curves obtained at a cantilever reproach velocity (V_r) of 5 μm/s on L-fibroblasts using nef-1 functionalized cantilever. Arrows indicate rupture of nef-1/nectin-1 homophilic trans-interactions. Only curves showing a single clear rupture event were used for generating histograms (b) The slope of the curve before rupture multiplied by the reproach velocity (V_r , expressed in μm/s) defines the loading rate (r_f , expressed in pN/s). The rupture height gives the bond strength (F_r) (expressed in pN)[123].

For control experiments, force curves were obtained on L-fibroblasts using cantilevers functionalized with anti-F_c antibody only. The force histograms so obtained showed few adhesion events (~3%, Fig. 4.6, Table 4.1). To rule out the possibility of non-specific interactions of Nef-1 with other proteins on the cell surface, force curves were also obtained on glass cover slips on which Nef-1 was immobilized, under similar conditions of contact force and time. The force histogram so obtained, showed a higher frequency of interactions compared to both the control experiment as well as the histogram obtained on cells (Fig. 4.6, Table 4.1). This was to be expected since the average concentration of endogenous nectin-1 expressed by the L-fibroblasts is very low. These control experiments strongly supported the fact that only specific interactions mediated by nectin-1 were being probed.

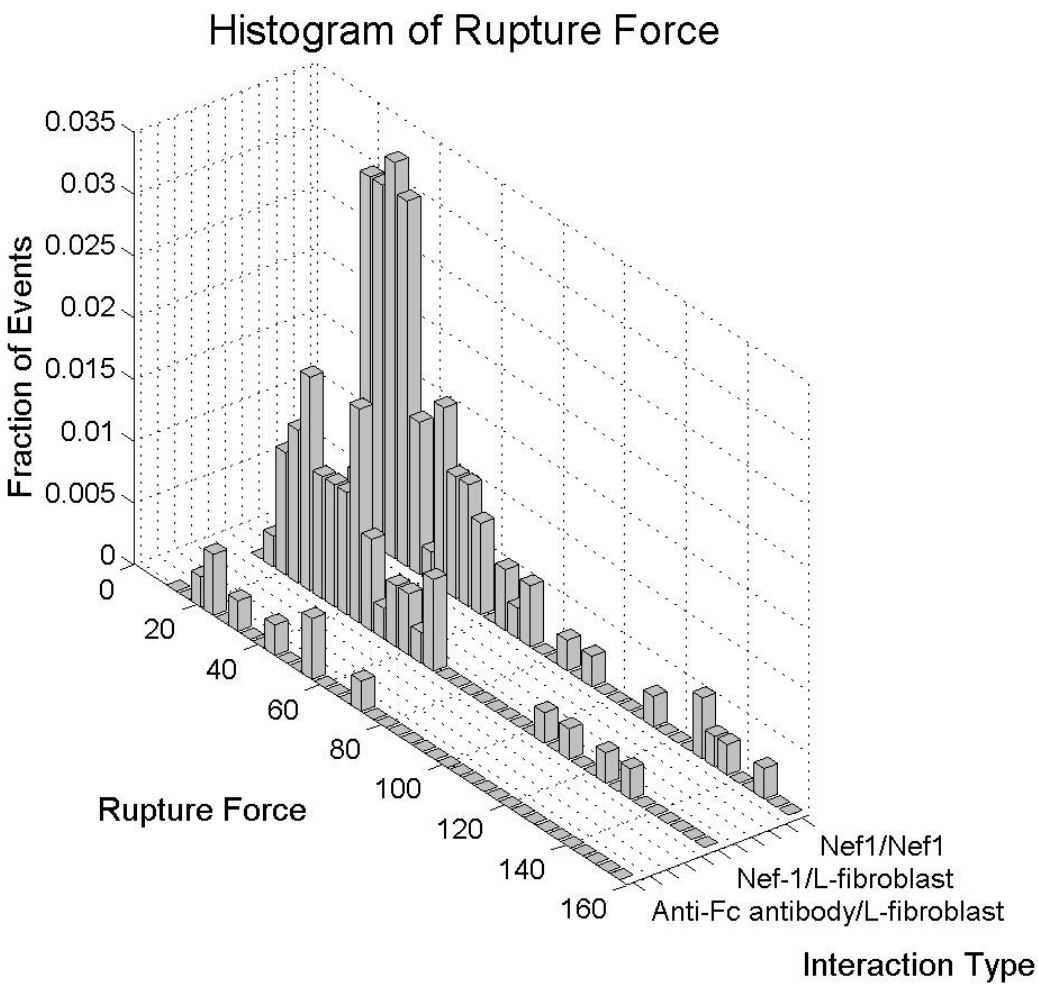

Figure 4.6 Rupture force histograms of interactions between Nef-1 functionalized tips and L-fibroblasts (Nef-1/L-fibroblast), anti-Fc antibody functionalized tips and L-fibroblasts (anti-Fc antibody/L-fibroblast), Nef-1 functionalized tips and Nef-1 functionalized cover slips obtained at a reproach velocity of 5μm/s[123].

Table 4.1 List of different interactions probed corresponding to histograms depicted in Fig. 4.6.

Interaction Type	**AFM Tip**	**Substrate**
1. Anti-Fc antibody/L-	Anti-Fc	L -cells
2. Nef-1/L-fibroblasts	Nef-1	L -cells
3. Nef-1/Nef-1	Nef-1	Nef-1 on cover slips

All the receptor/ligand pairs tested, corresponding to the histograms shown in Fig. 4.6, are listed in Table 4.1.

To analyze the biophysical nature of nectin-1 mediated homophilic interactions, the magnitude of the rupture events and the corresponding loading rates was extracted for all F-D curves showing a single clear rupture event. As mentioned in chapter 3, the most commonly used Bell-Evans model predicts a linear relation between the bond rupture force and logarithm of the applied loading rate. For nectin-1 mediated interactions, when the magnitude of rupture force was plotted against the logarithm of the applied loading rate, the data points appeared to be scattered instead of clustering into a single region (Fig. 4.7).

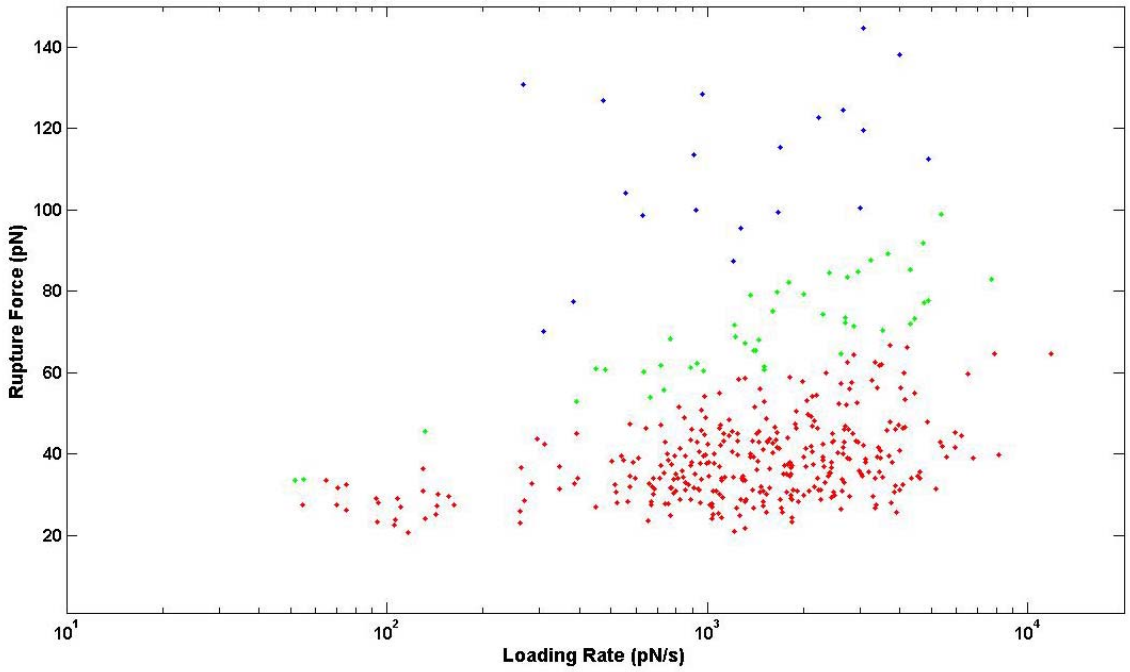

Figure 4.7 Rupture force magnitude plotted against the logarithm of loading rate for homophilic nectin-1 interactions. Data points appear to be scattered into different clusters.

One possible explanation for such a distribution pattern is that the data points clustering in the lower strength regime correspond to the rupture of a single bond whereas the data points in the higher strength regime correspond to the rupture of double and triple bonds in parallel (Fig. 4.8). Such clustering of data points has previously been observed in interactions of the protein mucin-1 and its antibody[124]. Alternatively, such pattern could also arise due to the existence of multiple binding configurations between two proteins. Such multiple binding configurations have been proposed for interactions between E-cadherins[125].

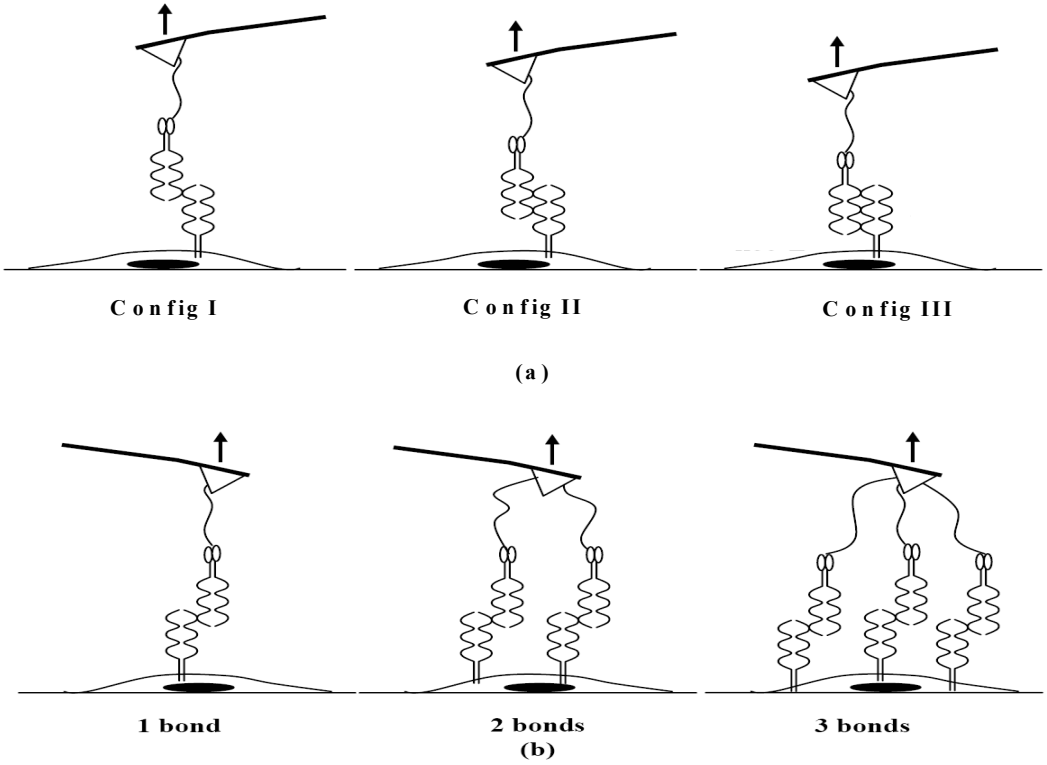

Figure 4.8 Schematic depiction of (a) proposed multiple interaction configurations of Nef-1/nectin-1 trans-interactions (b) Possible cases of simultaneous rupture of one, two or three bonds. Multiple bonds can rupture either in parallel or in zipper fashion.

We propose that the observed clustering is the result of multiple binding configurations between nectin-1 mediated interactions rather than multiple bond formation due to the following reasons. Firstly, such multiple binding interactions have been observed in heterophilic interactions between nectin-1 and nectin-3[125]. Since there is a significant homology between nectins, it is very likely that such multiple binding configurations can also occur in homophilic nectin-1 interactions. Secondly, it is reasonable to assume that the cantilever, intermolecular bond between the interacting protein molecules and the cell constitute a system of three springs in series. Since the stiffness of the cantilever ($k_{cantilever}$) and the cell (k_{cell}) is much greater than that of the intermolecular bond (k_{linker}), the effective stiffness of the cantilever-linker-cell system is dominated by the stiffness of the intermolecular bond. If the scatter was a result of double or triple bonds rupturing in parallel, the effective stiffness of the system for rupture events in the higher strength regime would be expected to be twice or three times that observed for the rupture events observed in the low strength regime. However, the effective spring constant for bond ruptures in the low and high strength regime (as calculated from the slope of the retrace curve just before bond rupture) did not show a significant difference (0.334 ± 0.170 pN/nm and 0.320 ± 0.195 pN/nm, respectively). Taken together these facts make it highly unlikely that the clustering of the data points is a result of multiple bond rupture.

4.3.2 Kinetic Parameter Extraction for the Different Interaction Configurations of Nectin-1 Mediated Interactions

To extract the biophysical characteristics of the different interaction configurations of homophilic nectin-1 interactions, it is necessary to fit the data points to a theoretical

model. Since rupture events in the high strength regime were very few compared to those in the low strength regime, individual force histograms obtained at different velocities did not show three distinct peaks. To overcome this problem, maximum likelihood estimation (MLE) method was used for curve fitting the rupture force histogram comprising all the F-D curves obtained at different velocities. The theoretical basis for the MLE method is as follows:

The conditional bond strength probability density function, $P_n(f \mid r_f)$ for a particular loading rate is given by[94, 95]:

$$P_n(f \mid r_f) = \left(\frac{k_{off}^0}{r_f}\right)\exp\left(\frac{f}{f_b}\right)\exp\left[\left(-\frac{f_b k_{off}^0}{r_f}\right)\left(\exp(\frac{f}{f_b})-1\right)\right] \tag{4.1}$$

Where $f_b = k_B T / x_\beta$, k_B is Boltzmann constant, T is temperature, x_β is potential length of the transition state and k^0_{off} is unstressed dissociation rate.

Thus, the bond strength distribution can be obtained by integrating out the prior probability density function of parameter R_f, where $R_f = r_f^{-1}$ is the inverse loading rate:

$$P_n(f) = \int_{R_f} P_n(f \mid R_f) P(R_f) dR_f \tag{4.2}$$

In our experiments, the prior distribution of R_f was found to follow an exponential distribution; $P(R_f) = (1/u_R)\exp(-R_f/u_R)$, where u_R = 8.22 ± 1.19 x 10^{-3} (Fig. 4.9, $p<0.05$, χ^2 test).

Using Eq. 4.2, the bond strength distribution can be rewritten as:

$$P_n(f) = u_R^{-1} A(f) / B^2(f) \tag{4.3}$$

where $A(f) = k_{off}^0 \exp(f / f_b)$

and $B(f) = f_b k_{off}^0 \left[1 - \exp(f / f_b)\right] - u_R^{-1}$

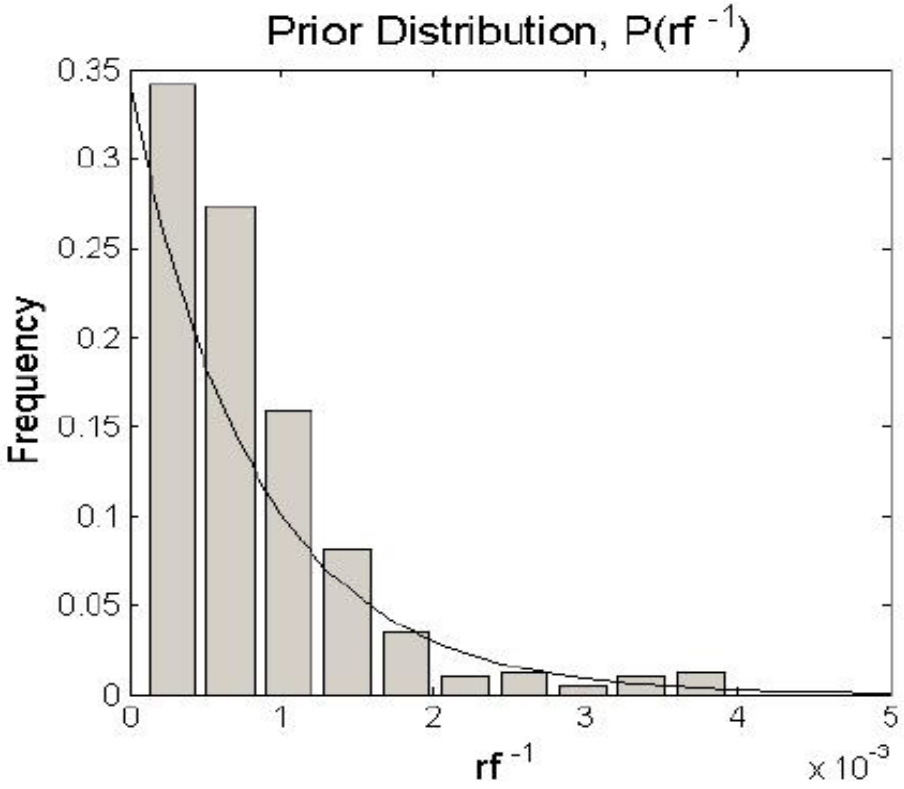

Figure 4.9 Histogram showing the prior distribution of the inverse loading rate (r_f^{-1}) obtained in the experiment fitted with an exponential distribution ($p<0.05$, χ^2 test).

Rupture force (f) between nef-1/nectin-1 pairs (n=1779) at different loading rates (r_f) were pooled into a single histogram. The histogram showed three well defined force peaks corresponding to the three different configurations of homophilic nef-1/nectin-1 trans-interactions (Fig. 4.10).

Fitting of bond strength distributions to multiple bond strength probability density function $P(f) = \sum a_n P_n(f)$ (black dotted curve in Fig 3c), where a_n are freely adjustable parameters to compensate the fraction of subpopulations and n is the number of subpopulations, resulted in three different values for the unstressed off-rate k_{off}^0 and the reactive compliance x_β corresponding to each of the bound states (Table 4.2).

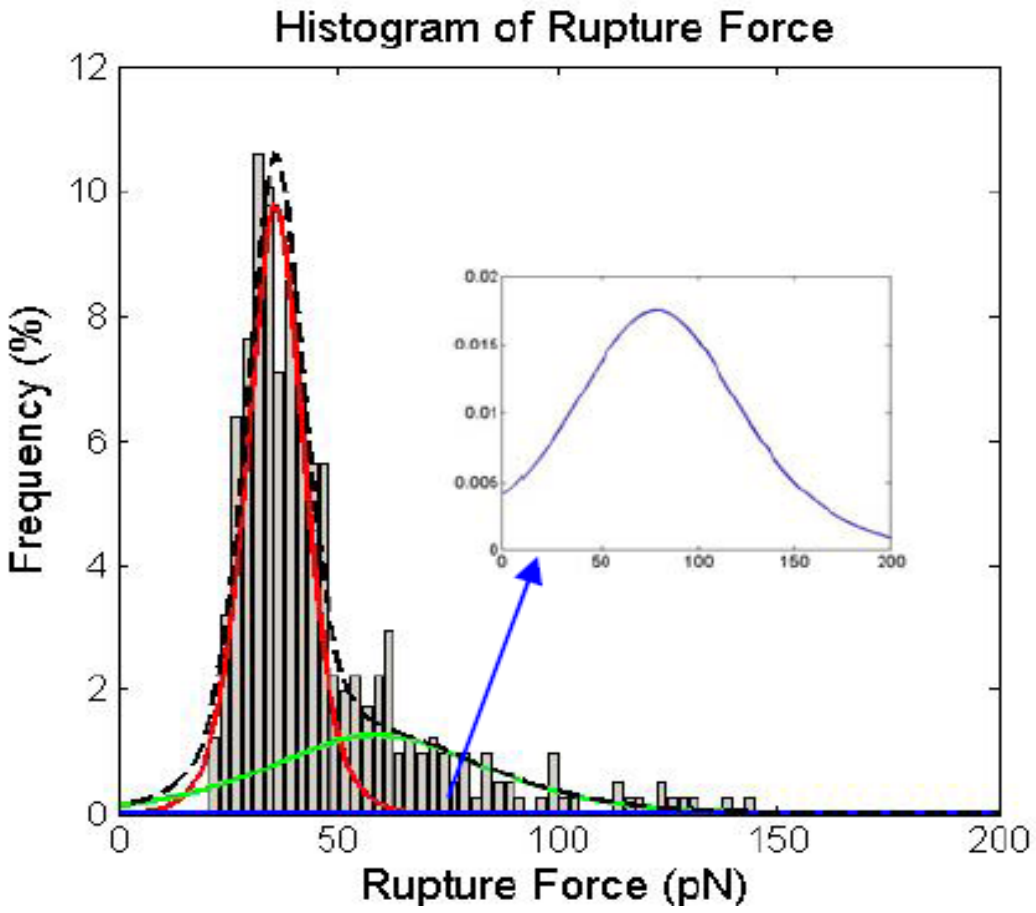

Figure 4.10 All rupture forces (Fr) recorded (interaction probability of 0.23 for n=1779) at different loading rates (r_f) were pooled into a single histogram. Red, green and blue continuous curves represent fittings including parameters to compensate for the fractions of subpopulations of the bond strength probability density function (Eq. 4.1). The black dashed curve represents sum of the three bond strength probability densities while the first, second and third distributions represent Config I (red), Config II (green) and Config III (blue) (corresponding to binding architectures shown in Fig. 4.8). Blue line is enlarged and displayed in the inset figure[123].

Table 4.2 Unstressed off rates and reactive compliance for different interaction configurations of nectin-1.

Molecular Pairs	Rate of dissociation k_{off}^0 (s^{-1})	Reactive Compliance x_β (nm)
E-cad/E-cad*	0.5-1	0.67
	10^{-2}-10^{-6}	1.3
Nef-1/nectin-1 (I)	0.038 ± 0.019	0.962 ± 0.071
Nef-1/nectin-1 (II)	1.155 ± 0.572	0.251 ± 0.032
Nef-1/nectin-1 (III)	1.465 ± 0.779	0.143 ± 0.072

*Data for E-cadherin has been taken from a previous study for comparison[102]. The two unstressed off rates shown correspond to values obtained for interactions between recombinant E-cadherin molecules containing only the N-terminal two domains and full length E-cadherin molecules, respectively.

Since configuration I physically represents the same set of rupture events as a single bond rupture, the kinetic parameters obtained for configuration I can be used to extract the kinetic parameters for the rupture of double and triple bonds either in a parallel fashion or in a zipper manner. Using the Markovian model for uncorrelated rupture of multiple parallel molecular bonds, it has been shown that for parallel attachment (where the load is shared between all of the bonds), the relationship between the loading rate (r_f) , the most probable rupture force (f*), and the number of bonds N is given by[126]:

$$r_f = k_{off}^0 f_b \left[\sum_{n=1}^{N} \frac{\exp(-f^* / nf_b)}{n^2} \right]^{-1} \tag{4.4}$$

Such a system has been studied in the dynamic force spectroscopy of parallel individual bond of the protein Mucin1 with its corresponding antibody[124]. For "zipper" connection, where only one of the bonds experiences the loading force at any given time, it is given by:

$$r_f = \frac{k_{off}^0 f_b \exp(f^*/f_b)}{N} \tag{4.5}$$

where $f_b = k_B T / x_\beta$ the thermal force, k_B is Boltzmann constant, T is absolute temperature, x_β is potential length of the transition state and k^0_{off} is unstressed dissociation rate. Using Eq. 4.4 and 4.5 and the kinetic parameters extracted for configuration I, theoretical curves were plotted corresponding to the rupture of double and triple bonds in parallel (Fig. 4.11a) and in a zipper fashion (Fig. 4.11b).

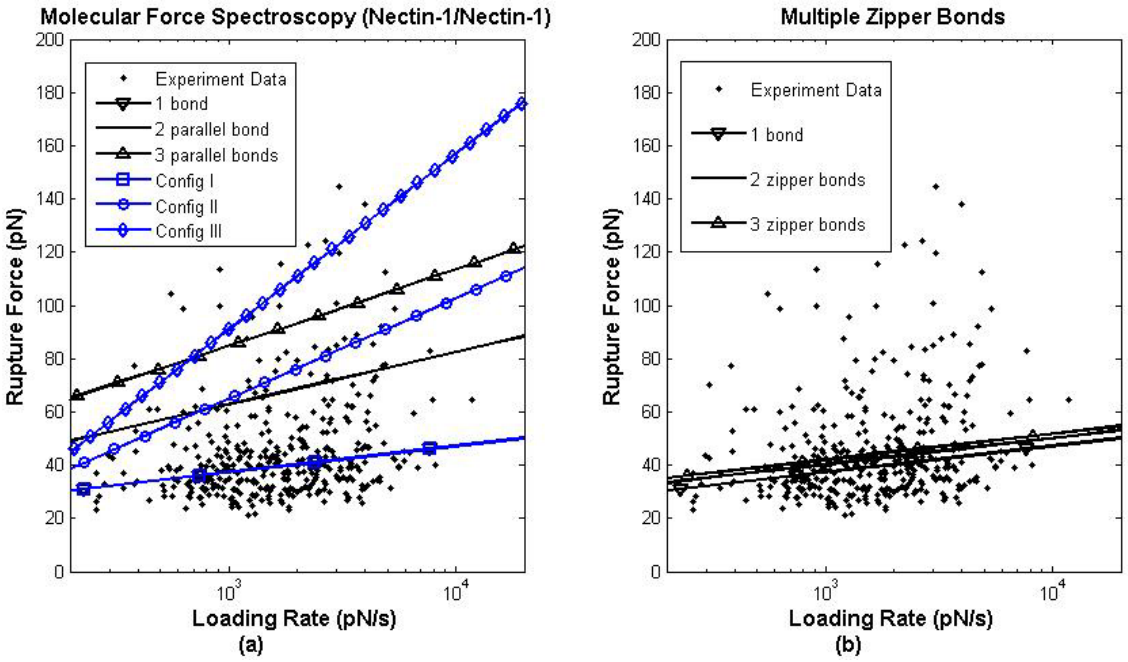

Figure 4.11 Theoretical lines (rupture force vs. loading rate lines) according to different models were fitted and superimposed on the experimental data (black dots). Blue lines: loading rate curves corresponding to the proposed binding architectures shown in Fig 4.8. Black line: loading rate curves according to the Markovian model of detaching identical parallel bonds (see supplementary information for details). (b) Loading rate lines were fitted according to the model of multiple zipper bonds (Eq. 4.5) and superimposed on the experimental data (black dots)[123].

The theoretical curves plotted based on the assumption that the rupture events were a result of multiple bond ruptures in parallel or in a zipper fashion, did not fit the data points well. On the other hand, the curves plotted based on the kinetic parameters obtained assuming multiple interaction configurations fit the data points relatively well (Fig. 4.11a).

4.4 Discussion and Conclusion

The adhesion kinetics of homophilic nectin-1 interactions were elucidated using SMFS. Results show that the interactions between nectin-1 can result from multiple binding configurations. Furthermore, a comparison between the adhesion kinetics of nectin-1 and E-cadherin interactions provides a strong support for a model of cell adhesion in which nectins initiate and stabilize the cell adhesion in the initial stages until the strong interactions mediated by E-cadherins take over to strengthen the adherens junction.

E-cadherins are well established as the major protein component responsible for the mechanical stability and integrity of the intercellular junction. However, initial SMFS experiments carried out on E-cadherin interactions showed that *trans*- interactions mediated by E-cadherin showed a very low $t_{1/2}$[26]. Such a low bond half life contradicted the established role of E-cadherin as cell adhesion stabilizers.

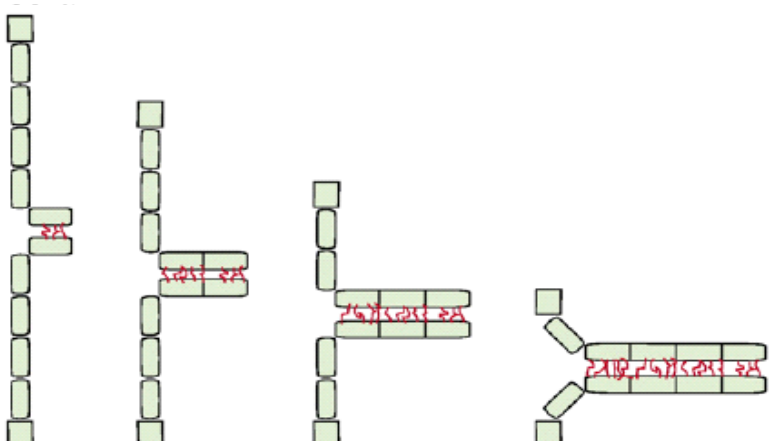

Figure 4.12 Schematic depiction of multiple binding configurations in E-cadherin mediated interactions. Initially, interactions involve only the N-terminal domains. Further recruitment of E-cadherins is followed by multiple domain overlap leading to strengthening of the interaction[125].

Further experiments using truncated recombinant E-cadherin proteins showed that adhesion mediated by E-cadherins expressing only the first two N-terminal domains was significantly weaker than that mediated by the full length E-cadherin. Moreover, interactions between full length E-cadherin molecules demonstrated the existence of multiple binding configurations[102]. These studies suggested that E-cadherin interactions occurred in hierarchical steps. Initial interactions occurring between the first N-terminal domains are weak and short lasting. This is followed by multiple domain overlap leading to the formation of different binding configurations (Fig. 4.13). Since the configurations involving multiple domain overlap show a significantly higher bond half life, the interactions are kinetically more stable (Table 4.2).

The discovery of nectins and their role in modulating E-cadherin mediated interactions has provided a better understanding of how adherens junction formation is initiated and stabilized. Biochemical studies suggest that the dissociation constant (K_d) for nectin-1 is

1μM while that of E-cadherin is 80μM which means that nectin-1 can undergo homophilic interactions even when they are present in low concentration[127-129]. Furthermore, it has been shown that recruitment of E-cadherins is enhanced by nectin-1 mediated interactions. Here, we show that the adhesion kinetics of nectin-1 mediated interactions, elucidated using SMFS experiments, provides a strong support for the role of nectin-1 in initiating adherens junction formation. The bond half life ($1/k^0_{off}$) of nectin-1 interactions (configuration I) is much longer than that of initial E-cadherin interactions (Table 4.2). Hence, in the initial stages of adherens junction formation (e.g. filopodia or lamellipodia of two cells coming in contact with one another) when E-cadherin mediated interactions are highly unstable and weak, nectin-1 mediated interactions help to stabilize them. Furthermore, they also help in the recruitment of E-cadherins to the junctions leading to a local increase in their concentration. Once a sufficiently high concentration of E-cadherins is reached, interactions with multiple domain overlap occur, leading to a significant strengthening of the adherens junction (Fig. 4.13).

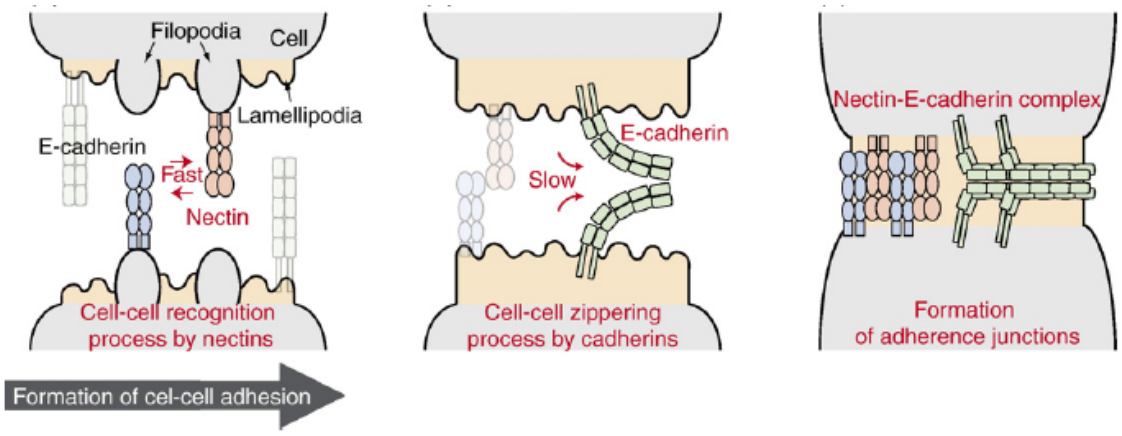

Figure 4.13 A cartoon showing the role of nectin-1 in the formation of adherens junction. Interactions between nectin-1 are followed by recruitment of E-cadherins[125].

In contrast to the interaction configuration I mediated by nectin-1 that shows a long bond half life, configuration II and configuration III show a much shorter bond half life (Table 4.2). However, the reactive compliance (x_β) of these interaction configurations is smaller than that of configuration I as well as that of E-cadherin mediated interactions. Phenomenologically, this parameter represents the sensitivity of dissociation of ligand-receptor complex to an applied force and is equivalent to the length scale of the transition state along the reaction coordinate[94]. According to the model proposed by Bell, the dissociation rate of a ligand receptor complex bears a direct exponential correlation to the external force acting on it as well as the reactive compliance of the interaction[95]. This means that the dissociation rate of interactions with a larger reactive compliance increases faster than the dissociation rate of interactions with a lower reactive compliance when they are subjected to an external force. Since the interaction configuration II and III mediated by nectin-1 have a low reactive compliance, they are much more resistant to dissociation under an externally applied force. However, since the observed frequencies of interaction configurations II and III are very small compared to configuration I, their physiological relevance is doubtful.

In conclusion, adhesion kinetics of homophilic nectin-1 interactions probed using SMFS provide us with a better understanding of their role in intercellular adhesion formation. Further experiments using truncated forms of nectin-1(e.g. expressing only first extracellular domain) could provide a more detailed insight into the role of individual loops of nectin-1 in initiating cell adhesion.

5 Single molecular force spectroscopy study of homophilic JAM-A interactions and JAM-A interactions with reovirus attachment protein σ1

5.1 Introduction

Junctional adhesion molecules (JAMs) are proteins that localize at intercellular tight junctions along with occludin and claudins[68]. Apart from endothelial cells and epithelial cells, JAM family members are expressed on leukocytes and platelets[69, 70]. JAMs belong to the immunoglobulin (Ig) superfamily of proteins and are implicated in tight junction formation[71], monocyte transmigration[68], platelet activation[70], angiogenesis[72, 73], cancer metastasis[130] and attachment of mammalian reovirus[8, 131]. The JAM family includes JAM-A, JAM-B, JAM-C, JAM-4, and JAML proteins[132].

JAM-A was first discovered as an antigen on platelets for the F11 monoclonal antibody; engagement of platelets by F11 mediates granule release, fibrinogen binding, and aggregation[76]. JAM-A was subsequently found to localize at regions of intercellular contact in epithelial and endothelial cell tight junctions[68]. While JAM-A is capable of undergoing only homophilic interactions within the JAM family, JAM-B and JAM-C are capable of both homophilic and heterophilic interactions with each other[133]. Support for JAM-A-mediated homophilic adhesion comes from the observation that transfected CHO cells show localization of JAM-A to regions of cell-cell contact formed between transfected cells[77]. Inhibition of monocyte transmigration by monoclonal antibody

BV11, which inhibits homophilic JAM-A interactions, strongly suggests that JAM-A-mediated interactions between monocytes and endothelial cells are important for transmigration[68]. JAM-A also can undergo heterophilic interaction with leukocyte function associated antigen-1 (LFA-1, $\alpha_L\beta_2$ integrin) expressed on neutrophils and T lymphocytes[80]. These findings suggest that a complex interaction of both heterophilic and homophilic interactions mediated by JAM-A facilitate the transmigration process. Furthermore, antibodies binding to the JAM-A homodimer interface have also been shown to delay the recovery of transepithelial resistance highlighting the importance of homophilic JAM-A interactions in regulating the tight junction barrier[71, 78]. Finally, JAM-A acts as a receptor for the reovirus attachment protein σ1.

Despite significant biochemical evidence for JAM-A homophilic interactions, neither the strength nor the kinetics of these interactions are well characterized. This chapter focuses on the use of single molecule force spectroscopy to understand the interactions of JAM-A with itself and with the reovirus attachment protein σ1.

5.1.1 Structure and organization of JAMs

Structurally, all JAM proteins contain an N-terminal signal peptide, an extracellular region composed of two Ig-like domains (a membrane-distal, N-terminal D1 domain and a membrane-proximal, C-terminal D2 domain), a single membrane-spanning domain and a short cytoplasmic tail (Fig. 5.1). The cytoplasmic tail interacts with PDZ domain-containing scaffolding proteins including ZO-1, while the D1 domain interacts with the D1 domain of an opposing JAM-A molecule to form physiologically relevant homodimers. While the extracellular domains of JAM-A undergo N-glycosylation, the

cytoplasmic segments have putative phosphorylation sites for protein kinase C (PKC) and protein kinase A (PKA). Evidence suggests that similar to occludin, phosphorylation might be critical for targeting JAMs to the intercellular junction complex[134]. The significance of N-glycosylation of the extracellular domains of JAMs currently remains unknown.

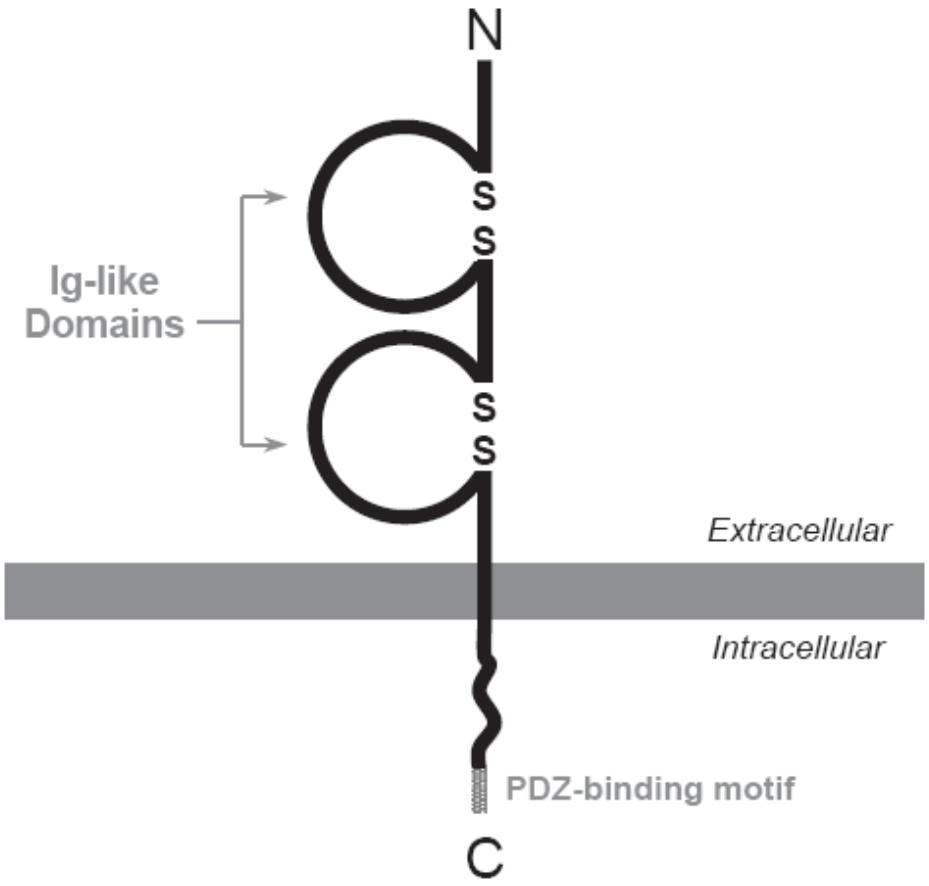

Figure 5.1 Schematic depiction of the basic structure of JAMs. The extracellular segment contains two Ig-like loops while the short cytoplasmic segment interacts with several adaptor molecules[135].

Crystal structures of murine and human JAM-A (mJAM-A and hJAM-A) show that the N-terminal D1 domains of two JAM-A monomers interact to form homodimers (Fig.

5.2). The model proposed for JAM-A organization at intercellular junctions, based on the crystal structure of murine JAM-A (which was determined before hJAM-A), was one in which JAM-A dimers belonging to one cell trans- interacted with corresponding dimers from the adjacent cell to form an extensive network (Fig. 5.3a)[74]. However, when the crystal structure of hJAM-A was resolved, similar contact between dimers was not observed[136]. The fact that hJAM-A crystal structure was different from that of mJAM-A strongly suggested that JAM-A interactions are extremely weak and that the observed networking was probably due to crystal packing forces rather than true interactions.

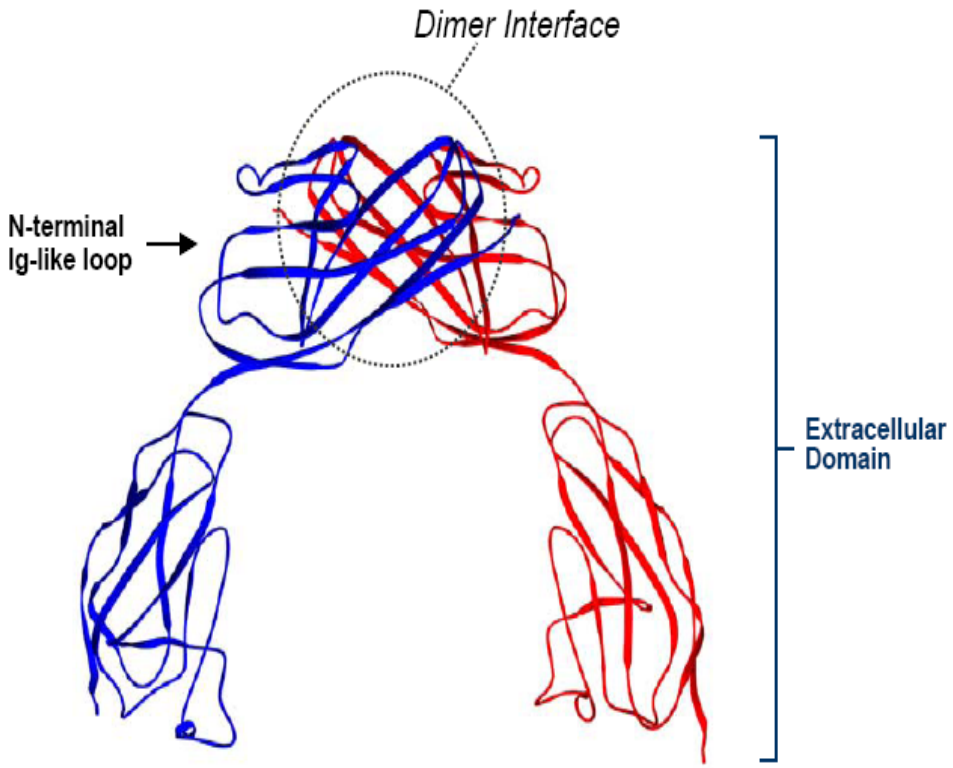

Figure 5.2 Crystal structure of JAM-A homodimers showing the interaction between the N-terminal D1 domains of two opposing molecules[135].

Furthermore, it was also proposed that JAM-A dimer itself could form the physiological contact between adjacent cells[136]. Combining the information from the crystal structures with the fact that a significant amount of JAM-A has been shown to exist in monomeric form in solution, strongly favors a model in which trans-interactions occur between JAM-A monomers from adjacent cells (Fig. 5.3b)[137].

5.1.2 Role of JAMs in physiological functions and in disease

As briefly referred to earlier, JAMs play an important role in several physiological as well as pathological functions. One of the most important physiological functions in which JAMs in general and JAM-A in particular, play an important role is inflammation. During inflammation, white blood cells adhere to the endothelial cells on the vessel wall. Following adhesion, the white blood cells transmigrate across the vessel wall through the endothelial cell junctions. Major steps in the process of inflammation include capture, rolling, adhesion and transmigration of the white blood cells (Fig. 5.4).

While capture, rolling and adhesion are primarily mediated by selectins and their ligands, transmigration is significantly dependent on interactions mediated by integrins (e.g. $\alpha_L\beta_2$) and JAMs. The importance of JAM-A in inflammation is further supported by the fact that antibodies against JAM-A inhibit infiltration and migration of white blood cells at sites of inflammation. It has been suggested that JAM-A on endothelial cells form a tunnel surrounding the transmigrating white blood cells.

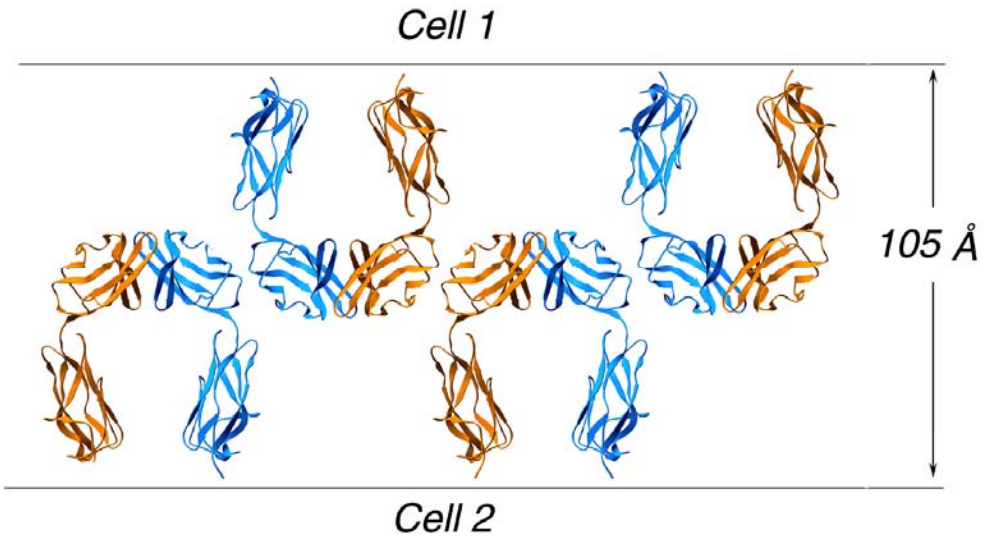

(a)

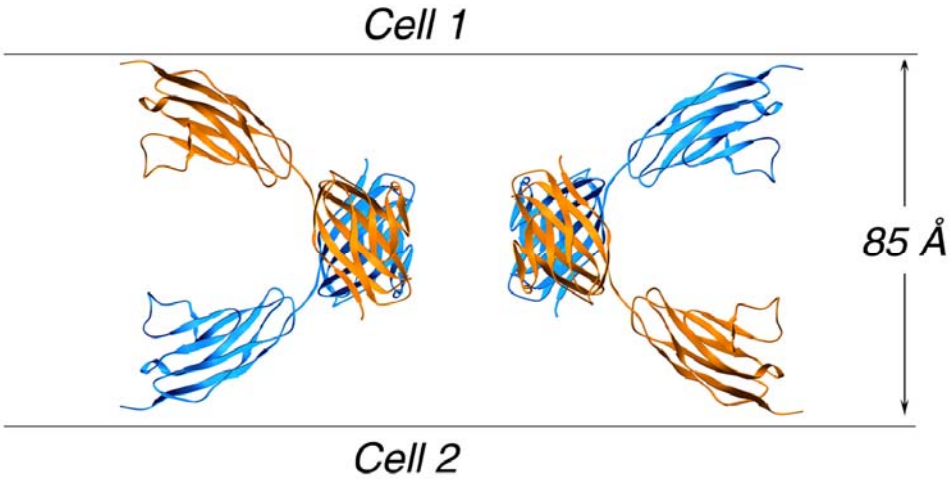

(b)

Figure 5.3 Models proposed for the organization of JAM-A at the intercellular contact sites (a) network of trans-interacting dimers (b) dimers of JAM-A formed between monomers from adjacent cells. (Courtesy: Dr. Stehle, University of Tubingen).

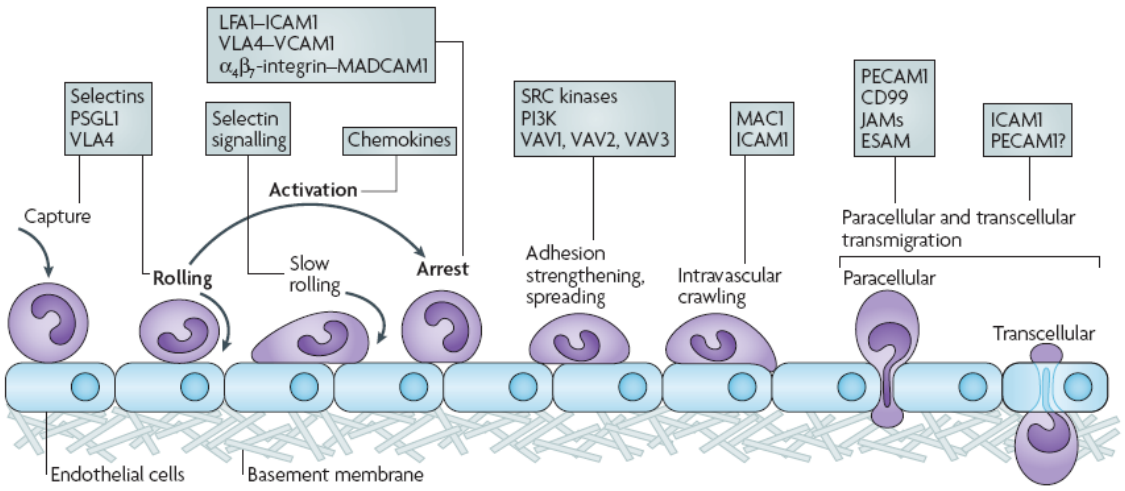

Figure 5.4 Schematic of the different processes constituting white blood cell transmigration across endothelial cells during inflammation. JAMs are important for the paracellular migration of the white blood cells[6].

Apart from its role in transmigration, JAM-A plays an important role in the formation and regulation of tight junctions. Monoclonal antibodies against the dimer interface of JAM-A have been shown to impede the re-formation of tight junction barrier when it was disrupted by calcium depletion. JAM-A expression has also been shown to enhance the localization of ZO-1 and occludin to intercellular contacts underlining its importance in the formation of tight junctions. Furthermore, JAM-A has also been shown to be important for targeting PAR-3, which is essential for the establishment of polarity in epithelial cells. JAM-A has also been shown to play an important role in regulating platelet function. Activation of JAM-A on platelets by antibodies has been shown to cause platelet aggregation, fibrinogen adhesion and degranulation. Using JAM-A deficient mice, it has been demonstrated that JAM-A plays an important role in fibroblast growth factor-2 (FGF-2) induced angiogenesis[73, 138]. Furthermore, it has been shown that FGF-2 induced angiogenesis requires the cytoplasmic domain of JAM-A. Based on

these results, it has been proposed that FGF-2 dissociates JAM-A/$\alpha_v\beta_3$ complex. The free JAM-A then activates the MAP kinase pathway resulting in downstream signaling that enhances angiogenesis[72]. JAM-A has also been shown to play an important role in regulating migration in cancer cells, dendritic cells and endothelial cells[139-141].

The functions of JAM-B and JAM-C have been less well studied in comparison to JAM-A. In contrast to JAM-A, which is widely distributed in various tissues, JAM-B and JAM-C have restricted tissue expression. JAM-B has been shown to be expressed in only endothelial cells while JAM-C is expressed by endothelial cells, epithelial cells and leukocytes[135]. JAM-B (also known as VE-JAM) on endothelial cells has been shown to undergo heterophilic interactions with JAM-C expressed on immune cells (T-cells, NK cells and dendritic cells)[133]. Antibodies to JAM-B and JAM-C have been shown to block leukocyte extravasation and inflammation in skin suggesting that they play an important role in contact dermatitis. Furthermore, apart from its role in inflammation, JAM-C has also been shown to mediate interactions between cancer cells and endothelial cells[130]. Taken together with the fact that JAM-A inhibition contributes to increased migration in breast cancer cells, this strongly suggests that JAMs may play an important role in cancer cell invasion and metastasis[139].

In addition to its physiological functions, JAM-A acts as a receptor for each of the three known serotypes of mammalian orthoreovirus (reovirus)[8]. Reoviruses are important experimental models for studying viral pathogenesis[142]. Both murine and human JAM-A proteins serve as receptors for reovirus. Reovirus engages JAM-A via the attachment protein σ1. σ1 is a filamentous trimer with an N-terminal tail and a C-terminal head. The

head domain of σ 1 binds to JAM-A, while the tail domain recognizes cell-surface carbohydrate, which is sialic acid for serotype 3 strains (Fig. 5.5)[143, 144].

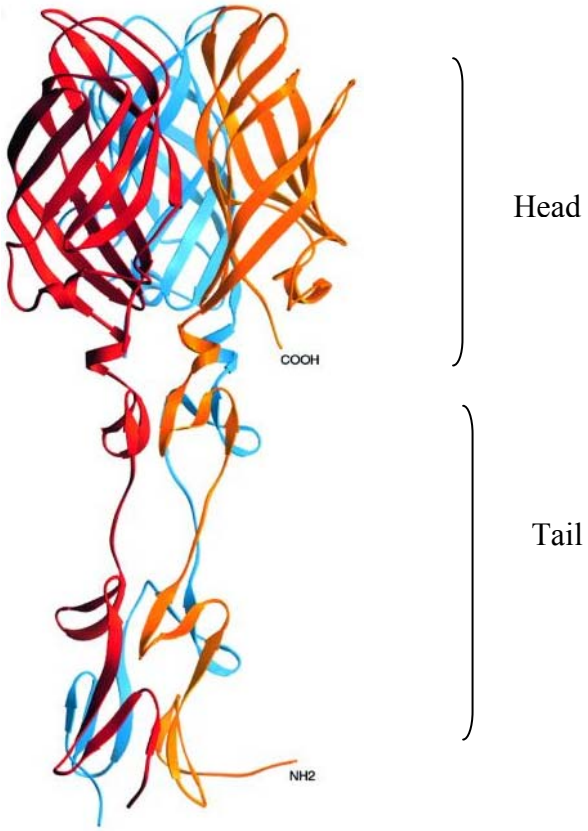

Figure 5.5 Schematic depiction of the crystal structure of the trimeric reovirus attachment protein σ1. The head segment engages JAM-A while the tail segment interacts with surface carbohydrate residues e.g. sialic acid residues[144].

Mutational and biochemical studies suggest that σ1interacts JAM-A via its dimer interface, probably by forming salt bridges similar to those formed between JAM-A monomers[145]. Also, surface cross linking of JAM-A in transfected CHO cells using BS^3 makes them resistant to reovirus infection strongly suggesting that σ1 engages monomeric JAM-A.

5.1.3 SMFS of homophilic JAM-A interactions and JAM-A interactions with reovirus attachment protein σ1

Though several biochemical and mutational studies have provided significant information on the role of JAM-A in various physiological functions and its interactions with reovirus attachment protein σ1, details of adhesion kinetics involving molecular interactions between these molecules have not been well studied. Recently, surface plasmon resonance (SPR) has been used to elucidate the kinetics of σ1/JAM-A interactions[145]. However, the SPR studies have several drawbacks. Firstly, the experiments were performed in non-physiological conditions using surface immobilized pure GST-JAM-A protein. Secondly, the GST-tag present on the N-terminal end of JAM-A is very likely to interfere with the interactions of σ1 with JAM-A. Finally, homophilic JAM-A interactions were undetectable using SPR. To overcome these disadvantages we have used single molecule force spectroscopy to characterize homophilic JAM-A interactions and interactions of σ1 with JAM-A. Cantilevers functionalized with either mouse JAM-A tagged with human F_c fragment on the C-terminal end (F_c/mJAM-A) or purified σ1 head domain were used to probe L-fibroblasts. L-fibroblasts are mouse fibroblasts that express JAM-A (mJAM-A) and are susceptible to infection by reoviruses[143, 146]. F_c tag on the C-terminal end ensured that there was no interference to the binding domains involved in the interactions. Using purified σ1 head domain ensured that interactions between the tail segment of σ1and sialic acid residues on L-cells were not probed. The use of L-cells ensured that JAM-A receptors were being probed in their natural state. Furthermore, since the JAM-A residues participating in the interactions with JAM-A and with σ1 are conserved between human mouse JAM-A, the results obtained are very likely applicable

to human JAM-A (hJAM-A). The results of the SMFS experiments provide a better insight into the biophysical basis for the different functions of JAM-A as a regulator of tight junctions and as a receptor for reovirus.

5.2 Methods and Materials

The atomic force microscopy setup for single molecule force spectroscopy experiments, cantilever functionalization with JAM-A/Fc fusion protein and σ1 head domain, data acquisition and analysis are described in detail in Chapter 3.

5.3 Results

5.3.1 Force spectroscopy of mJAM-A/L-cell interactions

The mJAM-A/Fc chimeric protein was linked to the AFM tip using an anti-Fc antibody. This strategy was chosen to provide optimal accessibility of the N-terminal D1 domain of mJAM-A, which is involved in both JAM-A dimer formation[74, 136] and interactions with σ1[145, 147]. Force-distance curves for homophilic mJAM-A interactions were obtained by probing L-fibroblasts using these functionalized cantilevers (Fig. 5.6). The functionalized cantilever was lowered onto a single well adherent L-cell. A contact force of 200pN was applied for 1ms by the cantilever before it was retracted at velocities of 1, 2.5, 5, or 10μm/s. More than 500 force-distance curves were obtained for each velocity at an adhesion probability of < 30%. Force-distance curves showing a clear single rupture event were analyzed for loading rate and rupture force as described in methods (Fig. 5.7).

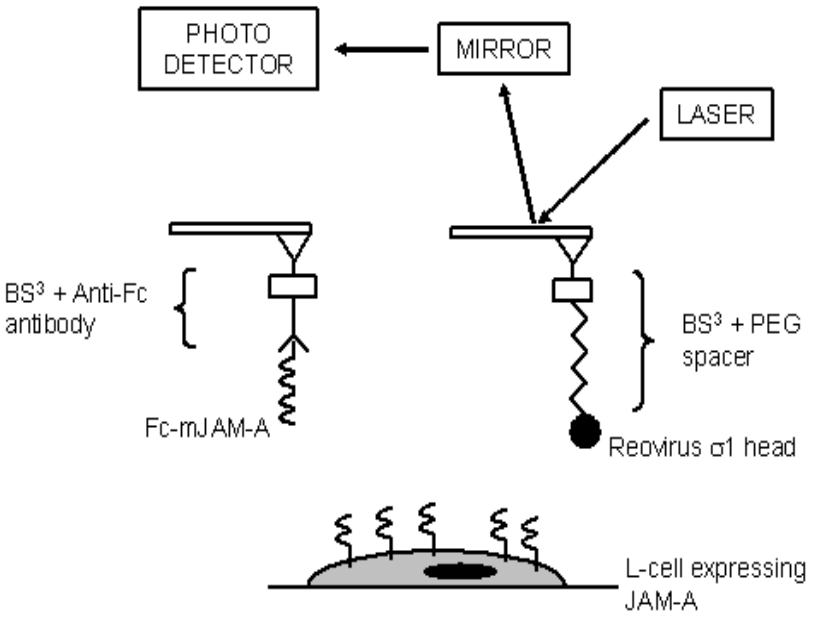

Figure 5.6 Schematic depiction of the SMFS setup for probing homophilic JAM-A interactions and JAM-A interactions with reovirus attachment protein σ1[148].

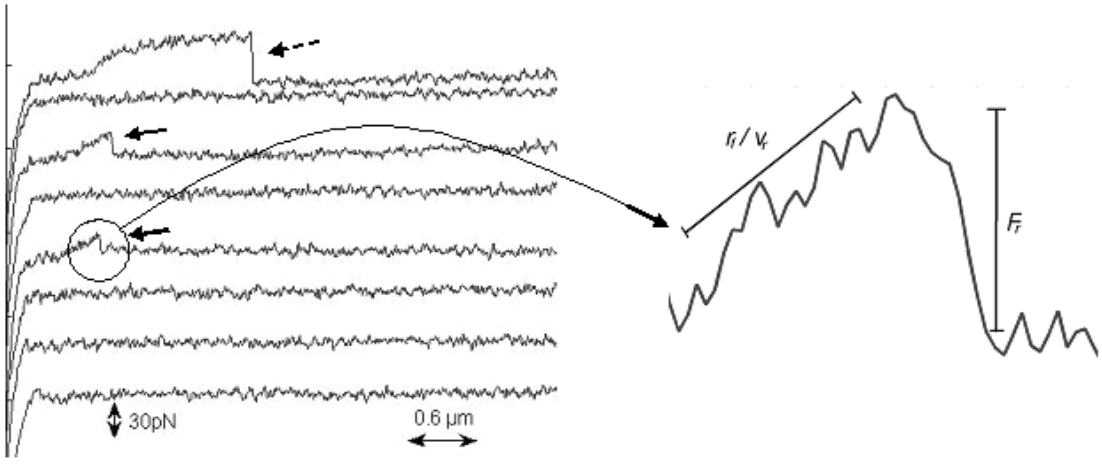

Figure 5.7 Typical force-distance curves with bond rupture events (bold arrows) and tether formation (dashed arrows). The loading rate for a given bond rupture event (F_r) was calculated by multiplying the slope (r_f/v_r) of the reproach curve prior to the rupture event by the reproach velocity of the cantilever.

Control experiments performed using anti-Fc antibody functionalized tips showed few adhesion events, indicating that the interactions being measured were specific to interactions mediated by JAM-A (Fig. 5.8).

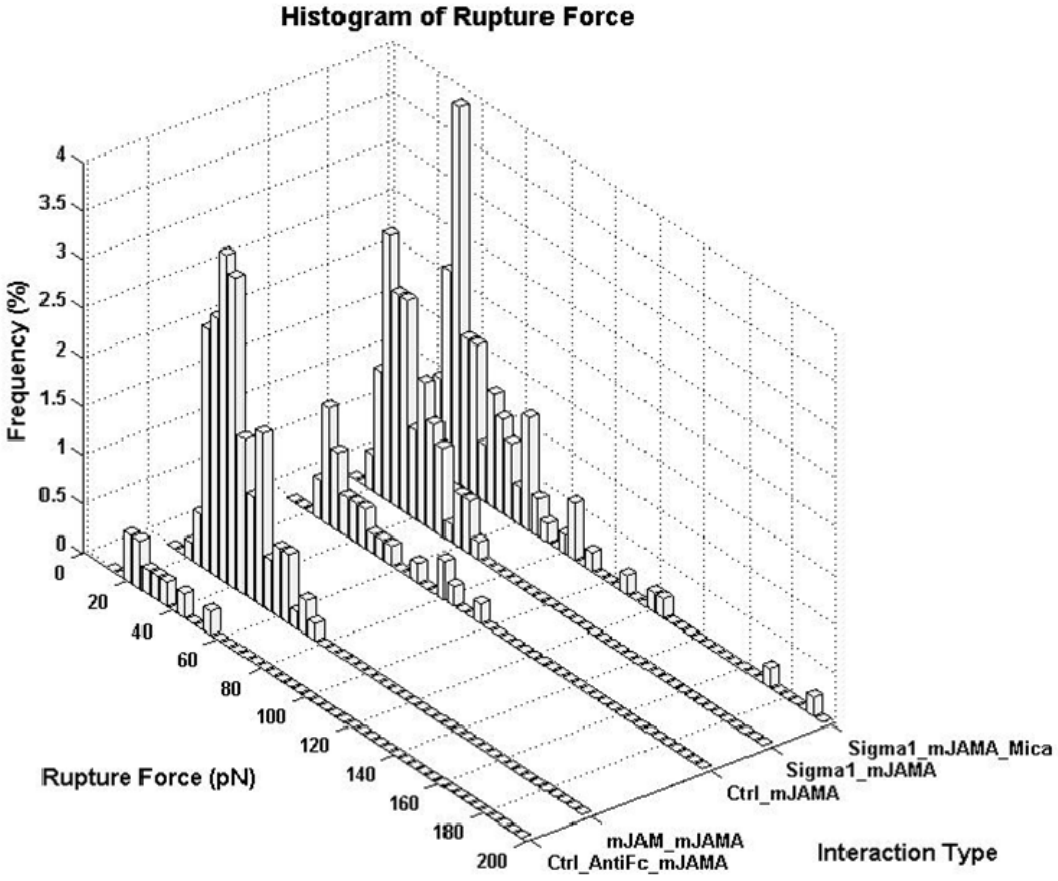

Figure 5.8 Histograms of bond rupture frequencies observed for different interaction types at reproach velocity of 5μm/s. A contact force of 200pN and a contact time of 1ms were used for all experiments. Control experiments showed few adhesion events. Each histogram represents data analyzed from over 500 force curves.

All the receptor/ligand pairs tested, corresponding to the histograms shown in Fig. 5.8, are listed in Table 5.1. Following the method used by Hanley et al.[83] and Panorchan et al.[85], rupture force measurements were binned by increments of 50 pN/s for loading

rates between 100 and 1000 pN/s and by increments of 500 pN/s for loading rates between 1000 and 10,000 pN/s. Each bin yielded a mean rupture force. By plotting the mean rupture force as a function of loading rate and extrapolating the fitted line, the unstressed dissociation rate (k^{o}_{off}) and reactive compliance (x_{β}) were extracted using Bell's model (Fig. 5.9 and Eq. 2.6 in Chapter 2).

Table 5.1 List of different interactions probed using AFM corresponding to the histograms depicted in Figure 5.8.

Interaction Type	**AFM Tip**	**Substrate**
1. Ctrl_antiFc_mJAM-A	Anti-Fc only	L cells
2. mJAM-A_mJAM-A	Fc-mJAM-A	L cells
3. Ctrl_mJAMA	PEG + BSA only	L cells
4. σ1_mJAM-A	PEG + σ1 head	L cells
5. σ1_mJAM-A_mica	PEG + σ1 head	Fc-mJAM-A on

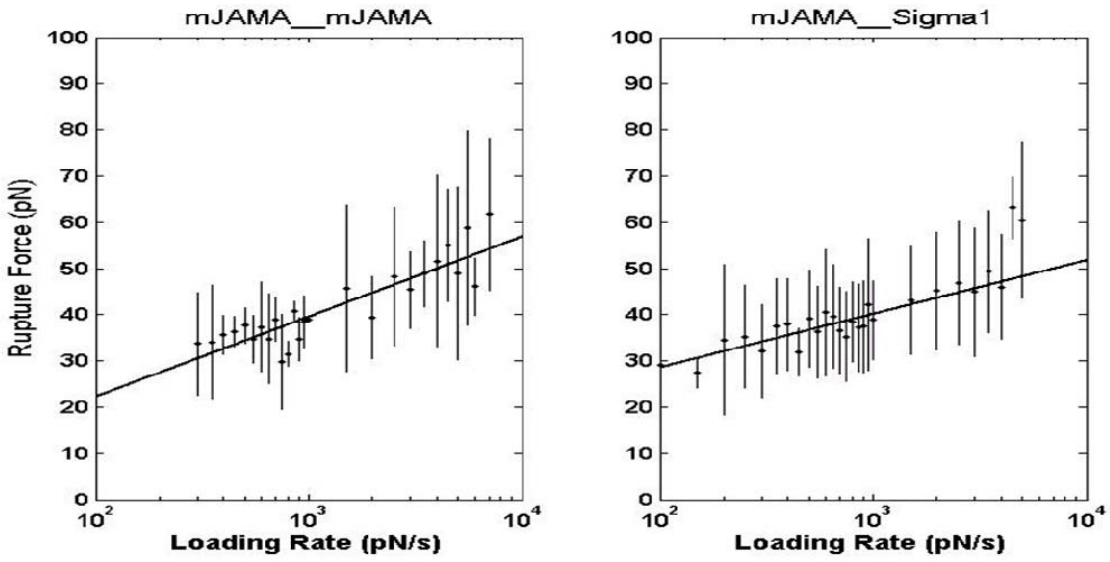

Figure 5.9 Loading rate curves for mJAM-A/mJAM-A and σ1 head/mJAM-A interactions. The loading rate and rupture force were obtained from the force curves. The data points were binned as described in the text. The mean rupture force values for each bin were plotted against the logarithm of the corresponding loading rate.

Homophilic mJAM-A interactions showed an increase in bond rupture force with increasing loading rate. Fitting the data points to a line, the k^{o}_{off} for mJAM-A interactions was found to be 0.688 ± 0.349 s^{-1} (Table 5.2). The bond dissociation time (1/ k^{o}_{off}) for mJAM-A interactions is very low when compared to that of σ1/mJAM-A interactions (see below). A low bond dissociation time is consistent with the physiological functions attributed to JAM-A in regulating tight junction permeability. The short bond life time imparts a highly dynamic nature to the interactions between JAM-A molecules necessary for the cell to regulate solute and solvent diffusion across the tight junction barriers. An interesting feature of the mJAM-A force-distance curves was the formation of occasional "tethers." These force-distance curves are distinguished by the fact that the bond rupture is preceded by a long horizontal stretch of cantilever movement without any deflection (dashed arrow, Fig. 5.7). This observation might be attributed to the formation of membrane tethers due to the interaction of mJAM-A on the tip with a free molecule of mJAM-A on the cell (not linked to the cytoskeleton).

Table 5.2 Parameters extracted by extrapolating the loading rate curves shown in Figure 5.9.

Molecular pairs	$\mathbf{k^{0}_{off}}$	$\mathbf{x_{\beta}}$	**Cell line**
mJAM-A / mJAM-A	0.688 ± 0.349	0.547 ± 0.060	L-cells
mJAM-A / σ1 head	0.067 ± 0.041	0.817 ± 0.073	L-cells
*Cldn1/Cldn1	1.35 ± 1.31	0.36 ± 0.06	Recombinant proteins[92]

*Data presented for claudin-1 has been taken from previous work.

Alternatively, this pattern could have been produced by dissociation of mJAM-A on the cell membrane from its cytoplasmic adaptor or cytoskeleton. Force-distance curves showing such tethers were excluded from the loading rate curve analysis.

5.3.2 Force spectroscopy of σ1/L-cell interactions

For functionalizing tips with σ1 head domain, one end of a homo-bifunctional polyethylene glycol spacer (approximately 15 nm in length and containing amino groups at both ends) was attached to the silanized AFM tips using bis (Sulfosuccinimidyl) suberate (BS^3) while the untagged σ1 head domain was linked to the other end of the spacer using 1-ethyl-3-[3-dimethylaminopropyl] carbodiimide hydrochloride (EDC). EDC is a "zero-length" cross linker that covalently links an amino group to a carboxylic acid group[117]. The PEG spacer was used to provide enhanced flexibility for the covalently attached σ1 head domain. The σ1 head domain has several surface-exposed aspartic and glutamic acid residues, which could engage the free amine group of the spacer in the presence of EDC via their carboxylic acid groups. The strategy chosen maximizes the probability that the JAM-A binding site of the σ1 head domain will contact JAM-A.

Force-distance curves for σ1/mJAM-A interactions were obtained on L-fibroblasts with tips functionalized with σ1using an analogous approach. The data were analyzed using Bell's model to extract the unstressed dissociation rate (k^o_{off}) and reactive compliance (x_β) (Fig. 5.9 and Table 5.2). The unstressed dissociation rate (k^o_{off}) obtained for σ1/mJAM-A interactions ($0.067 \pm 0.041\ s^{-1}$, Table 5.2) was much less than that obtained for homophilic mJAM-A interactions. These findings indicate that the bond half-life ($t_{1/2}$)

of the σ1/mJAM-A interaction is greater (by almost ten-fold) than that of the homophilic mJAM-A interaction. A long bond half life ($t_{1/2}$ or $1/k^{o}_{off}$) might facilitate stable adherence of the virus to the cell and help in its entry.

To ensure that the mJAM-A-binding domain of σ1remained accessible after it was cross-linked to the AFM tip, control force curves were obtained using mica cover slips functionalized with mJAM-A. The force histogram profile obtained using these functionalized mica cover slips probed with σ1-functionalized tips was similar to that obtained using L cells (Fig. 5.8, Table 5.1). Furthermore, mica functionalized with BSA showed few adhesion events when probed with the σ1-functionalized tips. Therefore, the method used to cross-link σ1to the AFM tip did not adversely affect interactions of the σ1head domain with mJAM-A.

5.3.3 Energy landscape for dissociation of mJAM-A/mJAM-A and σ1/mJAM-A complexes

Dissociation of mJAM-A/mJAM-A and σ1/mJAM-A complexes was found to follow a single step energy activation barrier process. The topography of the energy landscapes of the dissociation of mJAM-A/mJAM-A and mJAM-A/σ1 complexes can be compared by plotting the geometric locations of their bound states on the same reactive coordinates (Fig. 5.10). The unstressed off rate (k^{o}_{off}) for the two interactions can be used to estimate the energy difference (ΔG) between the activation barriers of mJAM-A/mJAM-A and mJAM-A/σ1 complex dissociation and is given by[149]:

$$\Delta G = -k_B T \ln(k^{0}_{mJAM} / A) \quad (5.1)$$

$$\Delta G = -k_B T \ln(k^{0}_{\sigma 1} / A) \quad (5.2)$$

Here k^0_{mJAM} and $k^0_{\sigma 1}$ denote the unstressed dissociation rate constants of the mJAM-A/mJAM-A and σ1/mJAM-A interactions respectively and A is a constant derived from frequency pre-factors in the dissociation process. The absolute energy values of each barrier from the level of the bound state cannot be confirmed due to the uncertainty of constant A. However, the relative positions of the energy barriers can be determined using x_β. To compare the topography of the energy landscape of the dissociation of mJAM-A/mJAM-A and σ1/mJAM-A interactions, the geometric locations of their bound states were plotted on the same reactive coordinates. It should be stressed that dissociation pathways for mJAM-A/mJAM-A and σ1/mJAM-A interactions may take different reactive coordinates in general. The analysis reveals that the activation barrier of the σ1/mJAM-A complex is $2.33\,k_BT$ higher than that of mJAM-A/mJAM-A complex (Fig. 5.10) indicating that σ1/mJAM-A forms a more stable bond when compared to mJAM-A/mJAM-A interaction.

5.4 Discussion and Conclusions

We used single molecule force spectroscopy to elucidate the kinetics of homophilic JAM-A/JAM-A interactions and interactions between JAM-A and the reovirus σ1 protein. Although mJAM-A was used in this study, residues mediating interactions between JAM-A dimers are conserved between mJAM-A and hJAM-A, and both mJAM-A and hJAM-A bind reovirus σ1[74, 136]. Thus, our results are likely applicable for both human and murine forms of JAM-A.

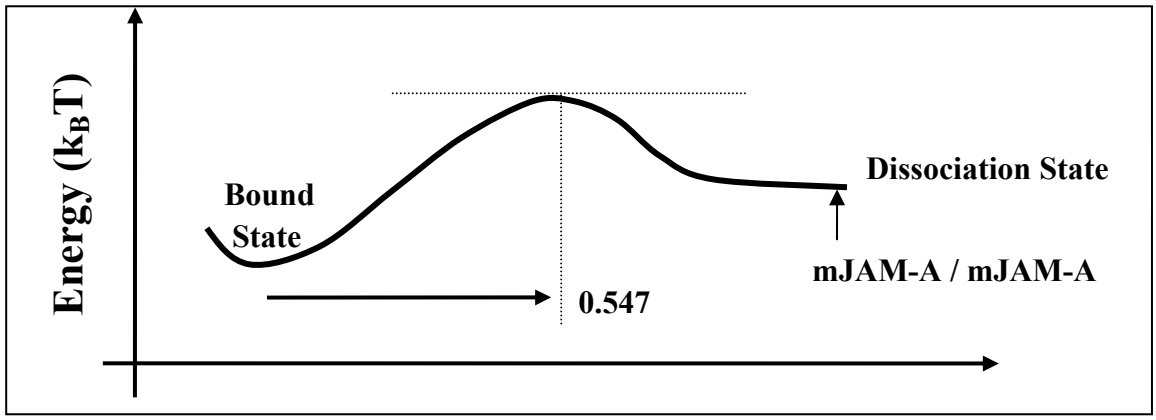

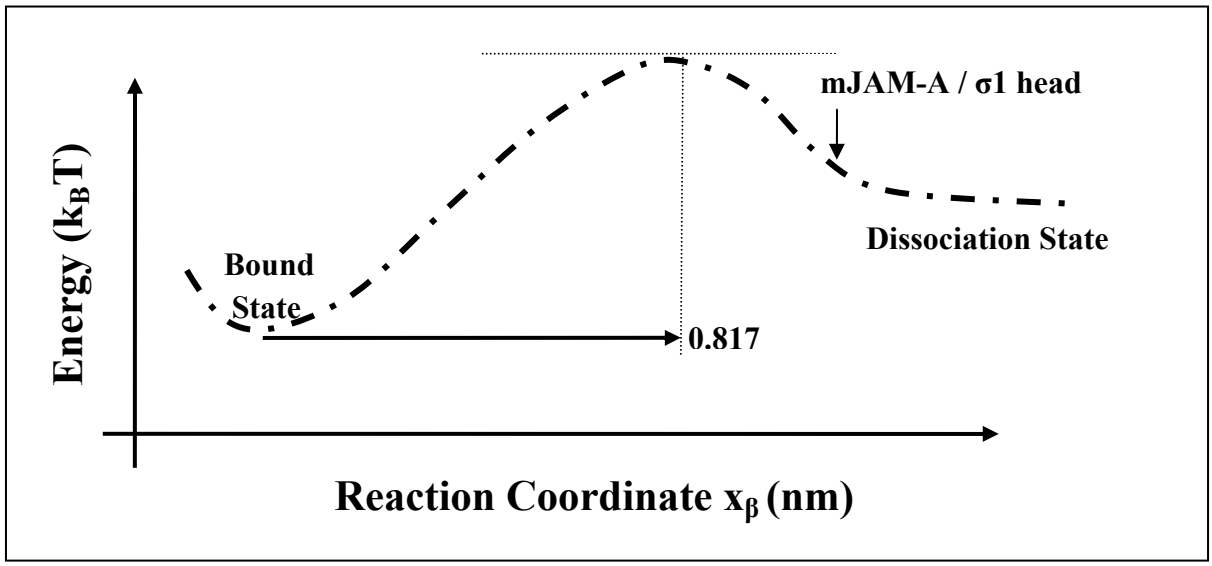

Figure 5.10 Energy landscapes for the dissociation of σ1/mJAM-A and mJAM-A/mJAM-A constructed based on the kinetic parameters obtained from SMFS experiments.

While both mJAM-A and σ1 interact specifically with L-cells, we find that σ1/L-cell interactions have a substantially longer half-life ($t_{1/2}$) than mJAM-A/L-cell interactions. The lack of adhesion events in control experiments strongly suggests that these measurements describe specific interactions with mJAM-A on the surface of L cells. The observed kinetic parameters of homophilic mJAM-A interactions closely resemble that of claudin-1(Table 5.2)[92]; another tight junction protein which is also involved in regulating paracellular permeability of solutes. For claudin-1, rapid lateral association

and dissociation between adjacent cells has also been observed using the corresponding GFP tagged proteins[150]. It is likely that such dynamic interactions provide the cell with a better platform to regulate solute flux. Furthermore, since JAM-A (and other TJ proteins) is linked to the actin cytoskeleton, it is likely that forces from within the cell are conveyed to the trans-interacting JAM-A molecules (and other TJ proteins) via the actin filaments. Based on Bells model, such externally acting forces on these molecules can alter their adhesion kinetics significantly. This could probably be an important method for the cell to regulate the permeability of the paracellular barrier in response to various extracellular signals.

The differences in half-life for homophilic JAM-A and σ1/JAM-A interactions are consistent with published findings. When JAM-A dimers are mixed with σ1 in solution, σ1 displaces JAM-A from the dimer interface, presumably by binding to a region near this interface. Therefore, once formed, the σ1/JAM-A complex is more stable in solution than the JAM-A/JAM-A homodimers. At this juncture it is not possible to ascertain the exact underlying cause for the difference in the unstressed off rate for the two interactions despite a significant overlap between the predicted σ1 binding site on JAM-A and the JAM-A dimer interface. However, we speculate that the differences could have arisen from (a) formation of additional contacts between σ1and JAM-A that could 'cement' or strengthen the σ1/JAM-A interaction after the initial complex formation (b) presence of an as yet unknown receptor for σ1 head domain that could be recruited following σ1 binding to JAM-A. It has been shown previously that the tail portion of σ1 can interact with sialic acid residues present on L-cells. We used purified σ1 head domain in our experiments that did not possess the tail portion and hence it is unlikely that the observed

difference was due to sialic acid residues. However, it is possible that the head domain has other binding partners which could strengthen the interaction following the initial complex formation with JAM-A.

An important aspect of homophilic interactions mediated by JAM-A is whether we are probing monomer-monomer interactions or dimer-dimer interactions. Such a difference cannot be resolved based on SMFS studies unless there are two distinct force peaks that belong to the different interactions. In our SMFS studies on homophilic JAM-A interactions, we neither observed multiple peaks in the force histograms nor clustering of data points into multiple regions in the loading rate curve. However, the crystal structure data of JAM-A and previous biochemical studies strongly suggest that the rupture events detected in our SMFS experiments arise from interactions between two JAM-A monomers. Firstly, it has been observed that a significant amount of JAM-A exists in monomeric form in solution[137]. Secondly, cross linking studies performed on JAM-A in solution using BS^3 followed by gel electrophoresis revealed bands corresponding to monomers and dimers only. No bands corresponding to higher order oligomers e.g. tetramers were observed[137]. Thirdly, crystal structures of hJAM-A and mJAM-A are significantly different from each other suggesting that the dimer-dimer interaction network proposed for mJAM-A probably results from crystal packing forces rather than actual interactions occurring between two dimers[136]. Finally, the antibody J10.4, which binds JAM-A and prevents its dimerization, also delays transepithelial resistance recovery following calcium switch[78]. Taken together, these facts strongly suggest that the dominant homophilic JAM-A interactions occurring in solution as well as between cells is mediated by monomers.

In conclusion, results presented here show how the kinetic differences of protein interactions probed using single molecule force spectroscopy experiments, bear correlation to their physiological functions. Future experiments using JAM-A with mutated residues could help in clarifying the observed differences in JAM-A/JAM-A and σ1/JAM-A interactions.

6 Mechanical Strain Induced Alterations in the Expression and Localization of Tight Junction Proteins in MDCK Cells

6.1 Introduction

All types of cells and organisms are continuously subjected to mechanical forces though the type and magnitude of these forces may differ. For example, bone and cartilage cells are subjected to large compressive and tensile forces, endothelial cells lining the blood vessels are subjected to shear stress and epithelial cells lining the airways and gut are subjected to mechanical strain during respiration and peristalsis. Apart from stresses arising from normal physiological processes, cells are subjected to mechanical strain in certain diseased states as well, e.g. during obstruction of the gut or ureters and during artificial ventilation. During such diseased states, cells can be subjected to mechanical strains of large magnitude.

Cells are, however, not passive absorbers of the stresses and strains that are imposed on them. Over time, they have developed a highly organized system of surface mechanosensors and signaling pathways that allow them to convert externally acting forces into biological processes. This phenomenon is termed as mechanotransduction. Important biological processes that are regulated by externally acting forces include cell morphology, orientation[151], proliferation[152], differentiation[153], migration, protein expression and protein localization[39]. Previous studies have been carried out to investigate the effect of mechanical strain on the expression of specific genes,

localization of proteins and organization of cytoskeleton in a wide variety of cell types like cardiomyocytes[154-157], fibroblasts[158-161], osteocytes[162-164] and chondrocytes[165-167]. However, few studies have focused on investigating the alterations in the expression and localization of intercellular adhesion proteins in response to external mechanical strain. Considering that tight junction proteins and the associated adaptor proteins act not merely as regulators of the paracellular pathway, but also as important regulators of cell proliferation; we have explored the possibility that intercellular adhesion proteins, particularly tight junction proteins and their associated adaptor molecules, play an important role in modulating cellular responses to external mechanical strain.

6.1.1 Mechanosensing, Mechanotransduction and Mechanoresponse

The effect of external stresses and strains on cells is a result of a complex interplay between the proteins that act as sensors for converting the force into biochemical signals (mechanosensors) and the intracellular signaling pathways that activate the downstream effectors (Fig. 6.1).

The most well established mechanosensors are mechanosensitive (MS) ion channels and integrins. The existence of MS channels was first predicted based on the ability of E. coli to resist osmotic shock. Experiments supported the presence of “emergency release valves” in these bacteria that allowed solutes to diffuse out when they were subjected to hypo-osmotic shock. The search for these “valves” finally led to the discovery of mechanosensitive (MS) ion channels in bacteria[168, 169]. While the MS channels in prokaryotes have been well characterized in terms of both structure and function, MS

channels in eukaryotes have been identified only recently and include TREK-1 and TRAAK in mammalian neurons, MEC in C.elegans, TRPC1 in Xenopus and SAKcaC in chick hearts.

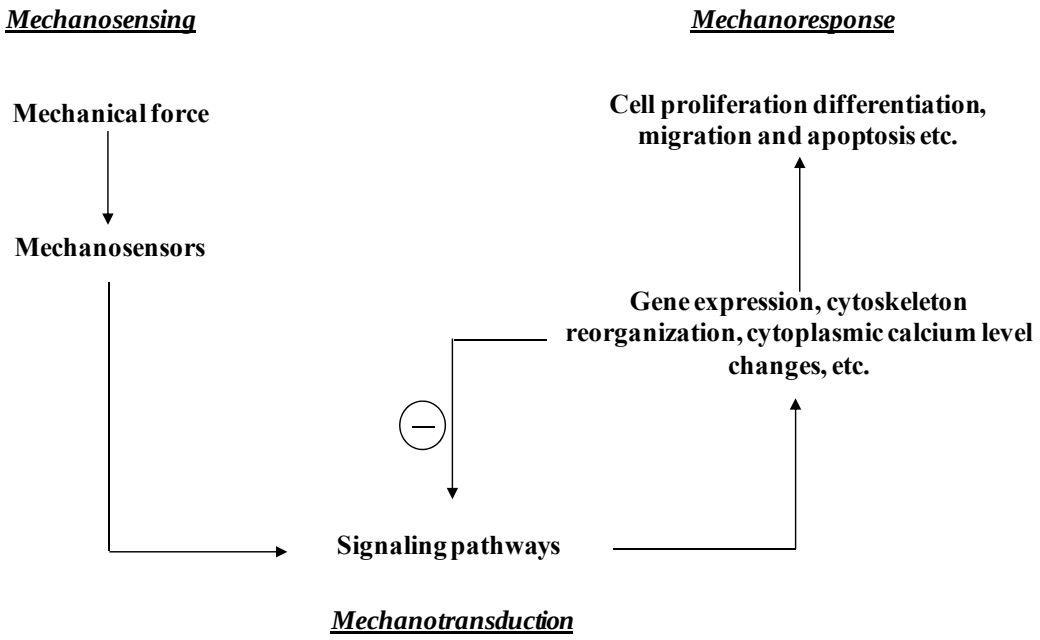

Figure 6.1 Schematic depiction of how externally applied mechanical forces are converted into observable cellular responses[12].

Functionally, MS channels form transmembrane pores. The opening and closing of these pores is regulated by the tension in the cell membrane. The influx of ions through these channels can trigger several signaling cascades. Though Na^+ and K^+ ion influx may play an important role in the down stream signaling activated by MS channels in some cases, the most important pathways seem to be mediated by Ca^{2+} and as discovered recently, by MS release of chemical transmitters, notably ATP.

Integrins and their cytoplasmic adaptor proteins have also been shown to play an important role in regulating cellular response to externally applied mechanical force. Integrins are heterodimeric transmembrane proteins that mediate cell-extracellular matrix interaction (ECM)[170, 171]. Interaction of integrins with ECM proteins is followed by recruitment of several adaptor proteins like paxillin and focal adhesion kinase on their cytoplasmic side. It has been proposed that there are two possible ways in which integrins could act as mechanosensors: the first is the possibility that they open MS channels existing in their vicinity, leading to ion influx and signal initiation[172]. Alternatively, external forces can induce a change in the structure and/or relative positions of the adaptor molecules associated with the cytoplasmic domain of integrins. This relative change in the position and/or structure could open up cryptic molecular recognition sites in the proteins that could trigger the cascading of the signals[173]. Integrins act as a starting point for a number of important signaling cascades among which are the FAK (focal adhesion kinase) pathway and the Fyn/SHC pathway[174]. While the FAK pathway activates both the classical Erk1/2 pathway and the JNK pathway, Fyn/SHC predominantly activates Erk1/2 pathway. Apart from MS channels and integrins, some other proteins have also been proposed to act as mechanosensors. Among these are the G-protein coupled receptors[175], receptor tyrosine kinases and intercellular adhesion molecules[176]. There are several important signaling pathways that are activated by mechanosensors important among which are the mitogen activated protein kinase (MAPK) pathway, the phospholipase C (PLC) pathway and the nitric oxide (NO) pathway.

(a) MAPK pathway: MAPK or Mitogen Activated Protein Kinase is one of the most important pathway that regulates several cellular activities. The three major MAPK pathways are the ERK1/2 (Extracellular signal-regulated kinase), JNK (c-jun NH_2-terminal Kinase) and p38 MAPK pathways (Fig. 6.2). The Erk1/2 pathway is activated by growth factors and other cell survival signaling factors. The first step in the activation of ERK1/2 pathway is the activation of Ras. Mechanical strain can activate Ras either through integrins, receptor tyrosine kinases or by Ca^{2+} influx through MS channels. Activated Ras can then activate Raf which activates MEK1 which in turn can activate ERK1/2. Activated ERK1/2 enters the nucleus and binds to several transcription factors and regulates the expression of a number of different genes necessary for cell survival and proliferation. Activation of the MEK1-ERK1 pathway followed by an increase in activated Elk1 in response to mechanical strain has been demonstrated in human dermal fibroblasts[177]. Similarly, mechanical strain induced mitogenic activity in a Caco-2 cell line has been shown to be mediated by ERK1[178]. Previous studies have also shown that mechanical stretch induces ERK1 activation in alveolar epithelial cells. However, the increase in ERK1 in these cells was mediated through G protein coupled receptors (GPCR) rather than through Ras and Raf[175]. These facts suggest that mechanical stretch mediated activation of ERK1/2 is probably a convergence point of multiple pathways. The SAPK/JNK (stress activated protein kinase or c-jun NH_2-terminal Kinase) pathway, on the other hand, is activated in cells in response to various kinds of stresses e.g. exposure to UV radiation, oxidative agents and osmotic shock[179, 180]. JNK can in turn regulate several transcription factors and has a significant inhibitory effect on cell proliferation[181]. Furthermore, activation of JNK pathway in response to mechanical

strain has been shown in cardiomyocytes[182] and tendon fibroblasts[183]. In endothelial cells, activation of JNK is associated with exposure to both fluid shear stress and cyclic mechanical strain[184]. The p38 MAPK pathway, similar to the JNK pathway, is also activated in response to cellular stress and has a predominantly inhibitory effect on cell proliferation. Several nuclear events are associated with the activation of MAPK pathways. Expression of a number of transcription factors is modulated by MAPK pathway e.g. AP-1, Elk-1 and Egr-1. These transcription factors in turn regulate various cellular processes such as protein expression, cell proliferation, and differentiation.

(b) PLC pathway: There are several isoforms of phospholipase C (PLC) and its activation is central to a number of signaling pathways. Activated PLC converts PIP2 (Phosphatidyl Inositol bisPhosphate) into IP_3 (Inositol triphosphate) and DAG (Diacyl Glycerol) (Fig. 6.3). IP_3 is a potent stimulator for intracellular Ca^{2+} release from the endoplasmic reticulum while DAG activates protein kinase C (PKC). Protein kinase C, in turn, is involved in regulating the transcription of several proteins that are involved in various cellular functions. Furthermore, PKC can also activate the MAPK pathway thereby controlling cell proliferation. Though the better established activators of PLC involve a variety of extracellular ligands that bind to G-protein coupled receptors, PLC has also been shown to be activated by mechanical stress. In fact, PLC activation has been shown to play an important role in regulating cell proliferation in response to mechanical strain in alveolar epithelial cells[112].

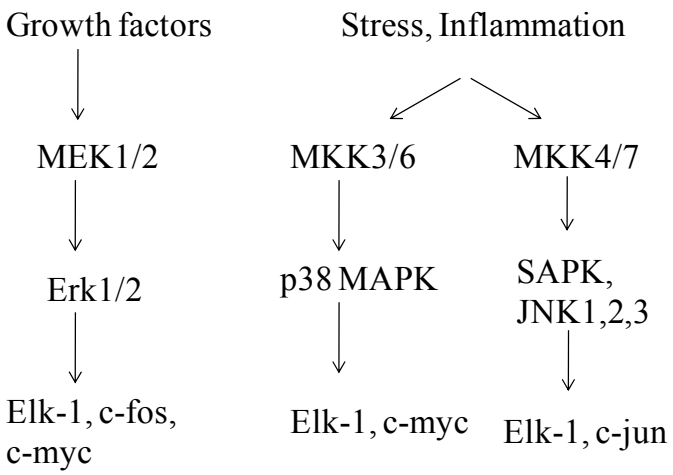

Figure 6.2 Schematic depiction of the three important MAPK pathways involved in controlling cell proliferation and apoptosis.

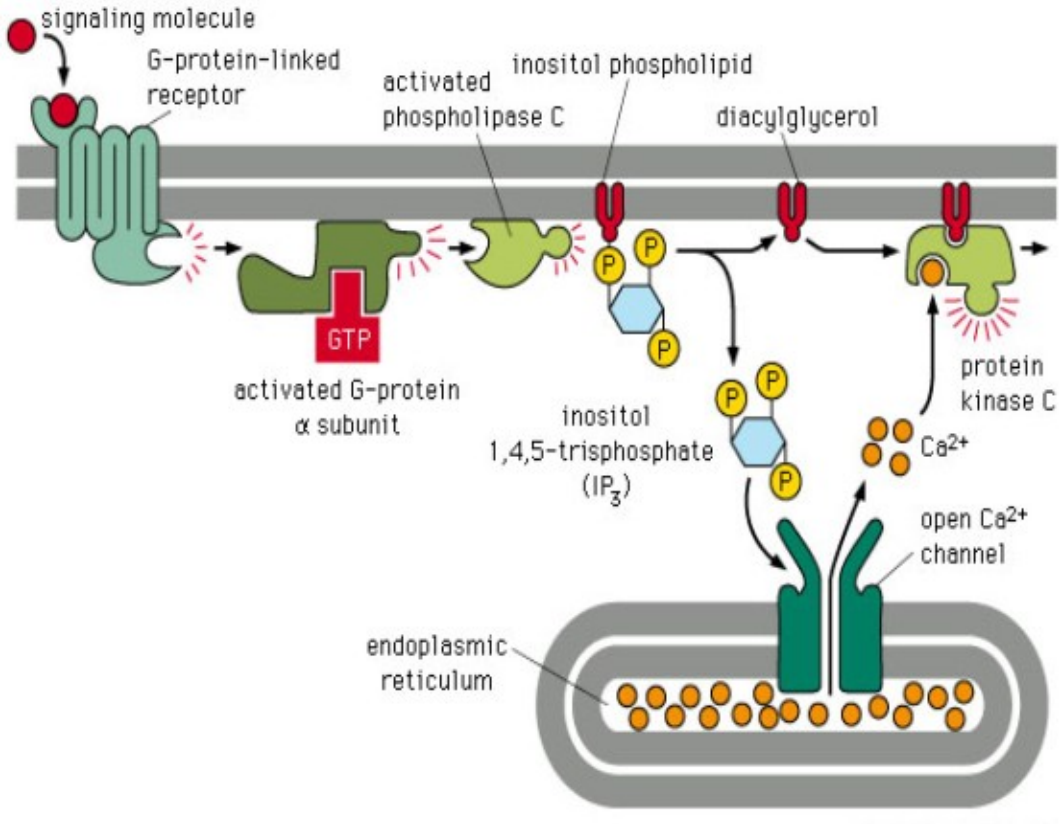

Figure 6.3 Schematic depiction of the PLC pathway. Activation of PLC can result from either ligand binding or mechanical stress[185].

(c) NO pathway: Nitric oxide (NO) is an important molecule that has been shown to be important in neuronal synapses, blood vessel dilatation and immune responses. There are three different enzymes that catalyze the production of NO. Endothelial NO synthase (eNOS) and neuronal NOS (nNOS) are constitutively expressed enzymes whose expression is regulated by Ca^{2+} levels in the cell. The inducible NO synthase (iNOS), on the other hand, is a Ca^{2+} independent enzyme whose regulation is transcriptionally regulated in response to a number of external stimuli[112]. NO can either act directly on target guanylyl cyclase (GC) leading to the formation of cyclic GMP (cGMP) (Fig. 6.4).

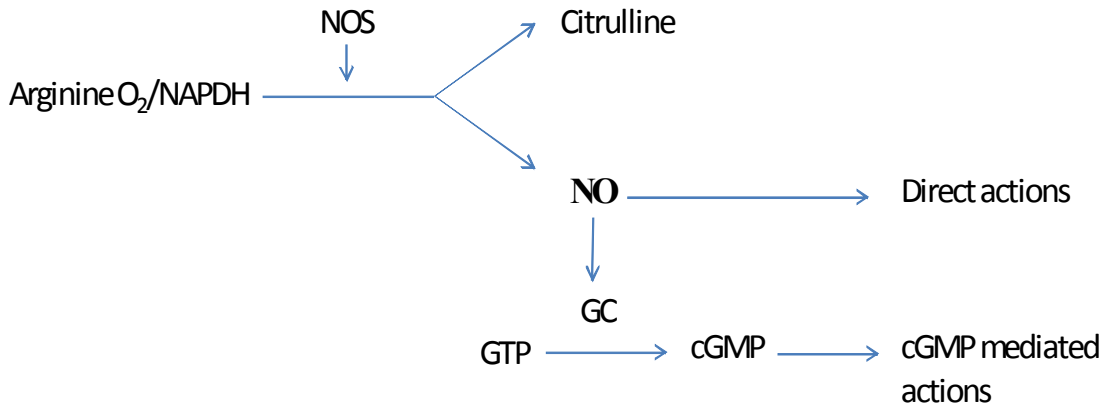

Figure 6.4 Schematic depiction of the NO pathway. NO generated from arginine by the action of NOS can regulate functions either directly or through formation of cGMP.

Mechanical strain and shear stress have been shown to modulate iNOS in a variety of different cell types including endothelial cell, osteoblasts, cardiomyocytes and epithelial cells. For example, cardiomyocytes subjected to mechanical strain show decreased NO, iNOS mRNA as well as iNOS levels[186]. Similarly MDCK cells subjected to mechanical strain have been shown to produce less NO compared to control cells[115]. However, osteoblasts and tendon fibroblasts subjected to mechanical strain have been

shown to produce increased NO[187, 188]. Furthermore, NO has been shown to inhibit cell proliferation as well as increase cell proliferation depending on the cell type[115, 189]. Together, these facts strongly suggest that mechanical strain induced NO expression as well as its effects on cellular processes are highly dependent on the type of cell being investigated.

6.1.2 Mechanical strain and intercellular adhesion proteins

As mentioned in the previous section, extensive work has been done to characterize the effect of mechanical strain on some of the important cell signaling pathways like MAPK and PLC pathway. However, few studies have focused on studying the possible involvement of intercellular adhesion molecules in relation to mechanical strain induced changes in cellular functions. Previous studies have focused on studying the role of e-cadherins and β-catenin in regulating cellular functions in response to mechanical strain as well as shear flow. For example, β-catenin activation has been shown to be inhibited in colon cancer cells subjected to shear flow[190]. Alteration in the expression of VE-cadherin and β-catenin in response to shear stress has also been observed in endothelial cells[191]. Furthermore, it was observed that application of mechanical force to e-cadherins using magnetic beads functionalized with antibodies directed against the cytoplasmic domain of e-cadherin leads to activation of ion channels[176].

Similar to e-cadherins, tight junctions are also localized at intercellular junctions. They are associated with adaptor molecules like ZO-1/-2/-3 which link them to the actin cytoskeleton. Furthermore, the ZO group of proteins are also important in regulating cell proliferation. Targeting of ZO-1 to the intercellular junctions is associated with the

sequestration of the transcription factor ZONAB from the nucleus to the cell periphery. Nuclear ZONAB is associated with an increase in cell proliferation which is mediated via cell division kinase (CDK) 4[192, 193]. Hence, localization of ZO-1 to the intercellular contact is associated with a decrease in cell proliferation due to ZONAB sequestration. Studies have also shown that ZO-2 can inhibit cell proliferation due to its ability to repress cyclin D1[194]. Furthermore, ZO-2 also modulates the expression of genes containing promoters for the transcription factor AP-1(Activated Protein-1)[195]. The localization of TJ protein at intercellular adhesion and their association with transcription factors that play an important role in cell proliferation make them highly likely candidates for responding to externally applied mechanical strain. However, few studies have explored this possibility. Moreover, the study of the effects of mechanical strain on cells not only helps us in understanding a number of physiological functions, but also provides an insight into the pathogenesis of several diseases.

6.2 Methods and Materials

The design and calibration of the cell stretching device has been described in detail in chapter 3. MDCK cells seeded on silicone membranes and grown to confluence were subjected to a mechanical strain of 20% for 24 hours at a frequency of 0.25Hz. These values of strain and frequency were used because they represent values corresponding to an in vitro model of hydronephrosis. Cells were then fixed and stained for immunofluorescence studies or lysed for protein gel electrophoresis analysis as described in chapter 3.

6.3 Results

6.3.1 Occludin expression is increased in response to mechanical strain

Immunofluorescence images of MDCK cells subjected to mechanical strain obtained using laser scanning confocal microscopy showed a marked increase in the intensity of staining for occludin. Images for control and stretched samples were obtained under identical acquisition parameters for relative comparison. The intercellular boundaries as well as the cytoplasm of the stretched cells showed a significantly more intense staining for occludin as compared to control cells (Fig. 6.5). Furthermore, the increase in occludin expression was also confirmed using Western blots performed on lysates of control cells and cells subjected to mechanical strain (Fig. 6.6). Occludin bands were observed at a molecular weight of ~ 60kD. The two bands observed for occludin represent either splicing variants or molecules phosphorylated to different extents[39]. Some bands of higher molecular weight were also detected and probably correspond to hyper-phosphorylated forms or oligomers of occludin. Multiple bands for occludin have also been observed by several other groups. Staining for JAM-A, another tight junction protein, did not show any significant changes either in the intensity or localization in cells subjected to mechanical strain (Fig. 6.7). A similar increase in occludin expression in response to mechanical strain has previously been observed in endothelial cells[39]. Considering that occludin expression directly correlates with the barrier properties of epithelial monolayers[64, 65], it is likely that increased occludin expression in response to mechanical strain is a protective mechanism on part of the cells to maintain the integrity of the epithelial barrier.

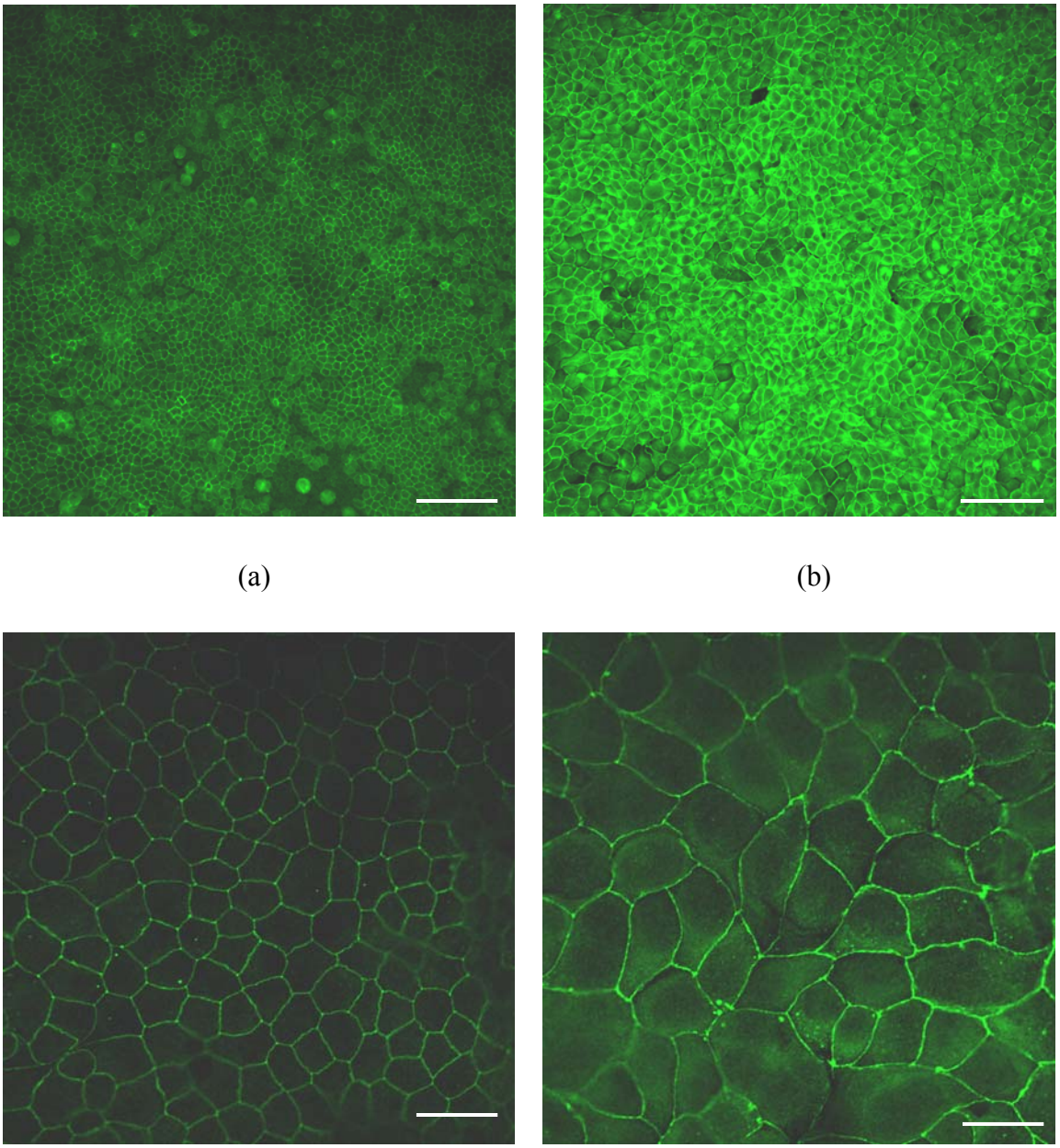

(a) (b)

(c) (d)

Figure 6.5 Laser scanning confocal microscopy images of control MDCK cells (a & c) or MDCK cells subjected to mechanical strain (b & d) stained for occludin obtained using a 20x or 100x objective (scale bars = 100 μm and 20 μm), respectively.

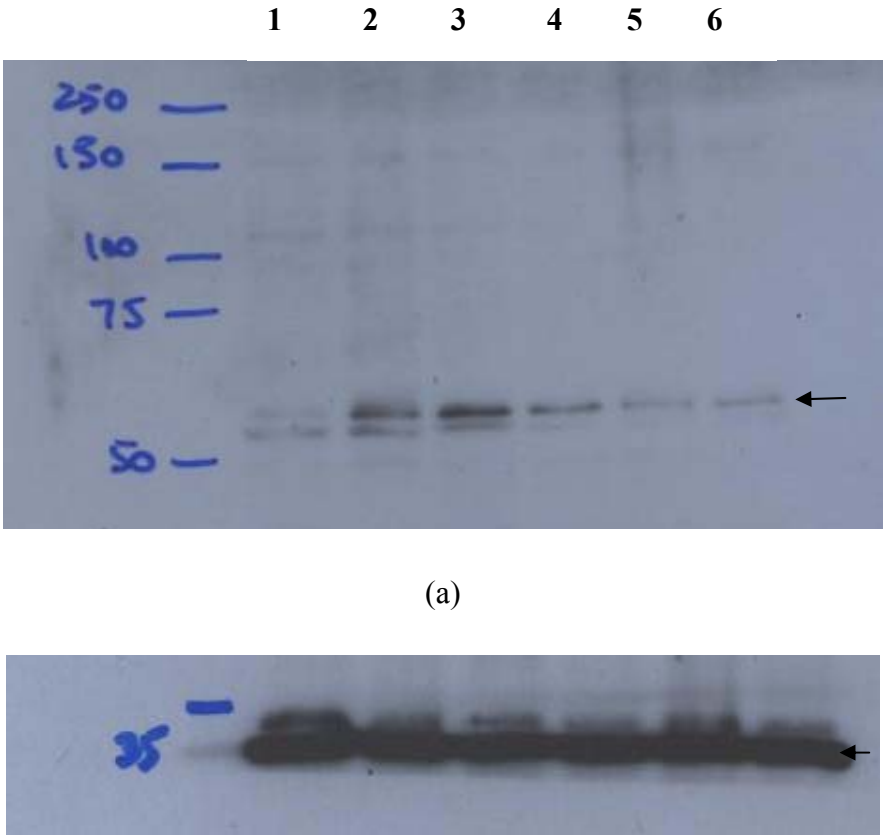

(a)

(b)

Figure 6.6 Western blot of lysates of control MDCK cells (Lanes 4, 5 and 6) and cells subjected to mechanical strain (Lanes 1, 2, and 3) stained for (a) occludin and (b) GAPDH as loading control. Molecular weight marker is shown on extreme left. Band intensities showed a significant difference using unpaired t test.

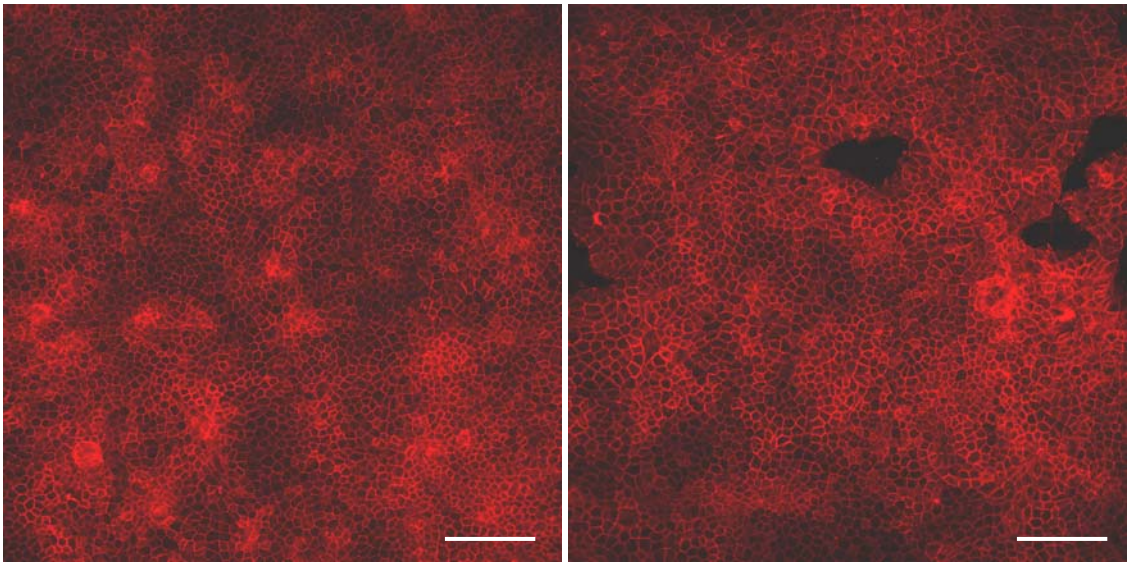

(a) (b)

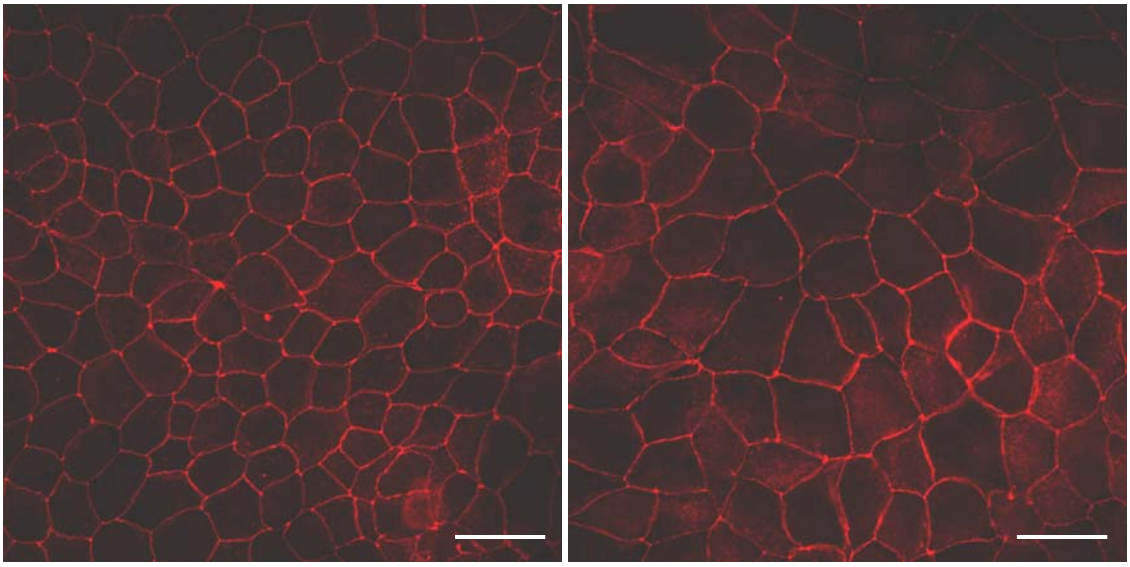

(c) (d)

Figure 6.7 Laser scanning confocal microscopy images of control MDCK cells (a & c) or MDCK cells subjected to mechanical strain (b & d) stained for JAM-A obtained using a 20x or 100x objective (scale bars = 100 μm and 20 μm) respectively.

6.3.2 Application of mechanical strain is associated with nuclear localization of ZO-2 but not ZO-1

ZO-1 and ZO-2 are adaptor molecules that localize at intercellular junctions in confluent monolayers[4, 58]. They link a number of cell adhesion proteins to the actin cytoskeleton. Furthermore, ZO-1 and ZO-2 also play an important role in regulating cell proliferation and gene expression[192, 194, 196]. To investigate whether mechanical strain has any influence on the localization or expression of ZO-1 or ZO-2, control cells and cells subjected to mechanical strain were immunostained for ZO-1 and ZO-2. Consistent with previous observations, it was observed that ZO-1 localized well to the cell boundaries and formed distinct intercellular junction boundaries in confluent cell monolayers. There were, however, no observable changes either in the localization or expression of ZO-1 in response to mechanical strain (Fig. 6.8 a&b).

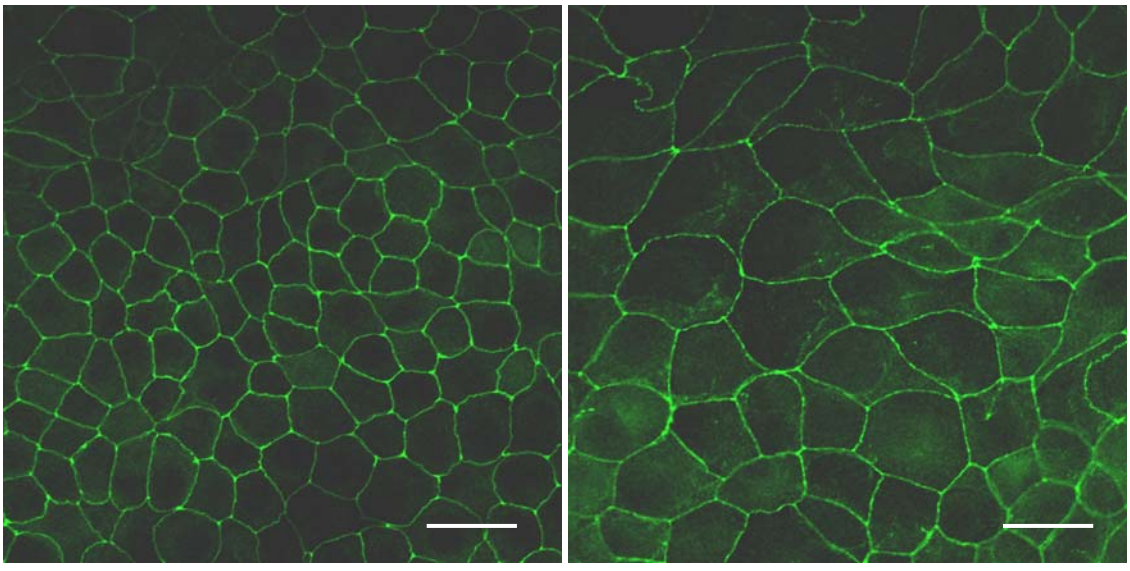

(a) (b)

Figure 6.8 Immunofluorescence images of (a) control or (b) cells subjected to mechanical strain stained for ZO-1 (scale bar = 20 μm).

ZO-2 also localized well to the cell boundaries and intercellular junctions in control cells. In contrast to ZO-1, however, ZO-2 showed a more uniform staining pattern throughout the cell body with a significant concentration in the nuclear region in cells subjected to mechanical strain (Fig. 6.9 a&b). Such a staining pattern strongly suggests that mechanical strain destabilizes ZO-2 localization at the intercellular junction. It has been shown that silencing of ZO-2 using siRNA leads to decreased occludin expression[196]. This suggests that nuclear localization of ZO-2 could, at least in part, be responsible for the mechanical strain induced increase in the expression of occludin.

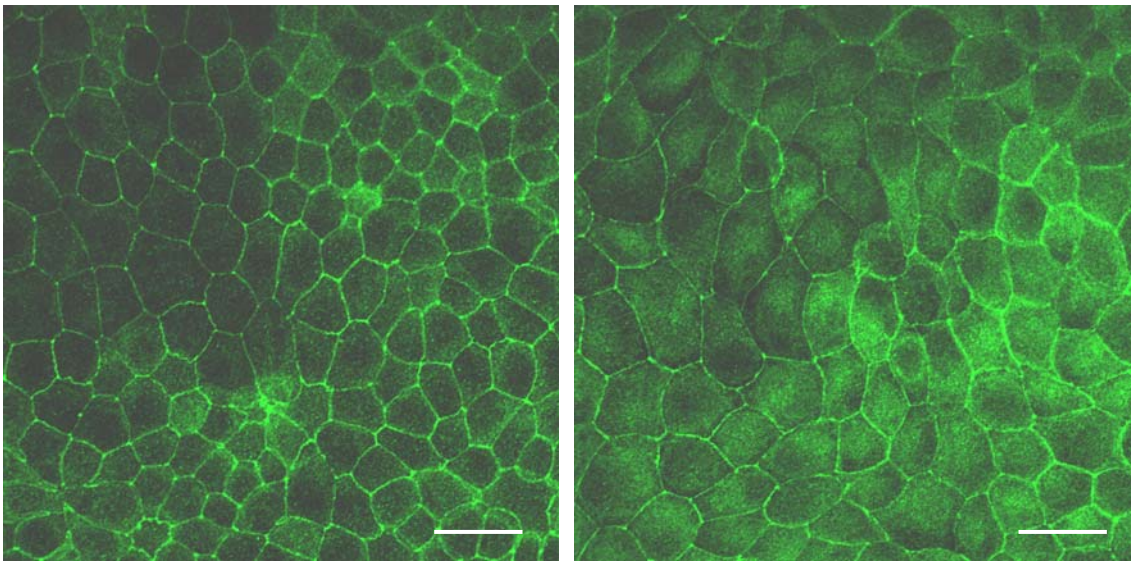

(a) (b)

Figure 6.9 Immunofluorescence images of (a) control cells or (b) cells subjected to mechanical strain stained for ZO-2. Significant amount of ZO-2 is observed in the cell cytoplasm and nuclear region in cells subjected to mechanical strain (scale bar = 20 μm).

6.3.3 Proliferation is inhibited in cells subjected to cyclical mechanical strain

Cell proliferation studies performed using Bromodeoxyuridine (BrdU) showed that mechanical strain inhibited cell proliferation rate (Fig. 6.10). BrdU is a synthetic

analogue of thymidine and is taken up by proliferating cells for incorporation into newly synthesized DNA[197]. Antibodies to BrdU stain those nuclei that have incorporated it into the DNA. These BrdU positive nuclei represent cells that are actively proliferating. The ratio of the BrdU positive nuclei to that of the total nuclei in a given region expressed as percentage represents the proliferation rate of the cells. BrdU method was used for assessing the proliferation in contrast to the widely used MTT assay because the latter is also affected by any changes occurring in the metabolic activity of the cells. The cell proliferation inhibition is also evident from the fact that cell density was lower (and cell size was larger) for cells subjected to mechanical strain (Fig. 6.11). Though there were small disruptions of the epithelial cell monolayer in some regions in cells subjected to mechanical strain, there were no large areas or patches of membrane devoid of cells suggesting that mechanical strain did not detach the monolayer form the membrane. There were also no obvious morphological changes in cells suggestive of apoptosis (e.g. bleb formation, nuclear fragmentation etc.).

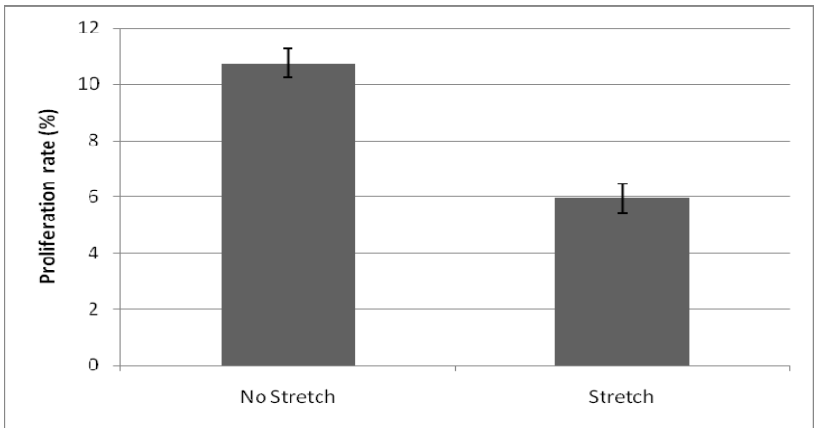

Figure 6.10 Cell proliferation rate assessed using BrdU uptake method. Cells subjected to mechanical strain show a significant decrease in proliferation rate ($p<0.01$ using students unpaired t-test). The values shown are an average of three independent experiments. Bars represent standard error.

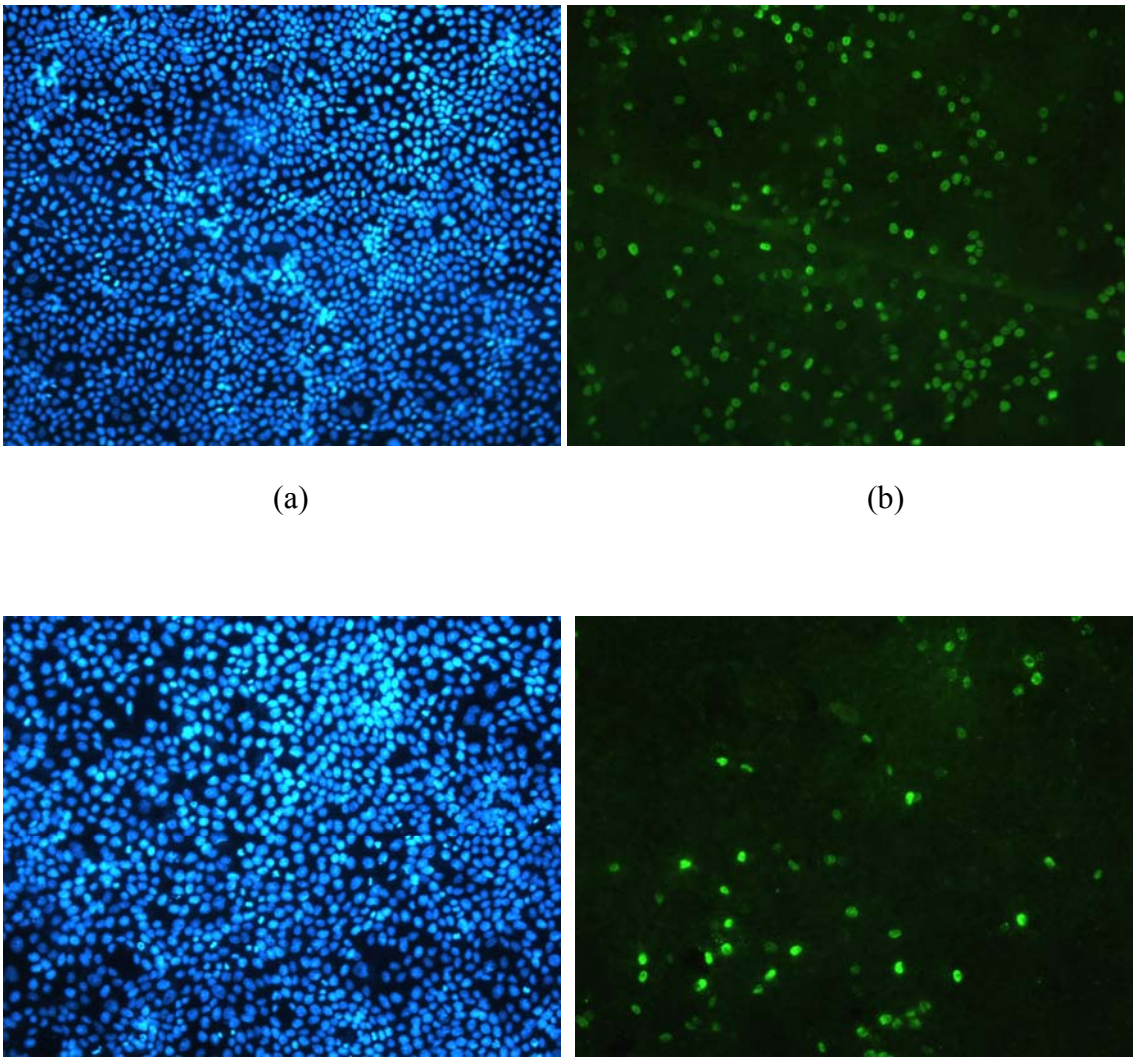

(a) (b)

(c) (d)

Figure 6.11 Control MDCK cells (a&b) or cells subjected to mechanical strain (c&d) double stained for DAPI (blue) and BrdU (green). The proliferation rate was determined as the ratio of BrdU positive nuclei (green) to that of the total number of nuclei (blue) for a given region. Images were obtained on an inverted fluorescence microscope (Leica) using a 20x objective.

It has been shown that ZO-2 can act as a tumor suppressor and can repress cyclin D1 promoter leading to inhibition of cell proliferation[194]. Together with the fact that mechanical strain is associated with an increased nuclear localization of ZO-2, it is likely

that the inhibition of cell proliferation in response to mechanical strain is a result of cyclin D1 repression by ZO-2.

6.4 Discussion and conclusions

Using a custom built cell stretcher, the influence of mechanical strain on the expression and localization of specific tight junction proteins as well as on proliferation rate was investigated in MDCK cells. It is observed that externally applied mechanical strain is associated with destabilization of ZO-2 at tight junctions and that this could be one of the important mechanisms influencing the observed cellular responses. This observation strongly supports the role of tight junctions as an important link in integrating external mechanical strain and cellular responses.

Previous studies carried on alveolar epithelial cells have shown that mechanical strain can result in disruption of occludin staining at the intercellular junctions as well as decrease in the overall expression of occludin[30, 113]. It was suggested that the disruption of occludin at the intercellular contacts could be responsible for the increased permeability of respiratory epithelia observed in clinical settings where alveolar epithelial cells are subjected to large mechanical strains e.g. artificial ventilation. Epithelial cells lining the renal tubules are also subjected to large mechanical strains in persons suffering from hydronephrosis. Hydronephrosis is the term used to refer to abnormal dilatation of the renal pelvis and collecting tubule system resulting from obstructions arising from the presence of stones, tumors, prostatic hypertrophy or congenital cysts. Large pressures build up in the lumen of the collecting ducts proximal to the site of obstruction resulting in the dilatation of the tubules and exertion of mechanical strain on the epithelial cells

lining the tubules. The high pressure is one of the most important causes of renal tubular cell death and chronic renal failure in patients suffering from hydronephrosis. We hypothesized that such large strains acting on renal epithelial cells could alter occludin expression and localization. To test this hypothesis, MDCK cells grown on flexible silicone membrane were subjected to external mechanical strain. MDCK cells (derived from epithelium of dog kidney) have been established as a model system for studying epithelial cells in general and as a cellular model for hydronephrosis in particular[115]. Contrary to expectation, there was no observable disruption in the regular and uniform staining pattern of occludin at the intercellular junctions. In fact, there was increased concentration of occludin along the intercellular junction observed as increased intensity in immunofluorescence staining. Furthermore, there was an overall increase in occludin expression in response to mechanical strain. Since renal tubular epithelial cells are involved in excretion of waste products of metabolism as well as in regulating the electrolyte balance in the body, the integrity and selectivity of the epithelial barrier is critical for maintaining homeostasis. It is very likely that the increase in occludin expression in response to mechanical strain has evolved as a protective mechanism to maintain the integrity of the paracellular barrier. An increase in occludin expression in response to mechanical strain has recently been demonstrated in endothelial cells also where it has been proposed to augment the paracellular barrier[39].

ZO-2 has been shown to play an important role in regulating the expression of genes involved in controlling cell proliferation. Since a direct association of ZO-2 with DNA has not been established, most of the regulatory functions of ZO-2 stem from its ability to bind to and modulate the activity of other transcription factors. It has previously been

shown that silencing ZO-2 using siRNA leads to a decrease in expression of occludin suggesting that ZO-2 has a positive effect on occludin expression[196]. Furthermore, occludin promoter has a number of putative sites for binding of AP-1, whose transcriptional activity is significantly modulated by ZO-2. Consistent with this fact, in our experiments, it was found that there was significant nuclear localization of ZO-2 in cells subjected to mechanical strain. Based on these observations, we propose a model in which externally acting mechanical strain destabilizes ZO-2 from the tight junctions. Some of the ZO-2 translocates to the nucleus leading to an increase in occludin expression probably by binding to and inhibiting an occludin repressor or as a result of AP-1 activation. Furthermore, ZO-2 has also been shown to repress the cyclin D1 promoter by binding to c-myc and recruiting HDAC[194]. Since activation of cyclin D1 is associated with an increase in cell proliferation, nuclear localization of ZO-2 also explains the mechanical strain induced inhibition of cell proliferation (Fig. 6.12). It is very likely that the observed inhibition of proliferation rate in response to mechanical strain is a net result of several signaling pathways. ZO-2 mediated inhibition is probably only one of the several possible mechanisms. For e.g. it has been shown previously that MDCK cells subjected to mechanical strain show decreased production of nitric oxide (NO) and that supplementing the culture medium with NO donors like sodium nitroprusside had a protective effect on mechanical strain induced inhibition of cell proliferation rate.

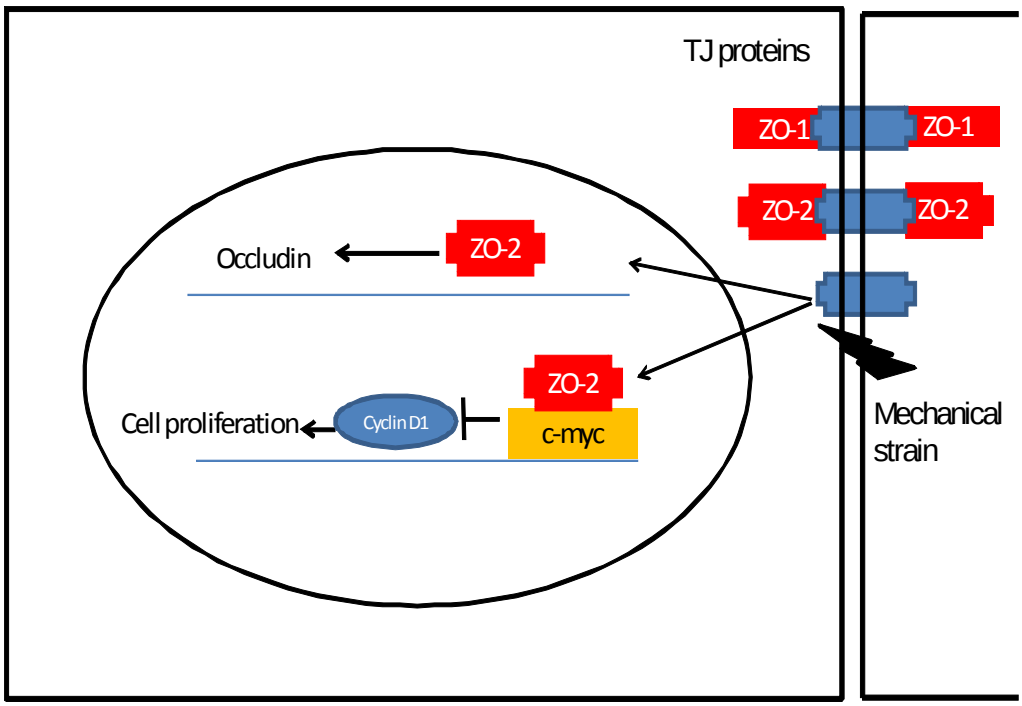

Figure 6.12 A model for explaining the mechanical strain induced changes in MDCK cells. ZO-2 is destabilized by the external mechanical strain leading to an increase in its concentration in the cell nucleus and cytoplasm. ZO-2 in turn increases occludin expression and inhibits cell proliferation.

In conclusion, we show for the first time that mechanical strain induces occludin expression and inhibits cell proliferation in MDCK cells. Furthermore, these effects are probably a result of nuclear re-localization of ZO-2 as well as involvement of the MAPK pathway. It is highly likely that these responses have evolved to protect the cells from large mechanical strains.

7 Conclusions and Future Work

The focus of this thesis has been to understand the adhesion kinetics of specific intercellular adhesion molecules by applying single molecule force spectroscopy and to study the effect of mechanical strain on the expression and localization of specific tight junction proteins. The two main hypotheses around which experiments have been designed are that (a) single molecule force spectroscopy of interactions mediated by intercellular adhesion proteins can provide us with a better understanding of their role in regulating physiological functions and (b) expression and localization of specific intercellular adhesion molecules (tight junction proteins) is altered in response to externally applied mechanical strain.

7.1 Conclusions

The main contribution of this thesis has been the elucidation of the adhesion kinetics of specific intercellular adhesion proteins (nectin-1 and JAM-A) and the effect of mechanical strain on the expression and localization of tight junction proteins. The results and conclusions of this thesis can be summarized as follows:

(a) The adhesion kinetics of nectin-1 mediated interactions probed by SMFS experiments provides a biophysical basis for their role in forming adherens junctions. Furthermore, SMFS experiments also reveal the existence of multiple binding interactions configurations between nectin-1 molecules similar to E-cadherin. While configuration I has a long bond half life and helps to stabilize the initial adhesion formed, configurations II and III have a low reactive compliance making them highly resistant to externally

applied force. The results, for the first time, provide a strong biophysical support for a cell adhesion model that has been proposed based on biochemical evidence only.

(b) Homophilic interactions mediated by JAM-A have also been characterized, for the first time, using SMFS experiments. The dynamic nature of homophilic JAM-A interactions is physiologically consistent with its role in regulating paracellular diffusion as well as in trans-endothelial migration of leukocytes. Furthermore, SMFS experiments also reveal that interactions of reovirus attachment protein σ1 with JAM-A are much more stable than homophilic JAM-A interactions. Such stable interactions can not only help the virus in disrupting normal homophilic JAM-A interactions but also provide a strong foothold for the virus to enter the cell.

(c) Alterations in the expression and localization of specific tight junction proteins in epithelial cells in response to mechanical strain have been investigated. Mechanical strain was associated with an increase in the expression of occludin as well as re-localization of ZO-2 from cell boundaries in MDCK. Furthermore, mechanical strain also inhibited cell proliferation in these cells. Since ZO-2 has previously been established as a regulator of occludin expression as well as cell proliferation, we propose that ZO-2 re-localization is one of the main causes for the observed cellular response. These results, for the first time, point towards the possible role of ZO-2 in modulating the response of cells to mechanical strain.

7.2 Future Work

The work presented in this thesis opens up three important and exciting research avenues for exploration in the future:

(a) Only representative components of intercellular adhesion molecules have been explored in this thesis. However, the same technique and principle can be applied to study and characterize other important protein interactions. In particular, the study of newly identified interactions of intercellular adhesion proteins e.g. hepatitis C virus (HCV) interaction with Claudins and herpes envelope glycoprotein with nectin-1 can provide a better understanding of viral adhesion and pathogenesis. Other interesting interactions involving tight junction proteins include Clostridium perfringens enterotoxin (CPE) with Claudin-3 & Claudin-4 and interactions of JAM-C expressed on cancerous cells with endothelial cells. This would help us in better understanding the role of intercellular adhesion molecules in the pathogenesis of several important diseases.

(b) The cell stretcher has been designed to allow the visualization of the protein localization and trafficking in response to mechanical strain in real time. Cells transfected with GFP (green fluorescent protein)-tagged tight junction proteins e.g. ZO-2 and occludin can be subjected to mechanical strain to visualize their dynamics in real time.

(c) The mechanism by which externally applied mechanical strain influences the expression and localization of tight junction proteins needs to be explored in depth. In particular, the potential role of MAPK pathway, PLC pathway and ion channels needs to be defined.

8 Bibliography

[1]E. Knust, Regulation of epithelial cell shape and polarity by cell-cell adhesion (Review). Mol Membr Biol, 19(2002.)(2): p. 113-20.

[2]A. L. Berrier,K. M. Yamada, Cell-matrix adhesion. J Cell Physiol, 213(2007.)(3): p. 565-73.

[3]B. M. Gumbiner, Breaking through the tight junction barrier. J Cell Biol, 123(1993.)(6 Pt 2): p. 1631-3.

[4]K. Matter,M. S. Balda, Signalling to and from tight junctions. Nat Rev Mol Cell Biol, 4(2003.)(3): p. 225-36.

[5]M. S. Balda,K. Matter, Epithelial cell adhesion and the regulation of gene expression. Trends Cell Biol, 13(2003.)(6): p. 310-8.

[6]K. Ley, C. Laudanna, M. I. Cybulsky, S. Nourshargh, Getting to the site of inflammation: the leukocyte adhesion cascade updated. Nat Rev Immunol, 7(2007.)(9): p. 678-89.

[7]C. Krummenacher, A. V. Nicola, J. C. Whitbeck, H. Lou, W. Hou, J. D. Lambris, R. J. Geraghty, P. G. Spear, G. H. Cohen, R. J. Eisenberg, Herpes simplex virus glycoprotein D can bind to poliovirus receptor-related protein 1 or herpesvirus entry mediator, two structurally unrelated mediators of virus entry. J Virol, 72(1998.)(9): p. 7064-74.

[8]E. S. Barton, J. C. Forrest, J. L. Connolly, J. D. Chappell, Y. Liu, F. J. Schnell, A. Nusrat, C. A. Parkos, T. S. Dermody, Junction adhesion molecule is a receptor for reovirus. Cell, 104(2001.)(3): p. 441-51.

[9]M. J. Evans, T. von Hahn, D. M. Tscherne, A. J. Syder, M. Panis, B. Wolk, T. Hatziioannou, J. A. McKeating, P. D. Bieniasz, C. M. Rice, Claudin-1 is a hepatitis C virus co-receptor required for a late step in entry. Nature, 446(2007.)(7137): p. 801-5.

[10]S. R. K. Vedula, T. S. Lim, W. Hunziker, C. T. Lim, Mechanistic insights into physiological functions of cell adhesion proteins using single molecule force spectroscopy. Molecular and cellular Biomechanics, (in press)(2008.)(

[11]S. Tsukita, M. Furuse, M. Itoh, Multifunctional strands in tight junctions. Nat Rev Mol Cell Biol, 2(2001.)(4): p. 285-93.

[12]S.R.K.Vedula, T.S. Lim, G. Rajagopal, W. Hunziker, Lane B, M. Sokabe, C.T. Lim, *Role of External Mechanical Forces in Cell Signal Transduction*, in *Biomechanics at micro- and nanoscale levels*, H. Wada, Editor. 2007, World Scientific: Singapore.

[13]C. E. Turner, Paxillin and focal adhesion signalling. Nat Cell Biol, 2(2000.)(12): p. E231-6.

[14]D. R. Critchley, Focal adhesions - the cytoskeletal connection. Curr Opin Cell Biol, 12(2000.)(1): p. 133-9.

[15]D. D. Schlaepfer, C. R. Hauck, D. J. Sieg, Signaling through focal adhesion kinase. Prog Biophys Mol Biol, 71(1999.)(3-4): p. 435-78.

[16]S. R. Vedula, T. S. Lim, P. J. Kausalya, W. Hunziker, G. Rajagopal, C. T. Lim, Biophysical approaches for studying the integrity and function of tight junctions. Mol Cell Biomech, 2(2005.)(3): p. 105-23.

[17]S. Oez, K. Welte, E. Platzer, J. R. Kalden, A simple assay for quantifying the inducible adherence of neutrophils. Immunobiology, 180(1990.)(4-5): p. 308-15.

[18]E. A. Price, D. R. Coombe, J. C. Murray, A simple fluorometric assay for quantifying the adhesion of tumour cells to endothelial monolayers. Clin Exp Metastasis, 13(1995.)(3): p. 155-64.

[19]P. Bongrand,P. Golstein, Reproducible dissociation of cellular aggregates with a wide range of calibrated shear forces: application to cytolytic lymphocyte target cell conjugates. J Immunol Methods, 58(1983.)(1-2): p. 209-24.

[20]F. Amblard, C. Cantin, J. Durand, A. Fischer, R. Sekaly, C. Auffray, New chamber for flow cytometric analysis over an extended range of stream velocity and application to cell adhesion measurements. Cytometry, 13(1992.)(1): p. 15-22.

[21]D. R. McClay, G. M. Wessel, R. B. Marchase, Intercellular recognition: quantitation of initial binding events. Proc Natl Acad Sci U S A, 78(1981.)(8): p. 4975-9.

[22]H. Urushihara, M. Takeichi, A. Hakura, T. S. Okada, Different cation requirements for aggregation of BHK cells and their transformed derivatives. J Cell Sci, 22(1976.)(3): p. 685-95.

[23]K. L. Sung, L. A. Sung, M. Crimmins, S. J. Burakoff, S. Chien, Determination of junction avidity of cytolytic T cell and target cell. Science, 234(1986.)(4782): p. 1405-8.

[24]C. T. Lim, E. H. Zhou, A. Li, S. R. K. Vedula, H. X. Fu, Experimental techniques for single cell and single molecule biomechanics. Materials Science and Engineering: C, 26(2006.)(8): p. 1278-1288.

[25]C. C. Wu, H. W. Su, C. C. Lee, M. J. Tang, F. C. Su, Quantitative measurement of changes in adhesion force involving focal adhesion kinase during cell attachment, spread, and migration. Biochem Biophys Res Commun, 329(2005.)(1): p. 256-65.

[26]W. Baumgartner, P. Hinterdorfer, W. Ness, A. Raab, D. Vestweber, H. Schindler, D. Drenckhahn, Cadherin interaction probed by atomic force microscopy. Proc Natl Acad Sci U S A, 97(2000.)(8): p. 4005-10.

[27]X. Zhang, E. Wojcikiewicz, V. T. Moy, Force spectroscopy of the leukocyte function-associated antigen-1/intercellular adhesion molecule-1 interaction. Biophys J, 83(2002.)(4): p. 2270-9.

[28]P. Panorchan, J. P. George, D. Wirtz, Probing intercellular interactions between vascular endothelial cadherin pairs at single-molecule resolution and in living cells. J Mol Biol, 358(2006.)(3): p. 665-74.

[29]H. Wan, H. L. Winton, C. Soeller, E. R. Tovey, D. C. Gruenert, P. J. Thompson, G. A. Stewart, G. W. Taylor, D. R. Garrod, M. B. Cannell, C. Robinson, Der p 1 facilitates transepithelial allergen delivery by disruption of tight junctions. J Clin Invest, 104(1999.)(1): p. 123-33.

[30]K. J. Cavanaugh, Jr., J. Oswari, S. S. Margulies, Role of stretch on tight junction structure in alveolar epithelial cells. Am J Respir Cell Mol Biol, 25(2001.)(5): p. 584-91.

[31]N. Sonoda, M. Furuse, H. Sasaki, S. Yonemura, J. Katahira, Y. Horiguchi, S. Tsukita, Clostridium perfringens enterotoxin fragment removes specific claudins from tight junction strands: Evidence for direct involvement of claudins in tight junction barrier. J Cell Biol, 147(1999.)(1): p. 195-204.

[32]K. D. Chen, Y. S. Li, M. Kim, S. Li, S. Yuan, S. Chien, J. Y. Shyy, Mechanotransduction in response to shear stress. Roles of receptor tyrosine kinases, integrins, and Shc. J Biol Chem, 274(1999.)(26): p. 18393-400.

[33]L. L. Demer, C. M. Wortham, E. R. Dirksen, M. J. Sanderson, Mechanical stimulation induces intercellular calcium signaling in bovine aortic endothelial cells. Am J Physiol, 264(1993.)(6 Pt 2): p. H2094-102.

[34]M. A. Haidekker, N. L'Heureux, J. A. Frangos, Fluid shear stress increases membrane fluidity in endothelial cells: a study with DCVJ fluorescence. Am J Physiol Heart Circ Physiol, 278(2000.)(4): p. H1401-6.

[35]C. L. Ives, S. G. Eskin, L. V. McIntire, Mechanical effects on endothelial cell morphology: in vitro assessment. In Vitro Cell Dev Biol, 22(1986.)(9): p. 500-7.

[36]K. Murata, I. Mills, B. E. Sumpio, Protein phosphatase 2A in stretch-induced endothelial cell proliferation. J Cell Biochem, 63(1996.)(3): p. 311-9.

[37]T. Osada, K. Iijima, H. Tanaka, M. Hirose, J. Yamamoto, S. Watanabe, Effect of temperature and mechanical strain on gastric epithelial cell line GSM06 wound restoration in vitro. J Gastroenterol Hepatol, 14(1999.)(5): p. 489-94.

[38]T. Osada, S. Watanabe, H. Tanaka, M. Hirose, A. Miyazaki, N. Sato, Effect of mechanical strain on gastric cellular migration and proliferation during mucosal healing: role of Rho dependent and Rac dependent cytoskeletal reorganisation. Gut, 45(1999.)(4): p. 508-15.

[39]N. T. Collins, P. M. Cummins, O. C. Colgan, G. Ferguson, Y. A. Birney, R. P. Murphy, G. Meade, P. A. Cahill, Cyclic strain-mediated regulation of vascular endothelial occludin and ZO-1: influence on intercellular tight junction assembly and function. Arterioscler Thromb Vasc Biol, 26(2006.)(1): p. 62-8.

[40]M. Takeichi, Cadherin cell adhesion receptors as a morphogenetic regulator. Science, 251(1991.)(5000): p. 1451-5.

[41]Y. Takai,H. Nakanishi, Nectin and afadin: novel organizers of intercellular junctions. J Cell Sci, 116(2003.)(Pt 1): p. 17-27.

[42]K. Mandai, H. Nakanishi, A. Satoh, H. Obaishi, M. Wada, H. Nishioka, M. Itoh, A. Mizoguchi, T. Aoki, T. Fujimoto, Y. Matsuda, S. Tsukita, Y. Takai, Afadin: A novel actin filament-binding protein with one PDZ domain localized at cadherin-based cell-to-cell adherens junction. J Cell Biol, 139(1997.)(2): p. 517-28.

[43]K. Tachibana, H. Nakanishi, K. Mandai, K. Ozaki, W. Ikeda, Y. Yamamoto, A. Nagafuchi, S. Tsukita, Y. Takai, Two cell adhesion molecules, nectin and cadherin, interact through their cytoplasmic domain-associated proteins. J Cell Biol, 150(2000.)(5): p. 1161-76.

[44]C. Martinez-Rico, F. Pincet, E. Perez, J. P. Thiery, K. Shimizu, Y. Takai, S. Dufour, Separation force measurements reveal different types of modulation of E-cadherin-based adhesion by nectin-1 and -3. J Biol Chem, 280(2005.)(6): p. 4753-60.

[45]L. Shapiro, A. M. Fannon, P. D. Kwong, A. Thompson, M. S. Lehmann, G. Grubel, J. F. Legrand, J. Als-Nielsen, D. R. Colman, W. A. Hendrickson, Structural basis of cell-cell adhesion by cadherins. Nature, 374(1995.)(6520): p. 327-37.

[46]F. Drees, S. Pokutta, S. Yamada, W. J. Nelson, W. I. Weis, Alpha-catenin is a molecular switch that binds E-cadherin-beta-catenin and regulates actin-filament assembly. Cell, 123(2005.)(5): p. 903-15.

[47]B. Nagar, M. Overduin, M. Ikura, J. M. Rini, Structural basis of calcium-induced E-cadherin rigidification and dimerization. Nature, 380(1996.)(6572): p. 360-4.

[48]K. Kubota, M. Furuse, H. Sasaki, N. Sonoda, K. Fujita, A. Nagafuchi, S. Tsukita, Ca(2+)-independent cell-adhesion activity of claudins, a family of integral membrane proteins localized at tight junctions. Curr Biol, 9(1999.)(18): p. 1035-8.

[49]C. M. Niessen, Tight junctions/adherens junctions: basic structure and function. J Invest Dermatol, 127(2007.)(11): p. 2525-32.

[50]M. E. Morrison,V. R. Racaniello, Molecular cloning and expression of a murine homolog of the human poliovirus receptor gene. J Virol, 66(1992.)(5): p. 2807-13.

[51]J. Aoki, S. Koike, H. Asou, I. Ise, H. Suwa, T. Tanaka, M. Miyasaka, A. Nomoto, Mouse homolog of poliovirus receptor-related gene 2 product, mPRR2, mediates homophilic cell aggregation. Exp Cell Res, 235(1997.)(2): p. 374-84.

[52]F. Eberle, P. Dubreuil, M. G. Mattei, E. Devilard, M. Lopez, The human PRR2 gene, related to the human poliovirus receptor gene (PVR), is the true homolog of the murine MPH gene. Gene, 159(1995.)(2): p. 267-72.

[53]F. Cocchi, L. Menotti, P. Mirandola, M. Lopez, G. Campadelli-Fiume, The ectodomain of a novel member of the immunoglobulin subfamily related to the poliovirus receptor has the attributes of a bona fide receptor for herpes simplex virus types 1 and 2 in human cells. J Virol, 72(1998.)(12): p. 9992-10002.

[54]M. Lopez, M. Aoubala, F. Jordier, D. Isnardon, S. Gomez, P. Dubreuil, The human poliovirus receptor related 2 protein is a new hematopoietic/endothelial homophilic adhesion molecule. Blood, 92(1998.)(12): p. 4602-11.

[55]T. Honda, K. Shimizu, T. Kawakatsu, M. Yasumi, T. Shingai, A. Fukuhara, K. Ozaki-Kuroda, K. Irie, H. Nakanishi, Y. Takai, Antagonistic and agonistic effects of an extracellular fragment of nectin on formation of E-cadherin-based cell-cell adhesion. Genes Cells, 8(2003.)(1): p. 51-63.

[56]T. Sato, N. Fujita, A. Yamada, T. Ooshio, R. Okamoto, K. Irie, Y. Takai, Regulation of the assembly and adhesion activity of E-cadherin by nectin and afadin for the formation of adherens junctions in Madin-Darby canine kidney cells. J Biol Chem, 281(2006.)(8): p. 5288-99.

[57]T. Honda, K. Shimizu, A. Fukuhara, K. Irie, Y. Takai, Regulation by nectin of the velocity of the formation of adherens junctions and tight junctions. Biochem Biophys Res Commun, 306(2003.)(1): p. 104-9.

[58]K. Matter,M. S. Balda, Functional analysis of tight junctions. Methods, 30(2003.)(3): p. 228-34.

[59]M. Furuse, T. Hirase, M. Itoh, A. Nagafuchi, S. Yonemura, S. Tsukita, Occludin: a novel integral membrane protein localizing at tight junctions. J Cell Biol, 123(1993.)(6 Pt 2): p. 1777-88.

[60]M. Furuse, K. Fujita, T. Hiiragi, K. Fujimoto, S. Tsukita, Claudin-1 and -2: novel integral membrane proteins localizing at tight junctions with no sequence similarity to occludin. J Cell Biol, 141(1998.)(7): p. 1539-50.

[61]A. S. Fanning, B. J. Jameson, L. A. Jesaitis, J. M. Anderson, The tight junction protein ZO-1 establishes a link between the transmembrane protein occludin and the actin cytoskeleton. J Biol Chem, 273(1998.)(45): p. 29745-53.

[62]C. M. Van Itallie,J. M. Anderson, Occludin confers adhesiveness when expressed in fibroblasts. J Cell Sci, 110 (Pt 9)(1997.)(p. 1113-21.

[63]M. S. Balda, J. A. Whitney, C. Flores, S. Gonzalez, M. Cereijido, K. Matter, Functional dissociation of paracellular permeability and transepithelial electrical resistance and disruption of the apical-basolateral intramembrane diffusion barrier by expression of a mutant tight junction membrane protein. J Cell Biol, 134(1996.)(4): p. 1031-49.

[64]T. Hirase, J. M. Staddon, M. Saitou, Y. Ando-Akatsuka, M. Itoh, M. Furuse, K. Fujimoto, S. Tsukita, L. L. Rubin, Occludin as a possible determinant of tight junction permeability in endothelial cells. J Cell Sci, 110 (Pt 14)(1997.)(p. 1603-13.

[65]C. G. Kevil, N. Okayama, S. D. Trocha, T. J. Kalogeris, L. L. Coe, R. D. Specian, C. P. Davis, J. S. Alexander, Expression of zonula occludens and adherens junctional proteins in human venous and arterial endothelial cells: role of occludin in endothelial solute barriers. Microcirculation, 5(1998.)(2-3): p. 197-210.

[66]M. Furuse, H. Sasaki, K. Fujimoto, S. Tsukita, A single gene product, claudin-1 or -2, reconstitutes tight junction strands and recruits occludin in fibroblasts. J Cell Biol, 143(1998.)(2): p. 391-401.

[67]M. Furuse, H. Sasaki, S. Tsukita, Manner of interaction of heterogeneous claudin species within and between tight junction strands. J Cell Biol, 147(1999.)(4): p. 891-903.

[68]I. Martin-Padura, S. Lostaglio, M. Schneemann, L. Williams, M. Romano, P. Fruscella, C. Panzeri, A. Stoppacciaro, L. Ruco, A. Villa, D. Simmons, E. Dejana, Junctional adhesion molecule, a novel member of the immunoglobulin superfamily that distributes at intercellular junctions and modulates monocyte transmigration. J Cell Biol, 142(1998.)(1): p. 117-27.

[69]S. A. Cunningham, M. P. Arrate, J. M. Rodriguez, R. J. Bjercke, P. Vanderslice, A. P. Morris, T. A. Brock, A novel protein with homology to the junctional adhesion molecule. Characterization of leukocyte interactions. J Biol Chem, 275(2000.)(44): p. 34750-6.

[70]M. B. Sobocka, T. Sobocki, P. Banerjee, C. Weiss, J. I. Rushbrook, A. J. Norin, J. Hartwig, M. O. Salifu, M. S. Markell, A. Babinska, Y. H. Ehrlich, E. Kornecki, Cloning of the human platelet F11 receptor: a cell adhesion molecule member of the immunoglobulin superfamily involved in platelet aggregation. Blood, 95(2000.)(8): p. 2600-9.

[71]Y. Liu, A. Nusrat, F. J. Schnell, T. A. Reaves, S. Walsh, M. Pochet, C. A. Parkos, Human junction adhesion molecule regulates tight junction resealing in epithelia. J Cell Sci, 113 (Pt 13)(2000.)(p. 2363-74.

[72]M. U. Naik, S. A. Mousa, C. A. Parkos, U. P. Naik, Signaling through JAM-1 and alphavbeta3 is required for the angiogenic action of bFGF: dissociation of the JAM-1 and alphavbeta3 complex. Blood, 102(2003.)(6): p. 2108-14.

[73]V. G. Cooke, M. U. Naik, U. P. Naik, Fibroblast growth factor-2 failed to induce angiogenesis in junctional adhesion molecule-A-deficient mice. Arterioscler Thromb Vasc Biol, 26(2006.)(9): p. 2005-11.

[74]D. Kostrewa, M. Brockhaus, A. D'Arcy, G. E. Dale, P. Nelboeck, G. Schmid, F. Mueller, G. Bazzoni, E. Dejana, T. Bartfai, F. K. Winkler, M. Hennig, X-ray structure of junctional adhesion molecule: structural basis for homophilic adhesion via a novel dimerization motif. Embo J, 20(2001.)(16): p. 4391-8.

[75]K. Ebnet, C. U. Schulz, M. K. Meyer Zu Brickwedde, G. G. Pendl, D. Vestweber, Junctional adhesion molecule interacts with the PDZ domain-containing proteins AF-6 and ZO-1. J Biol Chem, 275(2000.)(36): p. 27979-88.

[76]E. Kornecki, B. Walkowiak, U. P. Naik, Y. H. Ehrlich, Activation of human platelets by a stimulatory monoclonal antibody. J Biol Chem, 265(1990.)(17): p. 10042-8.

[77]U. P. Naik, M. U. Naik, K. Eckfeld, P. Martin-DeLeon, J. Spychala, Characterization and chromosomal localization of JAM-1, a platelet receptor for a stimulatory monoclonal antibody. J Cell Sci, 114(2001.)(Pt 3): p. 539-47.

[78]K. J. Mandell, I. C. McCall, C. A. Parkos, Involvement of the junctional adhesion molecule-1 (JAM1) homodimer interface in regulation of epithelial barrier function. J Biol Chem, 279(2004.)(16): p. 16254-62.

[79]A. Woodfin, C. A. Reichel, A. Khandoga, M. Corada, M. B. Voisin, C. Scheiermann, D. O. Haskard, E. Dejana, F. Krombach, S. Nourshargh, JAM-A mediates neutrophil transmigration in a stimulus-specific manner in vivo: evidence for sequential roles for JAM-A and PECAM-1 in neutrophil transmigration. Blood, 110(2007.)(6): p. 1848-56.

[80]G. Ostermann, K. S. Weber, A. Zernecke, A. Schroder, C. Weber, JAM-1 is a ligand of the beta(2) integrin LFA-1 involved in transendothelial migration of leukocytes. Nat Immunol, 3(2002.)(2): p. 151-8.

[81]G. Binnig, C. F. Quate, C. Gerber, Atomic Force Microscope. Physical Review Letters, 56(1986.)(9): p. 930 LP - 933.

[82]B. C. Hans-Jürgen Butta, Michael Kappl, Force measurements with the atomic force microscope: Technique, interpretation and applications. Surface Science Reports, 59(2005.)(1-6): p. 1-152.

[83]W. Hanley, O. McCarty, S. Jadhav, Y. Tseng, D. Wirtz, K. Konstantopoulos, Single molecule characterization of P-selectin/ligand binding. J Biol Chem, 278(2003.)(12): p. 10556-61.

[84]W. D. Hanley, D. Wirtz, K. Konstantopoulos, Distinct kinetic and mechanical properties govern selectin-leukocyte interactions. J Cell Sci, 117(2004.)(Pt 12): p. 2503-11.

[85]P. Panorchan, M. S. Thompson, K. J. Davis, Y. Tseng, K. Konstantopoulos, D. Wirtz, Single-molecule analysis of cadherin-mediated cell-cell adhesion. J Cell Sci, 119(2006.)(Pt 1): p. 66-74.

[86]P. Hinterdorfer,Y. F. Dufrene, Detection and localization of single molecular recognition events using atomic force microscopy. Nat Methods, 3(2006.)(5): p. 347-55.

[87]T. S. Lim, S. R. Vedula, P. J. Kausalya, W. Hunziker, C. T. Lim, Single-Molecular-Level Study of Claudin-1-Mediated Adhesion. Langmuir, (2007.)(

[88]C. Verbelen, H. J. Gruber, Y. F. Dufrene, The NTA-His6 bond is strong enough for AFM single-molecular recognition studies. J Mol Recognit, 20(2007.)(6): p. 490-4.

[89]A. Touhami, B. Hoffmann, A. Vasella, F. A. Denis, Y. F. Dufrene, Probing Specific Lectin-Carbohydrate Interactions Using Atomic Force Microscopy Imaging and Force Measurements. Langmuir, 19(2003.)(5): p. 1745-1751.

[90]C. Stroh, H. Wang, R. Bash, B. Ashcroft, J. Nelson, H. Gruber, D. Lohr, S. M. Lindsay, P. Hinterdorfer, Single-molecule recognition imaging microscopy. Proc Natl Acad Sci U S A, 101(2004.)(34): p. 12503-7.

[91]T. Haselgrubler, A. Amerstorfer, H. Schindler, H. J. Gruber, Synthesis and applications of a new poly(ethylene glycol) derivative for the crosslinking of amines with thiols. Bioconjug Chem, 6(1995.)(3): p. 242-8.

[92]T. S. Lim, S. R. Vedula, P. J. Kausalya, W. Hunziker, C. T. Lim, Single-molecular-level study of claudin-1-mediated adhesion. Langmuir, 24(2008.)(2): p. 490-5.

[93]M. Benoit,H. E. Gaub, Measuring cell adhesion forces with the atomic force microscope at the molecular level. Cells Tissues Organs, 172(2002.)(3): p. 174-89.

[94]E. Evans,K. Ritchie, Dynamic strength of molecular adhesion bonds. Biophys J, 72(1997.)(4): p. 1541-55.

[95]G. I. Bell, Models for the specific adhesion of cells to cells. Science, 200(1978.)(4342): p. 618-27.

[96]D. F. J. Tees, J. T. Woodward, D. A. Hammer, Reliability theory for receptor--ligand bond dissociation. The Journal of Chemical Physics, 114(2001.)(17): p. 7483-7496.

[97]M. Raible, M. Evstigneev, F. W. Bartels, R. Eckel, M. Nguyen-Duong, R. Merkel, R. Ros, D. Anselmetti, P. Reimann, Theoretical analysis of single-molecule force spectroscopy experiments: heterogeneity of chemical bonds. Biophys J, 90(2006.)(11): p. 3851-64.

[98]A. Taubenberger, D. A. Cisneros, J. Friedrichs, P. H. Puech, D. J. Muller, C. M. Franz, Revealing early steps of alpha2beta1 integrin-mediated adhesion to collagen type I by using single-cell force spectroscopy. Mol Biol Cell, 18(2007.)(5): p. 1634-44.

[99]T. R. Albrecht, S. Akamine, T. E. Carver, C. F. Quate, Microfabrication of cantilever styli for the atomic force microscope. Journal of Vacuum Science & Technology A: Vacuum, Surfaces, and Films, 8(1990.)(4): p. 3386-3396.

[100]J. P. Cleveland, S. Manne, D. Bocek, P. K. Hansma, A nondestructive method for determining the spring constant of cantilevers for scanning force microscopy. Review of Scientific Instruments, 64(1993.)(2): p. 403-405.

[101]J. L. Hutter,J. Bechhoefer, Calibration of atomic-force microscope tips. Review of Scientific Instruments, 64(1993.)(7): p. 1868-1873.

[102]E. Perret, A. Leung, H. Feracci, E. Evans, Trans-bonded pairs of E-cadherin exhibit a remarkable hierarchy of mechanical strengths. Proc Natl Acad Sci U S A, 101(2004.)(47): p. 16472-7.

[103]J. Waschke, C. Menendez-Castro, P. Bruggeman, R. Koob, M. Amagai, H. J. Gruber, D. Drenckhahn, W. Baumgartner, Imaging and force spectroscopy on desmoglein 1 using atomic force microscopy reveal multivalent Ca(2+)-dependent, low-affinity trans-interaction. J Membr Biol, 216(2007.)(2-3): p. 83-92.

[104]E. A. Evans,D. A. Calderwood, Forces and bond dynamics in cell adhesion. Science, 316(2007.)(5828): p. 1148-53.

[105]J. Miyoshi,Y. Takai, Nectin and nectin-like molecules: biology and pathology. Am J Nephrol, 27(2007.)(6): p. 590-604.

[106]M. D. Kottke, E. Delva, A. P. Kowalczyk, The desmosome: cell science lessons from human diseases. J Cell Sci, 119(2006.)(Pt 5): p. 797-806.

[107]M. A. van Steensel, Gap junction diseases of the skin. Am J Med Genet C Semin Med Genet, 131C(2004.)(1): p. 12-9.

[108]J. H. Wang,B. P. Thampatty, An introductory review of cell mechanobiology. Biomech Model Mechanobiol, 5(2006.)(1): p. 1-16.

[109]J. Sadoshima, L. Jahn, T. Takahashi, T. J. Kulik, S. Izumo, Molecular characterization of the stretch-induced adaptation of cultured cardiac cells. An in vitro model of load-induced cardiac hypertrophy. J Biol Chem, 267(1992.)(15): p. 10551-60.

[110]J. D. Kakisis, C. D. Liapis, B. E. Sumpio, Effects of cyclic strain on vascular cells. Endothelium, 11(2004.)(1): p. 17-28.

[111]P. R. Chess, L. Toia, J. N. Finkelstein, Mechanical strain-induced proliferation and signaling in pulmonary epithelial H441 cells. Am J Physiol Lung Cell Mol Physiol, 279(2000.)(1): p. L43-51.

[112]M. Liu, J. Xu, J. Liu, M. E. Kraw, A. K. Tanswell, M. Post, Mechanical strain-enhanced fetal lung cell proliferation is mediated by phospholipase C and D and protein kinase C. Am J Physiol, 268(1995.)(5 Pt 1): p. L729-38.

[113]K. J. Cavanaugh, Jr.,S. S. Margulies, Measurement of stretch-induced loss of alveolar epithelial barrier integrity with a novel in vitro method. Am J Physiol Cell Physiol, 283(2002.)(6): p. C1801-8.

[114]A. J. Banes, G. Lee, R. Graff, C. Otey, J. Archambault, M. Tsuzaki, M. Elfervig, J. Qi, Mechanical forces and signaling in connective tissue cells: cellular mechanisms of detection, transduction, and responses to mechanical deformation. Current Opinion in Orthopedics, 12(2001.)(5): p. 389-396.

[115]N. J. Hegarty, R. W. Watson, L. S. Young, A. J. O'Neill, H. R. Brady, J. M. Fitzpatrick, Cytoprotective effects of nitrates in a cellular model of hydronephrosis. Kidney Int, 62(2002.)(1): p. 70-7.

[116]P. Schelling, K. M. Guglielmi, E. Kirchner, B. Paetzold, T. S. Dermody, T. Stehle, The reovirus sigma1 aspartic acid sandwich: a trimerization motif poised for conformational change. J Biol Chem, 282(2007.)(15): p. 11582-9.

[117]G. R. Kunkel, M. Mehrabian, H. G. Martinson, Contact-site cross-linking agents. Mol Cell Biochem, 34(1981.)(1): p. 3-13.

[118]M. Frick, C. Bertocchi, P. Jennings, T. Haller, N. Mair, W. Singer, W. Pfaller, M. Ritsch-Marte, P. Dietl, Ca2+ entry is essential for cell strain-induced lamellar body fusion in isolated rat type II pneumocytes. Am J Physiol Lung Cell Mol Physiol, 286(2004.)(1): p. L210-20.

[119]K. Takahashi, H. Nakanishi, M. Miyahara, K. Mandai, K. Satoh, A. Satoh, H. Nishioka, J. Aoki, A. Nomoto, A. Mizoguchi, Y. Takai, Nectin/PRR: an immunoglobulin-like cell adhesion molecule recruited to cadherin-based adherens junctions through interaction with Afadin, a PDZ domain-containing protein. J Cell Biol, 145(1999.)(3): p. 539-49.

[120]M. Miyahara, H. Nakanishi, K. Takahashi, K. Satoh-Horikawa, K. Tachibana, Y. Takai, Interaction of Nectin with Afadin Is Necessary for Its Clustering at Cell-Cell Contact Sites but Not for Its cis Dimerization or trans Interaction
10.1074/jbc.275.1.613. J. Biol. Chem., 275(2000.)(1): p. 613-618.

[121]Y. Momose, T. Honda, M. Inagaki, K. Shimizu, K. Irie, H. Nakanishi, Y. Takai, Role of the second immunoglobulin-like loop of nectin in cell-cell adhesion. Biochem Biophys Res Commun, 293(2002.)(1): p. 45-9.

[122]Y. S. Chu, W. A. Thomas, O. Eder, F. Pincet, E. Perez, J. P. Thiery, S. Dufour, Force measurements in E-cadherin-mediated cell doublets reveal rapid adhesion strengthened by actin cytoskeleton remodeling through Rac and Cdc42. J Cell Biol, 167(2004.)(6): p. 1183-94.

[123]S. R. Vedula, T. S. Lim, S. Hui, P. J. Kausalya, E. B. Lane, G. Rajagopal, W. Hunziker, C. T. Lim, Molecular force spectroscopy of homophilic nectin-1 interactions. Biochem Biophys Res Commun, 362(2007.)(4): p. 886-92.

[124]T. A. Sulchek, R. W. Friddle, K. Langry, E. Y. Lau, H. Albrecht, T. V. Ratto, S. J. DeNardo, M. E. Colvin, A. Noy, Dynamic force spectroscopy of parallel individual Mucin1-antibody bonds. Proc Natl Acad Sci U S A, 102(2005.)(46): p. 16638-43.

[125]Y. Tsukasaki, K. Kitamura, K. Shimizu, A. H. Iwane, Y. Takai, T. Yanagida, Role of Multiple Bonds Between the Single Cell Adhesion Molecules, Nectin and Cadherin, Revealed by High Sensitive Force Measurements. J Mol Biol, 367(2007.)(4): p. 996-1006.

[126]P. M. Williams, Analytical descriptions of dynamic force spectroscopy: behaviour of multiple connections. Analytica Chimica Acta, 479(2003.)(1): p. 107-115.

[127]M. Yasumi, K. Shimizu, T. Honda, M. Takeuchi, Y. Takai, Role of each immunoglobulin-like loop of nectin for its cell-cell adhesion activity. Biochem Biophys Res Commun, 302(2003.)(1): p. 61-6.

[128]A. W. Koch, S. Pokutta, A. Lustig, J. Engel, Calcium binding and homoassociation of E-cadherin domains. Biochemistry, 36(1997.)(25): p. 7697-705.

[129]S. Fabre, N. Reymond, F. Cocchi, L. Menotti, P. Dubreuil, G. Campadelli-Fiume, M. Lopez, Prominent Role of the Ig-like V Domain in trans-Interactions of Nectins. Nectin3 and nectin4 bind to the predicted C-C'-C"-D beta -strands of the nectin1 V domain. J. Biol. Chem., 277(2002.)(30): p. 27006-27013.

[130]S. Santoso, V. V. Orlova, K. Song, U. J. Sachs, C. L. Andrei-Selmer, T. Chavakis, The homophilic binding of junctional adhesion molecule-C mediates tumor cell-endothelial cell interactions. J Biol Chem, 280(2005.)(43): p. 36326-33.

[131]J. A. Campbell, P. Schelling, J. D. Wetzel, E. M. Johnson, J. C. Forrest, G. A. Wilson, M. Aurrand-Lions, B. A. Imhof, T. Stehle, T. S. Dermody, Junctional adhesion molecule a serves as a receptor for prototype and field-isolate strains of mammalian reovirus. J Virol, 79(2005.)(13): p. 7967-78.

[132]C. Weber, L. Fraemohs, E. Dejana, The role of junctional adhesion molecules in vascular inflammation. Nat Rev Immunol, 7(2007.)(6): p. 467-77.

[133]T. W. Liang, H. H. Chiu, A. Gurney, A. Sidle, D. B. Tumas, P. Schow, J. Foster, T. Klassen, K. Dennis, R. A. DeMarco, T. Pham, G. Frantz, S. Fong, Vascular endothelial-junctional adhesion molecule (VE-JAM)/JAM 2 interacts with T, NK, and dendritic cells through JAM 3. J Immunol, 168(2002.)(4): p. 1618-26.

[134]H. Ozaki, K. Ishii, H. Arai, H. Horiuchi, T. Kawamoto, H. Suzuki, T. Kita, Junctional adhesion molecule (JAM) is phosphorylated by protein kinase C upon platelet activation. Biochem Biophys Res Commun, 276(2000.)(3): p. 873-8.

[135]K. J. Mandell,C. A. Parkos, The JAM family of proteins. Adv Drug Deliv Rev, 57(2005.)(6): p. 857-67.

[136]A. E. Prota, J. A. Campbell, P. Schelling, J. C. Forrest, M. J. Watson, T. R. Peters, M. Aurrand-Lions, B. A. Imhof, T. S. Dermody, T. Stehle, Crystal structure of human junctional adhesion molecule 1: implications for reovirus binding. Proc Natl Acad Sci U S A, 100(2003.)(9): p. 5366-71.

[137]G. Bazzoni, O. M. Martinez-Estrada, F. Mueller, P. Nelboeck, G. Schmid, T. Bartfai, E. Dejana, M. Brockhaus, Homophilic interaction of junctional adhesion molecule. J Biol Chem, 275(2000.)(40): p. 30970-6.

[138]T. U. Naik, M. U. Naik, U. P. Naik, Junctional adhesion molecules in angiogenesis. Front Biosci, 13(2008.)(p. 258-62.

[139]M. U. Naik, T. U. Naik, A. T. Suckow, M. K. Duncan, U. P. Naik, Attenuation of junctional adhesion molecule-A is a contributing factor for breast cancer cell invasion. Cancer Res, 68(2008.)(7): p. 2194-203.

[140]M. U. Naik,U. P. Naik, Junctional adhesion molecule-A-induced endothelial cell migration on vitronectin is integrin alpha v beta 3 specific. J Cell Sci, 119(2006.)(Pt 3): p. 490-9.

[141]M. R. Cera, A. Del Prete, A. Vecchi, M. Corada, I. Martin-Padura, T. Motoike, P. Tonetti, G. Bazzoni, W. Vermi, F. Gentili, S. Bernasconi, T. N. Sato, A. Mantovani, E. Dejana, Increased DC trafficking to lymph nodes and contact hypersensitivity in junctional adhesion molecule-A-deficient mice. J Clin Invest, 114(2004.)(5): p. 729-38.

[142]Max L. Nibert, Leslie A. Schiff, Bernard N. Fields., *Reoviruses*, in *Fields Virology*, P.M.H. David M. Knipe, Diane E. Griffin, Robert A. Lamb, Malcolm A. Martin, Bernard Roizman, Stephen E. Straus., Editor. 2007, Lippincott Williams & Wilkins: Baltimore. p. 1597-1624.

[143]E. S. Barton, J. L. Connolly, J. C. Forrest, J. D. Chappell, T. S. Dermody, Utilization of sialic acid as a coreceptor enhances reovirus attachment by multistep adhesion strengthening. J Biol Chem, 276(2001.)(3): p. 2200-11.

[144]J. D. Chappell, A. E. Prota, T. S. Dermody, T. Stehle, Crystal structure of reovirus attachment protein sigma1 reveals evolutionary relationship to adenovirus fiber. Embo J, 21(2002.)(1-2): p. 1-11.

[145]K. M. Guglielmi, E. Kirchner, G. H. Holm, T. Stehle, T. S. Dermody, Reovirus binding determinants in junctional adhesion molecule-A. J Biol Chem, 282(2007.)(24): p. 17930-40.

[146]A. P. Morris, A. Tawil, Z. Berkova, L. Wible, C. W. Smith, S. A. Cunningham, Junctional Adhesion Molecules (JAMs) are differentially expressed in fibroblasts and co-localize with ZO-1 to adherens-like junctions. Cell Commun Adhes, 13(2006.)(4): p. 233-47.

[147]J. C. Forrest, J. A. Campbell, P. Schelling, T. Stehle, T. S. Dermody, Structure-function analysis of reovirus binding to junctional adhesion molecule 1. Implications for the mechanism of reovirus attachment. J Biol Chem, 278(2003.)(48): p. 48434-44.

[148]S. R. Vedula, T. S. Lim, E. Kirchner, K. M. Guglielmi, T. S. Dermody, T. Stehle, W. Hunziker, C. T. Lim, A comparative molecular force spectroscopy study of homophilic JAM-A interactions and JAM-A interactions with reovirus attachment protein sigma1. J Mol Recognit, (2008.)(

[149]R. Merkel, P. Nassoy, A. Leung, K. Ritchie, E. Evans, Energy landscapes of receptor-ligand bonds explored with dynamic force spectroscopy. Nature, 397(1999.)(6714): p. 50-3.

[150]H. Sasaki, C. Matsui, K. Furuse, Y. Mimori-Kiyosue, M. Furuse, S. Tsukita, Dynamic behavior of paired claudin strands within apposing plasma membranes. Proc Natl Acad Sci U S A, 100(2003.)(7): p. 3971-6.

[151]N. Haghighipour, M. Tafazzoli-Shadpour, M. A. Shokrgozar, S. Amini, A. Amanzadeh, M. T. Khorasani, Topological remodeling of cultured endothelial cells by characterized cyclic strains. Mol Cell Biomech, 4(2007.)(4): p. 189-99.

[152]E. Wilson, Q. Mai, K. Sudhir, R. H. Weiss, H. E. Ives, Mechanical strain induces growth of vascular smooth muscle cells via autocrine action of PDGF. J Cell Biol, 123(1993.)(3): p. 741-7.

[153]N. Shimizu, K. Yamamoto, S. Obi, S. Kumagaya, T. Masumura, Y. Shimano, K. Naruse, J. K. Yamashita, T. Igarashi, J. Ando, Cyclic strain induces mouse embryonic stem cell differentiation into vascular smooth muscle cells by activating PDGF receptor beta. J Appl Physiol, 104(2008.)(3): p. 766-72.

[154]W. Craelius, Stretch-activation of rat cardiac myocytes. Exp Physiol, 78(1993.)(3): p. 411-23.

[155]I. Komuro, T. Kaida, Y. Shibazaki, M. Kurabayashi, Y. Katoh, E. Hoh, F. Takaku, Y. Yazaki, Stretching cardiac myocytes stimulates protooncogene expression. J Biol Chem, 265(1990.)(7): p. 3595-8.

[156]I. Komuro, S. Kudo, T. Yamazaki, Y. Zou, I. Shiojima, Y. Yazaki, Mechanical stretch activates the stress-activated protein kinases in cardiac myocytes. Faseb J, 10(1996.)(5): p. 631-6.

[157]J. Sadoshima,S. Izumo, Mechanical stretch rapidly activates multiple signal transduction pathways in cardiac myocytes: potential involvement of an autocrine/paracrine mechanism. Embo J, 12(1993.)(4): p. 1681-92.

[158]J. Zeichen, M. van Griensven, U. Bosch, The proliferative response of isolated human tendon fibroblasts to cyclic biaxial mechanical strain. Am J Sports Med, 28(2000.)(6): p. 888-92.

[159]C. C. Berry, C. Cacou, D. A. Lee, D. L. Bader, J. C. Shelton, Dermal fibroblasts respond to mechanical conditioning in a strain profile dependent manner. Biorheology, 40(2003.)(1-3): p. 337-45.

[160]T. E. Danciu, E. Gagari, R. M. Adam, P. D. Damoulis, M. R. Freeman, Mechanical strain delivers anti-apoptotic and proliferative signals to gingival fibroblasts. J Dent Res, 83(2004.)(8): p. 596-601.

[161]T. Grunheid,A. Zentner, Extracellular matrix synthesis, proliferation and death in mechanically stimulated human gingival fibroblasts in vitro. Clin Oral Investig, 9(2005.)(2): p. 124-30.

[162]L. Tang, Z. Lin, Y. M. Li, Effects of different magnitudes of mechanical strain on Osteoblasts in vitro. Biochem Biophys Res Commun, 344(2006.)(1): p. 122-8.

[163]A. Kusumi, H. Sakaki, T. Kusumi, M. Oda, K. Narita, H. Nakagawa, K. Kubota, H. Satoh, H. Kimura, Regulation of synthesis of osteoprotegerin and soluble receptor activator of nuclear factor-kappaB ligand in normal human osteoblasts via the p38 mitogen-activated protein kinase pathway by the application of cyclic tensile strain. J Bone Miner Metab, 23(2005.)(5): p. 373-81.

[164]D. Kaspar, W. Seidl, C. Neidlinger-Wilke, L. Claes, In vitro effects of dynamic strain on the proliferative and metabolic activity of human osteoblasts. J Musculoskelet Neuronal Interact, 1(2000.)(2): p. 161-4.

[165]T. C. Ng, K. W. Chiu, A. B. Rabie, U. Hagg, Repeated mechanical loading enhances the expression of Indian hedgehog in condylar cartilage. Front Biosci, 11(2006.)(p. 943-8.

[166]K. Lahiji, A. Polotsky, D. S. Hungerford, C. G. Frondoza, Cyclic strain stimulates proliferative capacity, alpha2 and alpha5 integrin, gene marker expression by human articular chondrocytes propagated on flexible silicone membranes. In Vitro Cell Dev Biol Anim, 40(2004.)(5-6): p. 138-42.

[167]K. W. Li, A. K. Williamson, A. S. Wang, R. L. Sah, Growth responses of cartilage to static and dynamic compression. Clin Orthop Relat Res, (2001.)(391 Suppl): p. S34-48.

[168]B. Martinac, M. Buechner, A. H. Delcour, J. Adler, C. Kung, Pressure-sensitive ion channel in Escherichia coli. Proc Natl Acad Sci U S A, 84(1987.)(8): p. 2297-301.

[169]B. Martinac, Mechanosensitive ion channels: molecules of mechanotransduction. J Cell Sci, 117(2004.)(Pt 12): p. 2449-60.

[170]N. Wang, J. P. Butler, D. E. Ingber, Mechanotransduction across the cell surface and through the cytoskeleton. Science, 260(1993.)(5111): p. 1124-7.

[171]D. M. Salter, J. E. Robb, M. O. Wright, Electrophysiological responses of human bone cells to mechanical stimulation: evidence for specific integrin function in mechanotransduction. J Bone Miner Res, 12(1997.)(7): p. 1133-41.

[172]M. Shakibaei,A. Mobasheri, Beta1-integrins co-localize with Na, K-ATPase, epithelial sodium channels (ENaC) and voltage activated calcium channels (VACC) in mechanoreceptor complexes of mouse limb-bud chondrocytes. Histol Histopathol, 18(2003.)(2): p. 343-51.

[173]A. Katsumi, T. Naoe, T. Matsushita, K. Kaibuchi, M. A. Schwartz, Integrin activation and matrix binding mediate cellular responses to mechanical stretch. J Biol Chem, 280(2005.)(17): p. 16546-9.

[174]A. Katsumi, A. W. Orr, E. Tzima, M. A. Schwartz, Integrins in mechanotransduction. J Biol Chem, 279(2004.)(13): p. 12001-4.

[175]E. Correa-Meyer, L. Pesce, C. Guerrero, J. I. Sznajder, Cyclic stretch activates ERK1/2 via G proteins and EGFR in alveolar epithelial cells. Am J Physiol Lung Cell Mol Physiol, 282(2002.)(5): p. L883-91.

[176]K. S. Ko, P. D. Arora, C. A. McCulloch, Cadherins mediate intercellular mechanical signaling in fibroblasts by activation of stretch-sensitive calcium-permeable channels. J Biol Chem, 276(2001.)(38): p. 35967-77.

[177]J. Laboureau, L. Dubertret, C. Lebreton-De Coster, B. Coulomb, ERK activation by mechanical strain is regulated by the small G proteins rac-1 and rhoA. Exp Dermatol, 13(2004.)(2): p. 70-7.

[178]W. Li, A. Duzgun, B. E. Sumpio, M. D. Basson, Integrin and FAK-mediated MAPK activation is required for cyclic strain mitogenic effects in Caco-2 cells. Am J Physiol Gastrointest Liver Physiol, 280(2001.)(1): p. G75-87.

[179]C. Rosette,M. Karin, Ultraviolet light and osmotic stress: activation of the JNK cascade through multiple growth factor and cytokine receptors. Science, 274(1996.)(5290): p. 1194-7.

[180]H. Gille, T. Strahl, P. E. Shaw, Activation of ternary complex factor Elk-1 by stress-activated protein kinases. Curr Biol, 5(1995.)(10): p. 1191-200.

[181]L. Du, C. S. Lyle, T. B. Obey, W. A. Gaarde, J. A. Muir, B. L. Bennett, T. C. Chambers, Inhibition of cell proliferation and cell cycle progression by specific inhibition of basal JNK

activity: evidence that mitotic Bcl-2 phosphorylation is JNK-independent. J Biol Chem, 279(2004.)(12): p. 11957-66.

[182]M. T. Ramirez, V. P. Sah, X. L. Zhao, J. J. Hunter, K. R. Chien, J. H. Brown, The MEKK-JNK pathway is stimulated by alpha1-adrenergic receptor and ras activation and is associated with in vitro and in vivo cardiac hypertrophy. J Biol Chem, 272(1997.)(22): p. 14057-61.

[183]M. Skutek, M. van Griensven, J. Zeichen, N. Brauer, U. Bosch, Cyclic mechanical stretching of human patellar tendon fibroblasts: activation of JNK and modulation of apoptosis. Knee Surg Sports Traumatol Arthrosc, 11(2003.)(2): p. 122-9.

[184]P. Lacolley, Mechanical influence of cyclic stretch on vascular endothelial cells. Cardiovasc Res, 63(2004.)(4): p. 577-9.

[185]B. Alberts, A. Johnson, J. Lewis, M. Raff, K. Roberts, P. Walter, *Molecular Biology of the Cell*. 4 ed. 2002, New York: Garland Science. 1463.

[186]K. Yamamoto, Q. N. Dang, R. A. Kelly, R. T. Lee, Mechanical strain suppresses inducible nitric-oxide synthase in cardiac myocytes. J Biol Chem, 273(1998.)(19): p. 11862-6.

[187]A. A. Pitsillides, S. C. Rawlinson, R. F. Suswillo, S. Bourrin, G. Zaman, L. E. Lanyon, Mechanical strain-induced NO production by bone cells: a possible role in adaptive bone (re)modeling? Faseb J, 9(1995.)(15): p. 1614-22.

[188]M. van Griensven, J. Zeichen, M. Skutek, T. Barkhausen, C. Krettek, U. Bosch, Cyclic mechanical strain induces NO production in human patellar tendon fibroblasts--a possible role for remodelling and pathological transformation. Exp Toxicol Pathol, 54(2003.)(4): p. 335-8.

[189]R. S. Costa,J. Assreuy, Nitric oxide inhibits irreversibly P815 cell proliferation: involvement of potassium channels. Cell Prolif, 35(2002.)(6): p. 321-32.

[190]C. L. Avvisato, X. Yang, S. Shah, B. Hoxter, W. Li, R. Gaynor, R. Pestell, A. Tozeren, S. W. Byers, Mechanical force modulates global gene expression and beta-catenin signaling in colon cancer cells. J Cell Sci, 120(2007.)(Pt 15): p. 2672-82.

[191]S. Noria, D. B. Cowan, A. I. Gotlieb, B. L. Langille, Transient and steady-state effects of shear stress on endothelial cell adherens junctions. Circ Res, 85(1999.)(6): p. 504-14.

[192]M. S. Balda, M. D. Garrett, K. Matter, The ZO-1-associated Y-box factor ZONAB regulates epithelial cell proliferation and cell density. J Cell Biol, 160(2003.)(3): p. 423-32.

[193]M. S. Balda,K. Matter, The tight junction protein ZO-1 and an interacting transcription factor regulate ErbB-2 expression. Embo J, 19(2000.)(9): p. 2024-33.

[194]M. Huerta, R. Munoz, R. Tapia, E. Soto-Reyes, L. Ramirez, F. Recillas-Targa, L. Gonzalez-Mariscal, E. Lopez-Bayghen, Cyclin D1 is transcriptionally down-regulated by ZO-2 via an E box and the transcription factor c-Myc. Mol Biol Cell, 18(2007.)(12): p. 4826-36.

[195]A. Betanzos, M. Huerta, E. Lopez-Bayghen, E. Azuara, J. Amerena, L. Gonzalez-Mariscal, The tight junction protein ZO-2 associates with Jun, Fos and C/EBP transcription factors in epithelial cells. Exp Cell Res, 292(2004.)(1): p. 51-66.

[196]S. Hernandez, B. Chavez Munguia, L. Gonzalez-Mariscal, ZO-2 silencing in epithelial cells perturbs the gate and fence function of tight junctions and leads to an atypical monolayer architecture. Exp Cell Res, 313(2007.)(8): p. 1533-47.

[197]H. G. Gratzner, Monoclonal antibody to 5-bromo- and 5-iododeoxyuridine: A new reagent for detection of DNA replication. Science, 218(1982.)(4571): p. 474-5.